Title
State-of-the-Art Methods for Evaluation of Angiogenesis and Tissue Vascularization

Journal
Circulation Research, 116(11)

ISSN
0009-7330

Authors
Simons, Michael
Alitalo, Kari
Annex, Brian H
et al.

Publication Date
2015-05-22

DOI
10.1161/res.0000000000000054

Peer reviewed

AHA Scientific Statement

State-of-the-Art Methods for Evaluation of Angiogenesis and Tissue Vascularization

A Scientific Statement From the American Heart Association

Michael Simons, MD, Co-Chair; Kari Alitalo, MD, PhD; Brian H. Annex, MD; Hellmut G. Augustin, MD; Craig Beam, CRE; Bradford C. Berk, MD, PhD, FAHA; Tatiana Byzova, PhD; Peter Carmeliet, MD, PhD; William Chilian, PhD, FAHA; John P. Cooke, MD; George E. Davis, MD, PhD; Anne Eichmann, PhD; M. Luisa Iruela-Arispe, PhD; Eli Keshet, PhD; Albert J. Sinusas, MD, FAHA; Christiana Ruhrberg, PhD; Y. Joseph Woo, MD, FAHA; Stefanie Dimmeler, MD, Chair;
on behalf of the American Heart Association Council on Basic Cardiovascular Sciences and Council on Cardiovascular Surgery and Anesthesia

Vascular dysfunction is causally contributing to many diseases, including but not limited to cardiovascular disease, which is still the leading cause of death in the Western world. The endothelium that lines the inner wall of the blood vessels plays a critical role in the pathobiology of these illnesses. Particularly after ischemia or injury, the growth of new blood vessels, driven by endothelial expansion, is essential to maintain oxygen supply to the ischemic or injured tissue. Recent studies additionally suggest that the endothelium acts as a paracrine source for signals that determine tissue regeneration versus fibrosis after injury. Excessive vascularization, however, might also be unwanted, as in the case of cancer, neovascular eye diseases including diabetic retinopathy, atheroma growth, or the expansion of vasa vasorum, which leads to adverse vessel wall remodeling.

Neovascularization is a tightly regulated and essential process that results in the formation of new blood vessels. Specific types of neovascularization include angiogenesis, the formation of new capillaries from existing capillaries, and arteriogenesis, the formation of new arteries from preexisting collaterals or de novo. Although endothelial cells (ECs) certainly are essential for both processes, the formation of functionally active vessels requires a complex molecular cross-talk of ECs with perivascular cells such as pericytes, smooth muscle cells, and macrophages. Simple in vitro models are best suited to examine specific aspects of particular processes involved in angiogenesis such as the biochemical interactions that regulate EC proliferation, motility, and apoptosis or lumen formation. However, in vivo models are required to understand the complex cellular interactions that enable the generation of functionally active and hierarchical blood vessel networks capable of providing an appropriate blood supply and paracrine stimuli to organs. In addition, the development of therapeutic strategies to either promote or inhibit vessel growth depends on reproducible measures and end points in experimental models that are relevant for the treatment of human diseases. Accordingly, the selection of an appropriate experimental model is critical to study specific aspects of the molecular and cellular mechanisms that are of physiological or pathological relevance. This scientific statement summarizes in vitro assays and in vivo models suitable for gaining insights into the basic mechanisms of vessel growth and provides an overview of models that are particularly useful for clinical translation.

1. In Vitro Assays

Considerable progress has been made over the past 20 years in the development of in vitro strategies to investigate the complex processes of vascular morphogenesis and maturation events in

The American Heart Association makes every effort to avoid any actual or potential conflicts of interest that may arise as a result of an outside relationship or a personal, professional, or business interest of a member of the writing panel. Specifically, all members of the writing group are required to complete and submit a Disclosure Questionnaire showing all such relationships that might be perceived as real or potential conflicts of interest.

This statement was approved by the American Heart Association Science Advisory and Coordinating Committee on December 15, 2014, and the American Heart Association Executive Committee on January 27, 2015. A copy of the document is available at http://my.americanheart.org/statements by selecting either the "By Topic" link or the "By Publication Date" link. To purchase additional reprints, call 843-216-2533 or e-mail kelle.ramsay@wolterskluwer.com.

The American Heart Association requests that this document be cited as follows: Simons M, Alitalo K, Annex BH, Augustin HG, Beam C, Berk BC, Byzova T, Carmeliet P, Chilian W, Cooke JP, Davis GE, Eichmann A, Iruela-Arispe ML, Keshet E, Sinusas AJ, Ruhrberg C, Woo YJ, Dimmeler S; on behalf of the American Heart Association Council on Basic Cardiovascular Sciences and Council on Cardiovascular Surgery and Anesthesia. State-of-the-art methods for evaluation of angiogenesis and tissue vascularization: a scientific statement from the American Heart Association. *Circ Res.* 2015;116:e99–e132.

Expert peer review of AHA Scientific Statements is conducted by the AHA Office of Science Operations. For more on AHA statements and guidelines development, visit http://my.americanheart.org/statements and select the "Policies and Development" link.

(*Circ Res.* 2015;116:e99-e132. DOI: 10.1161/RES.0000000000000054.)

3-dimensional (3D) extracellular matrixes[1,2] (Table 1). Most studies have used primary human ECs, in particular human umbilical vein ECs,[3–5] because they are easily available. Other studies have used the aortic ring assay from rat or mouse to study these processes.[6] Two major extracellular matrix environments that work well in these assays are 3D type I collagen and fibrin matrixes. Both types of matrixes are highly effective in inducing EC tube formation and sprouting and allow EC-pericyte interactions in models of vessel maturation, which occur in a 3D matrix environment.[4,7]

Many studies have also been performed by seeding ECs 2-dimensionally on the surface of Matrigel, a laminin-rich matrix,[8] which enables ECs to rearrange into cordlike, lumenless structures.[9] However, there is actually little evidence that this assay system provides a suitable in vitro representation of the process of vascular morphogenesis. In fact, many cell types, including vascular smooth muscle cells, fibroblasts, and tumor cells, form similar cordlike structures on Matrigel surfaces, suggesting that this alignment assay may reflect a competitive cell-cell versus cell-matrix adhesion assay.[9] Laminin-rich matrixes have been shown to inhibit tubulogenesis through integrin-laminin interactions.[10] Together, 3D collagen and fibrin models have been demonstrated to be superior for investigations of vascular tubulogenesis, sprouting, and EC-pericyte tube coassembly and maturation events, including vascular basement membrane matrix formation.

1.1. EC Tubulogenesis Models

A fundamental property of ECs is their ability to form tubes with lumen structures in 3D matrixes (ie, a property of arterial, capillary, venous, and lymphatic ECs).[1] Any cell type that is reported to be an EC (including cells derived from induced pluripotent stem cells or other stem/progenitor cells that have differentiated toward the EC lineage) should be able to form tubes in a 3D matrix environment in vitro. We propose that without such functional characterization, a cell type should not be classified as an EC even if it expresses EC markers.

Several model systems have been established over many years to elucidate fundamental mechanisms underlying how ECs assemble into tube structures with defined lumens in 3D collagen or fibrin matrixes.[3,4] In the most basic setup, ECs are seeded into a 3D matrix and align over time to form lumenized tubes. Tube formation has been demonstrated by cross sections of cultures and with the use of techniques such as thin sectioning of plastic embedded gels, confocal microscopy, and transmission electron microscopy. Importantly, one consequence of EC tubulogenesis is the creation of physical tunnel spaces in the extracellular matrix, called vascular guidance tunnels, that are generated through highly localized MT1-matrix metalloproteinase–dependent matrix degradation.[11,12] These tunnel spaces represent matrix conduits for EC motility, tube remodeling, and recruitment of mural cells to the abluminal surface of developing vessels to enable processes such as vessel remodeling and vascular basement membrane matrix assembly.[13]

In vitro models have been used as a primary discovery tool to identify critical regulators of the EC lumen and tube formation pathway, which were later confirmed with in vivo models. They have also have been extensively used to confirm in vivo findings that have been obtained through mouse knockout or zebrafish morpholino experiments. One point that should be

Table 1. Summary of Most Commonly Used In Vitro Assays

	Pro	Con
3D collagen or fibrin EC lumen formation and sprouting assays	Very reproducible	EC only conditions without mural cells
	Allows the study of EC tube formation and sprouting in physiologically relevant 3D matrix environments	Thus far, isolated rodent ECs have not worked well in these assay models
	Can be reproducibly performed under serum-free conditions with defined recombinant growth factors	Variable growth conditions for ECs may affect results with these models
	Can be performed with various human ECs (eg, HUVECs) that can be genetically manipulated	
	EC tubes that are formed can be subjected to flow forces	
EC-pericyte coculture assays in 3D collagen or fibrin matrixes	Allows the study of EC tubulogenesis and sprouting and the contribution of mural cells to these events	Can be difficult to establish; functionality depends on appropriate conditions
	Allows the study of ECM remodeling, including basement membrane matrix assembly around developing EC tubes	Potential variability concerning the sources of pericytes used for the assay systems
	Can be performed under serum-free defined conditions and functionally define ECs vs pericytes	
EC spheroid assay	Very reproducible	No mural cell contribution
	Angiogenic sprouting can be investigated	
Aortic ring assay	Very reproducible	Variability requires sufficiently high numbers
	Allows the study of the angiogenic effects of genes in genetic models ex vivo	Cellular contributions (eg, ECs, various mural cells, macrophages) may vary
Matrigel assay	Very reproducible	Is not a specific angiogenesis assay (other cells can also form cordlike networks)
	Can provide insight into EC survival and signaling activity	
		No tubulogenesis

3D indicates 3-dimensional; EC, endothelial cell; ECM, extracellular matrix; and HUVEC, human umbilical vein endothelial cell.

emphasized is that in vitro morphogenesis models with isolated ECs have used human ECs; thus, if differences arise with an in vivo model system, it is always possible that this discordance may reflect a species difference in the molecular requirements for vascular morphogenic events.

To date, it has been very difficult to successfully use isolated primary mouse or rat ECs in tube morphogenic assays in 3D collagen or fibrin matrixes. The reason for this discrepancy between human and rodent ECs is unclear. However, primary human ECs work extremely well in vascular tube morphogenesis and sprouting assays in 3D matrixes.

As a general rule, in vitro vascular morphogenesis assays should be performed under highly defined conditions. Ideally, the assay systems should be performed in serum-free defined media in 3D matrixes so that the additives are known, and this has been accomplished with the use of a number of in vitro models using human ECs and the aortic ring assay. In this manner, the actual growth factor, lipid, hormone, and so on, requirements for the various steps and events during vascular morphogenesis can be accurately assessed.

1.2. Sprouting Models

In contrast to 3D alignment assays, the process of sprouting angiogenesis can be studied in vitro by allowing ECs to form sprouting and lumen-forming capillary-like structures by seeding them from focal starting points into a collagen or fibrin matrix. A common strategy to focally seed ECs into a matrix is to coat beads with ECs and then embed these EC-coated beads into a 3D matrix.[14] Alternatively, ECs can be allowed to form 3D spheroidal aggregates that can similarly be delivered as focal starting points into a 3D matrix.[5] Spheroidal aggregates of human ECs have also been transplanted in a 3D matrix into immunocompromised mice to generate a 3D capillary network that anastomoses with the mouse vasculature and is perfused by mouse blood.[15,16] Sprouting angiogenesis can be demonstrated and qualitatively and quantitatively analyzed effectively in vitro and in vivo in these assays.

Sprouting angiogenesis has also been studied by allowing ECs seeded as monolayers on top of a matrix to invade into the matrix, which allows them to form lumenized structures.[17,18] Such 2-dimensional/3D hybrid assays have been established as 3D sprouting angiogenesis assays. They can be considered an appropriate representation of 3D sprouting angiogenesis. However, the proteolytic balance between matrix-degrading and matrix-invading forces needs to carefully controlled.

The aortic ring assay system is another widely used 3D sprouting angiogenesis assay.[6] This assay has some advantages in that animal tissues from normal versus genetically modified vessels can be directly assessed in an ex vivo assay. In turn, the multicellular nature of this assay can complicate the interpretation of results. The aortic ring assay has also been modified to study the sprouting of lymphatic ECs from explanted thoracic duct segments.[19]

A murine allantois assay system that is useful for investigating early vasculogenic tube assembly has also been described, although no exogenous extracellular matrix is used in this approach.[20]

1.3. Microfluidic Flow Models

A recent advance has been the development of microfluidic models of vascular morphogenesis whereby flow forces can be applied during the morphogenic event. To date, this has been performed primarily with sprouting models in which flow is applied to 1 monolayer surface and then the tube networks connect with 2 sides of the microfluidic device (containing flow channels).[21] Directional flow ensues through the tubes that connect the flow channels. Other variations of such models have been to create tube channels artificially in 3D matrixes to enable user-defined geometries of the vascular network and then seed the channels with ECs for the creation of tube networks in the absence of EC-driven tubulogenesis and vascular guidance tunnel formation.[22,23] Of note, these systems have so far not been tested by many laboratories, and the robustness and practicability at a larger scale remain to be established.

1.4. EC-Pericyte Tube Maturation Models

Several EC-pericyte coculture models in 3D matrixes have been established during the past 10 years. Such assays have highlighted the functional importance of both ECs and pericytes during capillary tube assembly in vitro.[7,12,13,24] A major function of ECs is to establish networks of tubes that reside within vascular guidance tunnels and that induce the recruitment of pericytes into tunnel spaces along the abluminal tube surface.[7] Both ECs and pericytes are highly motile during these events, and once pericytes reach the abluminal surface, they migrate along these surfaces in a polarized manner. Pericyte recruitment increases the length and decreases the diameter of EC tubes, which correlates with the deposition of vascular basement membrane matrix. Both cell types contribute basement membrane components, and both ECs and pericytes are necessary to generate basement membrane matrixes under defined serum-free conditions in 3D matrixes (demonstrated with transmission electron microscopy and immunofluorescence microscopy). Such systems enable a detailed analysis of EC tube maturation events and can assess the role of the key growth factors and signaling pathways that are necessary for these processes.

1.5. Summary

Overall, in vitro models of vascular morphogenesis and maturation have contributed greatly to our understanding of these events, and sprouting angiogenesis can be well studied by the established highly reproducible assays. The use of 3D coculture assays additionally allows investigators to gain insights into vessel maturation processes and to study EC-pericyte interactions. The development of 3D coculture models that include flow would allow the study of microcirculatory networks and vessel maintenance at least for some days. Clearly, these models should be used in conjunction with in vivo approaches and hybrid strategies in which ECs are manipulated in vitro and then introduced in vivo to interface with a host vasculature. This is essential because even the best in vitro model will not fully recapitulate the complex process of vessel growth under physiological or pathophysiological conditions. Furthermore, in vitro models cannot assess the impact of circulating humoral and cellular factors that interact with the endothelium and that could have major impact, particularly under disease conditions

such as diabetes mellitus, coronary artery disease, or heart failure, which systemically affect tissue homeostasis.

2. Developmental Angiogenesis and Arteriogenesis

In all vertebrate species, blood vessels form during embryogenesis in successive steps called vasculogenesis and angiogenesis, which are then followed by remodeling and maturation of the initial vascular plexus into adult vasculature.[25] The term vasculogenesis describes the de novo specification of endothelial precursor cells or angioblasts from the mesoderm. These newly formed cells coalesce into lumenized tubes that form the primary vascular plexus, which consists of a meshwork of homogeneously sized capillaries and the central axial vessels (ie, the dorsal aorta [DA] and cardinal veins). With the onset of heartbeat, this early vascular circuit expands and remodels, undergoing proliferation, sprouting, and pruning of preexisting vessels. This process of vascular remodeling transforms simple circulatory loops into a complex hierarchical network of branched endothelial tubes of varying diameter, length, and identity and depends on both genetically hard-wired events and hemodynamic forces (reviewed elsewhere[26]).

A large number of signaling pathways regulate vascular development (reviewed by Potente et al[27]). Because a properly formed cardiovascular system is essential for sustaining embryonic development, mutations in these pathways frequently cause phenotypes that result in embryonic lethality. Global deletion in vascular endothelial growth factor (VEGF), Delta/Notch, integrin, transforming growth factor-ß, ephrin/Eph, and angiopoietin/Tie signaling pathways (among others) impairs vascular development, causing lethality in the mouse embryo between embryonic day (E) 8.0 and E12.5 attributable to failure to establish a functional circulatory network. These studies have been instrumental in our understanding of pathways required for vasculogenesis, endothelial tube assembly and lumen formation, angiogenesis, and arteriovenous differentiation. In the following sections, we present currently available models in mice and other species. Because vascular phenotypes are often complex and we still have an incomplete understanding of the normal sequence of vascular remodeling events, delineating the primary defect caused by a specific gene manipulation may require the combinatorial use of >1 model system.

2.1. The Mouse Embryonic Hindbrain and Postnatal Retina as Model Systems to Study Developmental Angiogenesis

The developing mouse constitutes a model of choice to analyze vascular development and consequences of genetic manipulations on this process. Angioblasts in the mouse embryo first emerge from the mesoderm as VEGF receptor (VEGFR) 2^+ cells around E7.0 and assemble into a simple circulatory loop consisting of a heart, DA, yolk sac plexus, and sinus venosus by E8.0.

Several methodological improvements have allowed better understanding of early embryonic vascular development in the mouse. These include an expanded array of vascular markers and improved imaging techniques such as confocal imaging, optical projection tomography, and ultramicroscopy to visualize vascular networks in intact embryos with far greater degrees of resolution and 3D context compared with histological sections.[28,29] In addition, the culture of allantois, an extraembryonic appendage rich in blood vessels that develops from E6 onward in the mouse, can be used for live imaging of vascular network formation in explanted wild-type and mutant tissue and allows additional manipulations such as phenotypic rescue experiments (reviewed by Arora and Papaioannou[30]).

The most crucial technical innovation in recent years has been the generation of temporally inducible, endothelium-specific *Cre* alleles that can switch conditional null (floxed) target genes off during any required developmental time window, thus circumventing the early embryonic lethality seen with global knockout mice that impairs cardiovascular development (eg, Benedito et al[31]; Table 2). Likewise, refined inducible overexpression systems can be used to switch genes on at any defined time point during embryonic and postnatal development in the mouse (eg, Wang et al[47]; Table 2). Combined with novel in vivo models of central nervous system angiogenesis, discussed below, these methods have considerably refined our capacity to decipher molecular mechanisms governing vascular development and to understand the activities of pathways required for vascular development, which are not limited to early embryonic development but extend to organogenesis, maintenance of adult vascular homeostasis, and pathological angiogenesis.

The vertebrate central nervous system is made up of brain, spinal cord, and retina. All 3 organs are vascularized during embryonic and early postnatal development to provide oxygen and nutrients to both neuronal progenitors and the metabolically highly active and terminally differentiated neurons that relay information. Both brain and spinal cord acquire a vascular network before birth, although the complexity of this network increases after birth for some time. In contrast, the retina is initially supplied by the extraretinal choroidal vasculature and hyaloid arteries. Although the choroidal vasculature persists into adulthood, the hyaloid arteries are replaced during postnatal development with an intraretinal vascular system that is known as the retinal vasculature. Brain, spinal cord, and retinal vasculature all form through angiogenesis (reviewed by Ruhrberg and Bautch[48]). Because of the stereotypic nature of vessel sprouting in all 3 organs, they are extremely well suited to identify even subtle changes caused by the perturbation of environmental or genetic factors that regulate angiogenesis. This section summarizes the advantages and limitations of the mouse embryo hindbrain and postnatal retina as model systems to study physiological angiogenesis and introduces the perinatal retina as an additional model to identify factors that modulate pathological neovascularization. Importantly, all 3 experimental models have been described with much detail in recent publications and are therefore easily applied and suited to standardization of angiogenesis research between different investigators.[37,49,50]

2.1.1. Brief Description of Hindbrain Vascularization

The mouse hindbrain is vascularized before birth.[48] The vascularization of the mouse embryonic hindbrain begins about E9.5, when vessels sprout into the hindbrain from a perineural vascular plexus. These first hindbrain vessels grow perpendicular to the hindbrain surface toward the ventricular zone (radial vessels) but then change direction to sprout parallel to the ventricular

Table 2. Mouse Lines Expressing Blood ECs and Lymphatic EC-Specific Cre or a Fluorescent Protein Reporter

Mouse Line	Description of Mouse Line	Reference
EC-specific constitutive Cre-deleter mouse lines		
Tie1-Cre	The Tie1 gene promoter drives Cre expression in these transgenic mice in most embryonic ECs from E8-9 onward but not in all ECs in adult vasculature. There may be expression in some hematopoietic cells.	32
Tie2-Cre	Tie2 gene promoter and enhancer sequences linked to Cre drive expression in endothelium through embryogenesis and adulthood. May be expressed also in certain monocyte subpopulation and mesenchymal cells.	33
flk1-Cre	Vegfr-2 gene promoter and enhancer sequences driving Cre expression in transgenic mice. Cre is expressed in ECs in embryos from E11.5 or E13.5 onward, depending on the mouse line, except the lung microvasculature.	34
VE-cadherin–Cre	VE-cadherin gene promoter Cre. Early expression in ECs of yolk sac at E7.5; more contiguous EC expression by E14.5 and onward. Shows ubiquitous EC expression in the adult, including LECs and some hematopoietic cells.	35
LEC-specific constitutive Cre-deleter mouse lines		
Lyve1-Cre	GFP-Cre knock in construct in mouse Lyve-1 gene. Cre is expressed in LECs of the lymph nodes but also in a varying fraction of other ECs and in some hematopoietic cells.	36
EC-specific inducible Cre-deleter mouse lines		
VE-cadherin–Cre–ERT2	VE-cadherin (Cdh5) promoter–Cre–ERT2. Administration of tamoxifen (4-OHT) induces translocation of Cre-ERT2 to the nucleus where it mediates Cre-loxP site-specific combination. Allows EC-specific Cre recombination in a temporally and spatially controlled manner.	35, 37
Pdgfb-CreERT2	Platelet-derived growth factor B promoter–Cre. Allows EC-specific Cre recombination in most vascular beds of newborn mice but not in all organs in adults (eg, in central nervous system).	38
LEC-specific Cre-deleter mouse lines		
Prox1-CreERT2	Prox1 gene promoter–driven Cre-ERT2 deletes in the lymphatic vasculature and in other Prox1-expressing cells (eg, in heart and liver), but not in ECs except in venous valves.	39, 40
Genetic fluorescent protein reporter mouse lines for visualization of lymphatic vessels in living mice		
Vegfr3-EGFPLuc	GFP–luciferase fusion protein knock-in construct in mouse Vegfr3 gene, expressed in LECs. Allows fluorescent and luminescent imaging of lymphatic vasculature in embryos and during the first weeks after birth, but expression is strongly downregulated during postnatal development.	41
Prox1-GFP	Fluorescent GFP protein is expressed under the Prox1 promoter in LECs. Recapitulates faithfully the endogenous Prox1 expression. Allows fluorescent imaging of the lymphatic vasculature in embryos and adults.	42
Prox1-mOrange2	Fluorescent mOrange2 protein expressed under the Prox1 promoter in LECs. Similar expression pattern as in Prox1-GFP mice (Choi et al[42]). Allows fluorescent imaging of lymphatic vasculature in embryos and adults.	43
Prox1-tdTomato	Fluorescent tdTomato protein imaging of lymphatic vasculature.	44
Genetic fluorescent protein reporter mouse lines for visualization of blood vessels in living mice		
Tie2-GFP	Tie2 gene promoter and enhancer sequences control GFP expression in transgenic mice. Allows fluorescent imaging of blood vessels during embryogenesis and in adults.	45
Tie1-GFP	Tie1 promoter fragment GFP expression in transgenic mice. GFP is expressed in the ECs in embryos but is downregulated in the adult vasculature.	46

E indicates embryonic day; EC, endothelial cell; GFP, green fluorescent protein; and LEC, lymphatic endothelial cells.

hindbrain surface and anastomose with each other (subventricular vascular plexus; Figure 1A). As the hindbrain tissue thickens as a result of the addition of neurons and the formation of glia, sprouting and fusion move to deeper brain layers.

2.1.1.1. Advantages of the Hindbrain Model to Study Sprouting Angiogenesis

- Permits the spatiotemporal analysis of organ vascularization in normal mice and in mouse strains with genetic mutations that compromise viability or result in postmidgestation embryonic lethality; when combined with inducible Cre-LoxP technology, can be extended to the analysis of mouse strains with premidgestation lethality.
- Robust method for whole-mount labeling of ECs and interacting cell types that can be combined with high-resolution imaging for reliable quantification of angiogenic sprouting, network density, and vessel caliber ECs.
- Enables the analysis of blood vessel growth within a natural but relatively simple multicellular microenvironment where ECs interact with non-ECs to refine the 3D organ architecture (fewer cell types compared with retinal angiogenesis, ie, neural progenitors, differentiating neurons, and microglia precursors but not glia, complex neural networks, or inflammatory cells).

2.1.2. Retinal Vascularization

The mouse retina is vascularized only after birth.[38,51] The formation of the retinal vasculature begins on the day of birth, when vessels emerge from the optic nerve head,

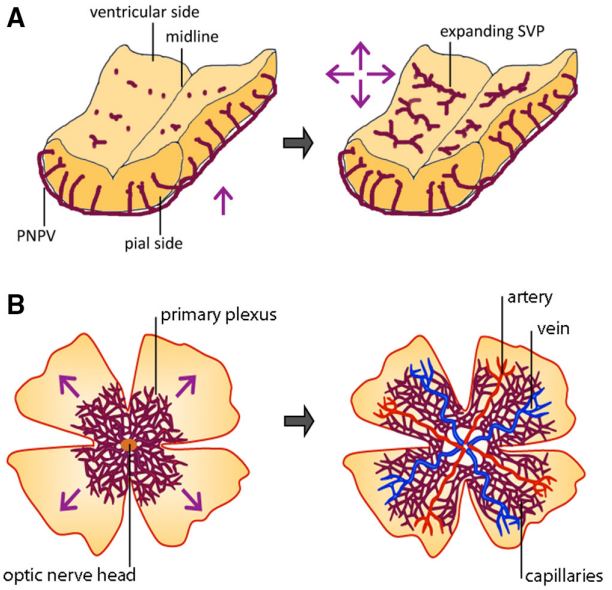

Figure 1. Hindbrain and retina models. Time course of blood vessel ingression into the mouse embryo hindbrain and the perinatal mouse retina. **A**, Vessels sprout from the perineural vascular plexus (PNVP) into the hindbrain at around embryonic day (E) 9.75 in the mouse and then grow radially toward the ventricular zone. Radial vessels do not invade the subventricular zone but sprout laterally and then anastomose to form a subventricular vascular plexus (SVP) by E12.5. **B**, Retinal vascularization proceeds from center to periphery in a radial manner during the first week of life and leads to an extensively remodeled superficial plexus composed of capillaries, arteries, and veins. Modified from Ruhrberg and Bautch.[48]

sprout perpendicularly over the surface of the retina on a network of astrocytes, and begin to anastomose (Figure 1B). While sprouting continues, in particular at the vascular front, vessels in the rear begin to remodel and form arteries and veins (Figure 1B). Pericytes are recruited at the vascular front, and smooth muscle cell maturation begins around arteries and veins. Therefore, multiple aspects of vascular development can be examined in a single 2-dimensional preparation. The formation of the primary vascular plexus is complete by about postnatal day 9, and the resulting vasculature remodels and matures for at least another 10 days. At postnatal day 9, vessels also begin to sprout from the primary retinal vessel plexus at nearly right angles into the inner retina to form first a deep vascular plexus followed by formation of an intermediate vascular plexus. This process is driven primarily by hypoxia/VEGF and is dependent on Notch signaling.

2.1.2.1. Advantages of the Retina Model to Study Sprouting Angiogenesis

- Permits the spatiotemporal analysis of organ vascularization in normal mice and in mouse strains with genetic mutations that are viable or live through the postnatal period until weaning; when combined with inducible Cre-LoxP technology, can be extended to the analysis of mouse strains with embryonic or early postnatal lethality.
- Robust method for whole-mount labeling of ECs and interacting cell types that can be combined with high-resolution imaging; enables reliable quantification of vascular migration and angiogenic sprouting; less suitable to quantify network density and vessel caliber because of temporal overlap in sprouting and vascular remodeling.
- Allows monitoring of angiogenesis alongside vascular remodeling in the same preparation, including visualization of vessel pruning and arteriovenous differentiation (advantage over hindbrain model).
- Permits the analysis of blood vessel growth within a natural multicellular microenvironment in which ECs interact with non-ECs to refine the 3D organ architecture; however, tissue interactions can be complex, with several types of neurons and glia, resident microglia, and recruited immune cells contributing to the process of vascularization.
- Model to study vascular pathology: oxygen-induced retinopathy.

2.1.3. Considerations When Choosing the Hindbrain Versus Retina to Study Physiological Angiogenesis

2.1.3.1. Developmental Stage

The mouse hindbrain can be used at earlier developmental stages than other angiogenesis models. For example, the mouse retina is suitable to analyze angiogenesis in the first 2 weeks after birth, whereas the neural tube is one of the earliest organs to develop and is vascularized earlier than kidneys, heart, or lung. As a result of its vascularization early in development, the hindbrain model is suitable for studying mouse mutants that survive the period of vasculogenesis but are lethal after E12.5 unless an inducible Cre-LoxP system is used.

2.1.3.2. Experimental Manipulation

An advantage of the retina is accessibility to experimental manipulation, for example, by local (intravitreal) or systemic (intraperitoneal) injection of growth factors or function-blocking reagents to examine their impact on retinal vascularization. Although vessel networks rapidly degenerate in organotypic culture, a retinal explant method suitable for short-term live imaging or ex vivo pharmacological manipulation has been described.[52]

2.1.3.3. Immunolabeling

The increasing thickness of the mouse hindbrain from E13.5 on inhibits the penetration of antibodies into the deeper tissue parts, and changes in organ shape prevent flat mounting for whole-mount imaging. Therefore, the hindbrain vasculature at later developmental or postnatal stages is best visualized in immunolabeled tissue sections. In contrast, even the adult retinal vasculature of the mouse is easily labeled in whole-mount preparations.

2.1.3.4. Physiology Versus Pathology

Because of its postnatal development, the development of the retinal vasculature is more easily affected by environmental influences than the hindbrain vasculature, which develops in utero. In particular, the influence of oxygen tension on vascular development is readily studied in a mouse model of oxygen-induced retinopathy, which is discussed below.

2.1.4. Brief Description of Pathological Retinal Vascularization

Pathological retinal neovascularization has been studied extensively in a mouse model of oxygen-induced retinopathy

in which neonatal mice are sequentially exposed to hyperoxia and then normal air. In these circumstances, hyperoxia first causes loss of central retinal capillaries because sufficient oxygen is released from retinal arteries to downregulate factors such as VEGF that are essential to maintain immature retinal capillaries. The ensuing return to normoxia then leads to oxygen deficiency in the vaso-obliterated area, which in turn results in hypoxia-induced VEGF upregulation and therefore the induction of abnormal neovascularization. Because of the ability to study both normal and abnormal vascular development in similar developmental time frames, the retina allows a comparison of hard-wired genetic and environmental influences on physiological and pathological angiogenesis. A detailed description of the method for inducing and analyzing oxygen-induced retinopathy has been published recently.[49]

2.2. Avian Models of Developmental Angiogenesis

Avian embryos, in particular chick (*Gallus gallus domesticus*) and quail (*Coturnix coturnix japonica*) embryos, are classic models for in vivo studies of various developmental processes, including angiogenesis and lymphangiogenesis. A hallmark advantage of avian embryos is their development inside the eggshell, which can be used as a natural culture dish by creating a window that allows visual inspection of embryo development over extended periods of time on a microscope stage. Furthermore, the large size of the embryos allows the exchange of cells and tissue fragments between different embryos. The behavior of the grafted cells in the host can be followed by various labeling techniques, the most well-known technique being the tracing of quail cells grafted into chick hosts with a quail nucleolar marker or with a monoclonal antibody that recognizes only quail cells.[53] Of particular interest for the study of vascular development is the monoclonal antibody QH1, which recognizes ECs from the quail but not the chick.[54] In this way, the capacity of different embryonic donor tissues to generate ECs can be determined, and their destiny in the chick host can be fate mapped. For example, grafting experiments have shown that tissues developing in contact with the endoderm (visceral organs such as lung, liver, and intestine) have the capacity to generate their own ECs, whereas tissues developing in contact with the ectoderm (brain, dermis) cannot generate their own ECs and rely on vascularization from external sources through angiogenic sprouting.[54] Grafting experiments can also be used to show how the environment into which the grafted ECs are placed alters their differentiation. For example, it has been shown that brain ECs, which would normally form a blood-brain barrier, develop fenestrations when grafted into the liver and conversely that liver ECs develop tight junctions when grafted into the brain. Furthermore, heterotopic grafts of arterial ECs can generate venous ECs and vice versa, together demonstrating that ECs can profoundly alter their phenotypes and have considerable plasticity to adapt to novel tissue environments in response to external stimuli.

The most popular avian angiogenesis model is the chorioallantois membrane (CAM).[55] The CAM is a richly vascularized extraembryonic appendage that provides nutrients and oxygen to the chick embryo during the second half of the incubation period and is situated right beneath the eggshell. Its easy accessibility allows application of proangiogenic and antiangiogenic growth factors and monitoring of vessel growth in response to such factors in real time; therefore, the CAM has often been used to test the angiogenic activity of diverse molecules in vivo. For example, the angiogenic activity of fibroblast growth factor-2 in vivo was first demonstrated with the CAM assay. The chicken genome has been sequenced, and growth factor receptors such as fibroblast growth factor, VEGF, and angiopoietin receptors are highly conserved between birds, rodents, and human, enabling the testing of vascular response to mammalian growth factors in the CAM model. However, validating the relevance of the CAM response for intraembryonic angiogenesis by knockdown of the relevant receptor(s) in birds is technically challenging.

2.2.1. Advantages of the Avian Model to Study Angiogenesis

- The embryos are large in size and develop as a flat disk on top of the egg yolk, and they can be grown in ovo or in vitro for extended periods of time. Therefore, avian embryos are readily accessible for experimental manipulations and visual inspection.
- The avian embryo is ideally suited for grafting experiments because a piece of tissue from a quail can be placed into a chicken embryo, either into the corresponding location (homotopic grafting) or into a different location (heterotopic grafting). Additionally, tissues can be exchanged between embryos of different ages (heterochronic grafting).
- An important recent advance has been the generation of transgenic quail expressing fluorescent markers in ECs.[56] Time-lapse imaging of vascular development or grafting of tissues derived from such transgenic quail allows monitoring of EC migration and behavior in real time and provides a powerful means to understand vascular development in complex tissue environments.
- The avian model is suitable for studies of flow-dependent vascular remodeling

2.3. Aquatic Animal Models to Study Vascular Development

The aquatic animal models *Danio rerio* (zebrafish) and *Xenopus* (African clawed frog) represent powerful models for in vivo studies of developmental and pathological angiogenesis and lymphangiogenesis. Hallmark advantages of these models are the (semi)transparency of the embryos and larvae, their external and rapid development, and the availability of transgenic lines reporting the vasculature by fluorescent protein expression. The last advantage enables easy, noninvasive visualization of the vasculature and allows direct observation of angiogenic processes in live embryos in a dynamic manner. Together with the easy breeding and amenability of the models to genetic and pharmacological interference with gene/protein function, these characteristics have led to the extensive use of these models to study candidate (lymph)angiogenesis genes. In addition, their small size and abundance facilitate high-throughput mutagenesis or drug screens. The high extent of gene and pathway conservation with higher vertebrates provides relevance of findings from these small vertebrate models for the human situation. This is exemplified, for instance, by the various discoveries and characterizations in mutant zebrafish models of genes involved in human congenital vascular diseases.[57]

2.3.1. Zebrafish Embryos as Genetic Models for Vascular Research

Zebrafish are tropical freshwater fish, ≈3 to 4 cm long in the adult stage but only a few millimeters long in the embryonic and early larval (hatched) stages. Up to ≈3 weeks of age, embryos and larvae are transparent; early pigmentation can be inhibited chemically by adding a melanogenesis inhibitor to the water[58] to preserve full transparency and to improve detection of signal in whole-mount in situ hybridization analyses. Within 24 to 36 hours, all major organs have been laid out, the major axial trunk vessels have been formed, and the heart is beating.[59]

A particular advantage of the zebrafish model for vascular studies is its small size; up to 4 to 5 days after fertilization, most cells remain within the passive diffusion distance of oxygen (≈100 μm). Hence, unlike mammalian embryos, zebrafish embryos can survive for several days even when vascular development is disrupted or when the vessels are dysfunctional. This allows studies of genes that, on knockout in mice, result in early embryonic lethality; it also allows the study of angiogenic processes and their flow dependency in mutants that have no blood flow.[60]

Techniques for both forward and reverse genetics can be applied in zebrafish such as chemical mutagenesis, Tol2 transposase–based transgenesis, morpholino oligonucleotide–mediated knockdown, and the recent knockout and knock-in technologies based on zinc finger nucleases, transcription activator-like effector nucleases, or Cas9/Crispr for targeted gene modification.[61,62] The zebrafish genome contains orthologs for most human genes, although because of zebrafish genome duplication paralog pairs are present for a subset of the zebrafish genes. Often, the paralogs each cover part of the functions of their human ortholog. This can complicate genetic studies if both paralogs have to be manipulated to observe phenotypic effects. It can also be highly useful because differential functions of the paralogs can then be studied independently in zebrafish.[63]

2.3.1.1. Visualization of the Vasculature and Transgenic Fluorescent Reporter Lines

A hallmark anatomic analysis of vascular development in zebrafish embryos and larvae was based on extensive confocal microangiography.[64] Studies of vascular development in zebrafish embryos further rely heavily on expression analysis, mostly via in situ hybridization on whole-mount zebrafish embryos (see ZFIN, the Zebrafish Model Organism Database, at www.zfin.org for protocols). Microangiography and in situ stainings are quite labor intensive and time consuming. In addition, microangiography is an invasive technique and visualizes only perfused vessels. Vascular research in zebrafish has therefore benefited enormously from the generation of transgenic reporter lines with fluorescent protein expression specifically in vascular ECs. These lines allow developmental and morphological documentation of vessel formation at subcellular resolution, uniquely suited for dynamic live imaging of actively forming vessels by time-lapse confocal microscopy. In the past decade, the availability of reporter lines distinguishing between endothelial subtypes (arterial, venous, lymphatic) and endothelial subcellular structures (eg, cytoplasmic versus nuclear or membrane-restricted) has further expanded the zebrafish model toolbox significantly.[59,65–68] The existence of these reporters also allows intercrosses and the analysis of EC types by flow cytometry or fluorescence-activated cell sorting for further characterization of isolated cells.

2.3.1.2. Angioblast Migration, Vasculogenesis, and Arteriovenous Specification

Specified angioblasts in the trunk that originate in the posterior lateral plate mesoderm migrate from 14 hours after fertilization onward in 2 waves between somites and endoderm toward the midline immediately ventral to the hypochord. They coalesce there to form a primordial vascular cord as a precursor of the DA and posterior cardinal vein (PCV; Figure 2A and 2B). Angioblasts likely already become specified to the arterial or venous cell fate at the lateral plate mesoderm. The DA and PCV primordia in the primitive vascular cord segregate between 21 and 23 hours after fertilization. Vascular lumen formation occurs concomitantly with segregation[59] (Figure 2C and 2D). Expression analysis by in situ hybridization for arterial markers such as Notch1b, Dll4, Tbx20 (hrT), gridlock, and ephrinB2 and venous markers such as DAB2, EphB4, and VEGFR3 is typically used to document arteriovenous EC specification at the level of the DA and PCV. In contrast, vasculogenesis in the trunk can be documented by imaging of DA/PCV formation and segregation via fluorescent microscopy of whole-mount reporter-line embryos or of their transverse sections.[57,71]

2.3.1.3. Sprouting Angiogenesis, Branching, and Tip/Stalk Cell Phenotypes

On establishment of the major axial vessels in the trunk, the vascular tree expands by sprouting angiogenesis. From 23 hours after fertilization, bilateral sprouts branch off the DA and, led by a migratory tip cell extending long filopodia scanning the environment for guidance cues, grow dorsally along the intersomitic boundaries (reviewed elsewhere[70]). Follower proliferative stalk cells elongate the sprout and eventually form the vascular lumen (Figure 2E and 2F). Tip and stalk cells can compete for the tip cell position on alteration of the relative expression levels of tip or stalk cell genes. Furthermore, the genetic "tip" or "stalk" instructions can be counteracted or even overruled by the metabolic status of the cell.[72] Derived from the DA and as the first sprouts to emerge, these vessel branches are called arterial or primary intersomitic vessels (ISVs).

Secondary sprouts develop from a second wave of intersomitic sprouts that, in contrast to the primary arterial ISVs, emanate from the PCV between 30 and 50 hours after fertilization. About half of these sprouts will give rise to the trunk lymphatic vasculature. The others connect to primary arterial ISVs, which lose their original connection with the DA and thereby become venous ISVs, in this way establishing the circulation in the trunk.[64]

Angiogenic sprouting also occurs in the hindbrain when central artery sprouts emerge from the primordial hindbrain channels and grow toward the midline in an arch-shaped fashion to connect to the basilar artery.[73]

2.3.1.4. Anastomosis and Lumen Formation

During dorsal outgrowth, the ISVs emerging from the DA undergo cell divisions, ultimately comprising 4 to 6 cells that overlap along the ventrodorsal axis of the vessel. Cellular rearrangements will then form a lumen in a process involving cell

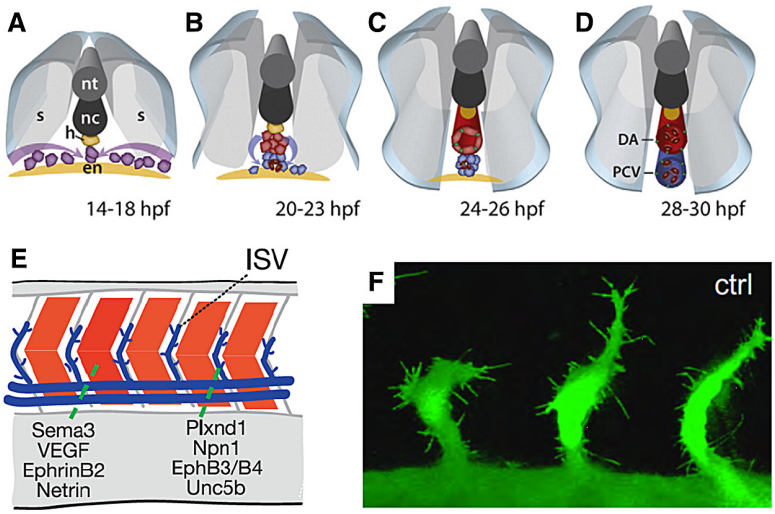

Figure 2. Zebrafish vessel development. **A** through **D**, Angioblast migration and vasculogenesis in the zebrafish embryo trunk region during formation of the dorsal aorta (DA) and posterior cardinal vein (PCV). **E** and **F**, Guided sprouting of intersomitic vessels (ISV) between somite boundaries. ctrl Indicates controls; en, endoderm; h, hypochord; hpf, high-power field; nc, notochord; nt, neural tube; s, somite; and VEGF, vascular endothelial growth factor. **A** through **D**, Modified from Ellertsdóttir et al[69] with permission from the publisher. Copyright © 2009, Elsevier Inc. **E**, Modified from Carmeliet and Tessier-Lavigne.[70]

hollowing (intracellular vacuolar fusion followed by intercellular lumen fusion) or cord hollowing (by exocytosis of vacuoles into the intercellular space common to multiple ECs).[66]

On reaching the roof of the neural tube, tip cells of the ISVs connect and anastomose with the tip cell of their neighboring ISVs to form the paired dorsal longitudinal anastomosing vessels. This process is initiated by filopodial connections, evolving into the formation of cell junctions and lumenization via junctional remodeling and cell rearrangement.[66]

2.3.1.5. Functional Testing

Functional testing at the level of the vessel can be done via microangiography with the use of fluorochrome-tagged dextran to evaluate the perfusion and integrity (absence of leakage) of lumenized vessels.[64] Angiography also visualizes vessel morphology of patent vessels and their 3D localization in the embryo.[64] Perfusion can also be tested on the basis of circulating DsRed$^+$ blood cells in Tg(kdrl:GFP;gata1:DsRed) embryos.[74] EC proliferation and apoptosis can be assessed by counting of nuclei using specific transgenic reporter lines with nuclear expression of the respective fluorescent protein in ECs[65]; by using standard assays such as DAPI, TOPRO, or BrDU staining; or, for apoptosis, by terminal deoxynucleotidyl transferase dUTP nick-end labeling staining. Transgenic lines expressing Lifeact–enhanced green fluorescent protein fusion proteins marking F-actin based structures have been used to visualize filopodia, anastomosis, cellular contacts/junctions, and lumenization (see above).

2.3.2. Xenopus *Tadpoles as Genetic Models for Vascular Research*

A complementary aquatic animal model is the *Xenopus* tadpole, a favored amphibian model organism in developmental biology for decades.[75] Similar to zebrafish, *Xenopus* embryos develop fast and ex utero, are semitransparent, and are amenable to forward and reverse genetics and chemicogenetics.[75,76] The longer generation time (1–2 years) and pseudotetraploid genome make the generation of transgenic lines of *X laevis* challenging. This is much less the case for *X tropicalis*, which has a shorter generation time (4–6 months) and a diploid genome.

2.3.2.1. Visualization of the Vasculature and Transgenic Fluorescent Reporter Lines

Previous reports on vascular development in *Xenopus* embryos were dependent mainly on in situ hybridization, dye injections into blastomers or directly into the vasculature, or corrosion casting.[76,77] However, none of these methods allows a detailed, noninvasive, long-term visualization of the developing vasculature. Whole-mount in situ hybridization also is technically challenging in tadpoles beyond stage 42 (4 days after fertilization). Fluorescent vascular reporters are available, although only a few to date, so far all in *X laevis* (for references, see the work by Ny et al[78]).

2.3.2.2. Vasculogenesis in Xenopus *Tadpoles*

Formation of the large axial vessels begins when a portion of endothelial progenitor cells in the lateral plate mesoderm ventral to the somites migrate to the midline to form the DA and endothelial progenitor cells that remain in place form the 2 paired PCVs.[79] This mechanism resembles a situation closer to higher vertebrates (DA and PCV each develop from a pair of vessels that then fuse to form a single DA and single PCV) compared with zebrafish (DA and PCV develop from a common precursor vessel; see above).

2.3.2.3. Angiogenesis in the Trunk and Fin

After the formation of the primitive vascular system by vasculogenesis, new blood vessels arise via sprouting. Formation of the ISVs occurs from stage 35 onward, with the first intersomitic veins and arteries starting to sprout off from the PCV and DA, respectively.[77] Thus, unlike zebrafish embryos, which display only 1 vessel, that of initially arterial character at each intersomitic junction, *Xenopus* embryos present 1 pair of artery and vein at each intersomitic junction (Figure 3A), similar to mammals. ISVs reaching the dorsal side of the trunk then form the dorsal longitudinal anastomosing vessel, which drains into the PCV near the head. Further vascular expansion is achieved by the sprouting of a capillary network, starting from the rostral-most vessels, ultimately covering the complete tail by stage 46[77] (Figure 3B).

Blood vessel sprouting from the axial arteries and veins into the fin can be visualized easily with the use of transgenic reporters. It starts around stage 46 (6 days after fertilization) and

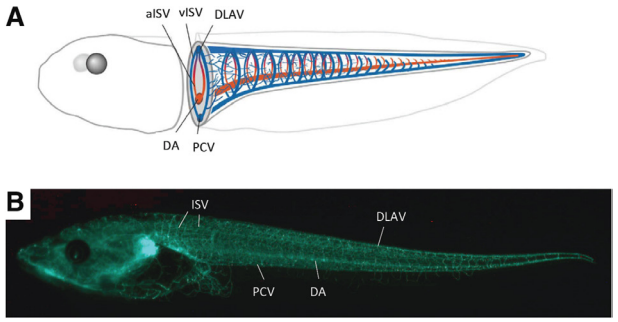

Figure 3. A, Schematic of the trunk vessels in a *Xenopus laevis* embryo. **B**, Stage 45 Tg(Flk1-eGFP) *X laevis* reporter embryo visualizing the vasculature. aISV indicates arterial intersomitic vessel; DA, dorsal aorta; DLAV, dorsal longitudinal anastomosing vessel; ISV, intersomitic vessel; PCV, posterior cardinal vein; and vISV, venous intersomitic vessel. **A**, Reproduced from Levine et al[77] with permission from Elsevier. Copyright © 2003, Elsevier. **B**, Modified from Ny et al.[78]

occurs in a random pattern. Loop formation by turning back of the sprouts toward the axial vessels and further branching of the sprouts establishes the vascular network of the fin.[78] The blood vessel sprouting is followed by a similar lymphatic sprouting of the dorsal and caudal axial lymph vessels into the fin.[78]

3. Adult Angiogenesis Models

The process of angiogenesis in the postnatal period is in most cases associated with tissue or organ growth, which requires an increasing supply of oxygen and nutrients. With rare exceptions, such postnatal expansion of tissues is caused by reproductive demands or pathologies such as neoplastic processes. Alternatively, new blood vessels are required for tissue and organ repair processes resulting from injury or vascular occlusion. Tadpoles allow for the study of developmental lymphangiogenesis in a more complex vertebrate animal model.[78]

3.1. Placental Angiogenesis

Even though angiogenesis in the healthy adult is generally a downregulated process, physiological angiogenesis occurs in the female reproductive system, most notably during the menstrual cycle and pregnancy-associated placental development.[80] Fetoplacental vascularization is critical for an exchange of oxygen and nutrients between maternal and embryonic tissues and therefore determines fetal growth and well-being. Impaired angiogenesis in the placenta inevitably leads to fetal growth retardation or preeclampsia. In rodents, the most vascularized part of the placenta is a labyrinth. Angiogenesis in this labyrinth is known to be driven by key proangiogenic factors, including VEGF-A and placental growth factor.[81] Both vascular density and the thickness of the labyrinth in mammals depend on successful angiogenesis; therefore, any abnormalities in these parameters might indicate the presence of angiogenic defects in knockout or transgenic models. Importantly, placental defects might occur in situations of maternal and embryonic angiogenic deficiencies. Therefore, when evaluating the phenotype of a new knockout or transgenic model in mammals, one might consider an analysis of placental vascularization. Initial characterization can be performed by a macroscopic inspection of the entire placenta in which vascularization is rather obvious at ×4 to ×10 magnification.[82,83] This can be followed by tissue sectioning through the center of the placenta and measurements of the labyrinth thickness.[84] Vascular density and area can be assessed in tissue section with CD31 or CD34 staining. The frequency and severity of placental defects might provide the very first evidence of a potential angiogenic activity of a studied gene product. Despite the major importance of angiogenesis in the female reproductive system, the measurement of angiogenesis during the menstrual cycle is rarely or never used as a method of measuring angiogenesis because of the difficulties in synchronizing the experiments, leading to a high variability.

3.2. Wound Angiogenesis Assay

One of the most visual and physiologically relevant assays to measure angiogenesis is the cutaneous wound assay. Tissue repair is associated with increased cell proliferation, intense matrix deposition, and timely clearance of cell debris, and naturally, tissue repair depends heavily on blood supply. It is important to remember that vessel density as a function of time follows a bell-shaped curve in this model. During intense wound healing, new blood vessels are formed, thereby increasing vascular density several-fold compared with intact skin before wounding. When the repair process is complete, vascular density returns to its normal levels. In the punch wound model using 10-week-old C57/Black6 mice, the peak of neovascularization occurs between days 4 and 8 after wounding (Figure 4). Vessel density generally returns to initial levels ≈3 weeks later. Therefore, before and at the peak of vascularization, this model reports on the angiogenic response; however, after this peak, this model might be an indicator of vascular stability and remodeling. Wound healing is highly dependent on vascularization, and most, if not all, known angiogenic inhibitors will delay this process, whereas proangiogenic factors generally accelerate it. Importantly, wound angiogenesis is driven by endogenously produced proangiogenic factors, which makes this model physiologically relevant. In particular, inhibition of VEGF or its receptors substantially slows wound healing. However, the amount and specificity of angiogenic growth factors cannot be controlled in this model.

Several specifics of this model should be considered when measuring angiogenesis:

1. It is advisable to evaluate vessel density by staining ECs at various time points after wound healing to detect differences at the early and late stages of tissue repair.
2. Tissues sections of wounds need to be cut through the center of the wound. For evaluation of the vasculature, it is important to consider an entire area of the wound and surrounding skin (≈10 mm from the wound border). Vessel density, blood vessel diameter, and the state of vessel maturation vary substantially, depending on the distance from the center of the wound.
3. The process of vascularization and the timing of wound healing depend on the age of the experimental animals. Typically, both angiogenesis and wound healing slow down in older mice.
4. Angiogenesis in wounds not only is influenced by vascular cells but also is highly dependent on the blood coagulation system, inflammatory cells, keratinocyte/fibroblast

migration and proliferation, and matrix deposition. At early time points, the wound is a site of activation of platelets and the coagulation cascade to enable thrombus formation and, later on, fibrinolysis. Successful and timely blood clotting and timely fibrinolysis are prerequisites for a well-balanced angiogenic response. Delayed angiogenesis in this model and therefore slow wound closure might be caused by hemostatic rather than vascular defects. Therefore, the results of wound healing assays need to be interpreted with care.

5. Inflammatory responses are another important issue to consider in the evaluation of angiogenesis in wounds. The results of this assay might differ if animals are kept in pathogen-free conditions compared with regular housing. In addition, defects of the immune system may affect the angiogenic response. Monocytes and macrophages are important sources of proangiogenic growth factors, and any abnormalities in their recruitment and activation may eventually slow the angiogenic response.

Overall, wound healing is a relatively robust model to assay angiogenesis dependent on endogenously produced growth factors. It is important to remember that angiogenesis in wounds is strongly influenced by tissue injury–induced responses such as hemostasis and inflammation. This assay is also useful for the analysis of angiogenesis in species other than mice, including rats, pigs, dogs, and primates.

3.3. Matrigel Plug Assay and Angioreactors

The Matrigel plug assay is in principle an easy, doable angiogenesis assay. This assay involves subcutaneous injection of Matrigel with or without growth factor supplementation and analysis of the ingrowing capillaries after 7 to 14 days.[85]

3.3.1. Advantages of the Matrigel Plug Assay:

- The Matrigel plug assay is relatively easy to perform, and it is possible to control both the amount and type of proangiogenic growth factors. Alternatively, one can use a combination of proangiogenic factors.
- The readout is based on the measurement of vascularization and hemoglobin contents in excised plugs. Thus, one can assay multiple samples in 1 experiment, making this method suitable for analyzing a variety of stimuli and conditions.
- Matrigel plugs can be fixed and sectioned to obtain additional information about their cellular content.
- This assay can be conducted with exogenous cells mixed in the Matrigel before its implantation. Examples include various populations of macrophages and ECs. Human ECs premixed in Matrigel will also form blood vessels if implanted in mice in the presence of a sufficient amount of the growth factor(s).
- Adenoviruses carrying genetic constructs of interest can be incorporated into Matrigel, leading to effective transduction of invading cells.

3.3.2. Limitations and Caveats

The assay has a number of inherent limitations that make it rather unreliable and not robust. Notably, when no growth factor is implanted and the assay is pursued under clean (ie, sterile conditions), there is essentially very little ingrowth of capillaries. In turn, when growth factors are included in the gel, then the response is heavily dependent on the presence of heparin. Without heparin, growth factors rapidly diffuse from the plug. With heparin, one needs to deal with the side effects of heparin such as increased bleeding. Specifically, the following aspects need to be considered when the Matrigel plug assay is used:

- Consistency of this method might be problematic. Often, 2 plugs excised from the same mouse yield different amounts of capillaries and hemoglobin, and measuring hemoglobin is not very reliable. This issue, however, may be overcome by increasing the number of experimental animals per group.
- Similar to wound angiogenesis, this method is highly influenced by hemostatic abnormalities. Deficiencies in platelet function or blood coagulation defects leading to excessive bleeding often affect blood content in excised plugs. Therefore, using hemoglobin measurement as the sole end point is not appropriate. Extra-"bloody" plugs might be a manifestation of bleeding problems in animals. Likewise, treating experimental animals with anticoagulants might affect the results of this assay.
- The vasculature generated by ingrowing capillaries in Matrigel plugs consists primarily of "naked" and leaky endothelial tubes with only a limited number of more mature, smooth muscle cell–covered blood vessels, which are typically present at the periphery of Matrigel plugs. The cotransplantation of cells may lead to more mature vessels.[16]
- The assay is highly dependent on an inflammatory response to the Matrigel. Mice with abnormal

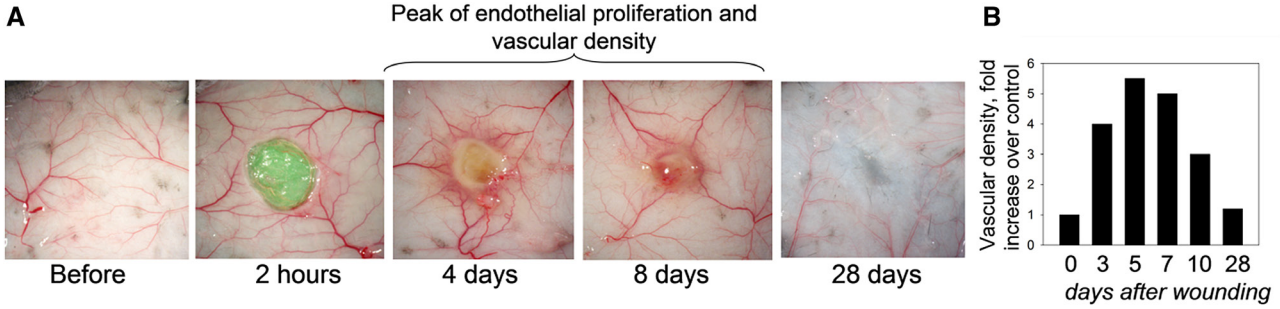

Figure 4. Various stages of punch wound healing in C57/Black6 mice. **A**, The peak of vascularization occurs at days 4 through 8. **B**, Wound tissue was collected at the indicated time points after wounding (0, 3, 7, 10, and 28 days), fixed, sectioned, and stained with CD31 to identify blood vessels. Vascular density in wound tissue sections was measured by ImagePro. Bars show increase in vascular density over control (before wounding).

inflammatory/immune responses may show impaired angiogenesis as a result of this feature.

In addition, to monitor vessel ingrowth, disks or other types of angioreactors have been implanted.[86,87] Angioreactors are silicone cylinders that are closed at one end and filled with a relatively small volume (eg, 20 μL) of matrix premixed with or without angiogenic-modulating factors before they are subcutaneously implanted in the dorsal flank of mice.[86] At 7 to 10 days after implantation, there are enough cells to determine an effective dose response to angiogenic modulating factors. In contrast to Matrigel plugs, which often are not homogeneously distributed in the subcutaneous space, disks or angioreactors have a defined volume and may be better standardized; however, reliability may also be a major problem with these types of assays.

3.4. Tumor Angiogenesis

The critical impact of vascular growth on tumor expansion and metastatic tumor progression has made angiogenesis an important process in tumor biology. The assessment of vessel density is an inherent requirement in the evaluation of tumors. Furthermore, the identification and clinical application of antiangiogenic therapies have required histological, physiological, and metabolic readouts of the vasculature within a tumor.

Vessel density, defined as the number of vessels per area, has been the most frequently used parameter to evaluate the tumor vasculature. Essential questions in assessments of vessel growth and vessel density include the following: Which method should be used to visualize and quantitate tumor vessels? Which method should be used to obtain an accurate representation of average and local vascularity in a tumor? Finally, it is important to note that vessel density is an important angioarchitectural parameter suitable to describe the vasculature in a given tissue. However, vessel density is a static parameter that should not be confused with active angiogenesis, the assessment of which requires the analysis of endothelial turnover, for example, by counting the number of proliferating ECs.

3.4.1. Visualization of Blood Vessels in Tumors

Antibodies to detect platelet EC adhesion molecule (PECAM)/CD31 are the best choice for the identification of tumor-associated vessels because CD31 antibodies are commercially available and relatively easy to use. However, preparation of the sample should be standardized because the antibodies are sensitive to overfixation. Other frequently used antibodies include MECA32, CD105, VEGFR2, and CD34, although some of these do not comprehensively detect vessels in all tumor types.[88,89] However, one should keep in mind that antibodies on sections do not distinguish between occluded and functional (lumenized) vessels.

In addition, intravascular perfusion, particularly with *Lycopersicum esculentum lectin,* frequently preconjugated with fluorophores, has provided investigators a means to visualize vessels and offers information on the functional status of perfused vessels, in addition to providing excellent labeling.[90] However, the perfusion technique can be affected by vascular clotting if not performed correctly.

3.4.2. Morphometric Assessment

Parameters to be considered during morphometric evaluation are what, how and where to count.

3.4.2.1. What to Count

A simple procedure is to evaluate vascular profiles per area (for comparative purposes, profiles per 1 mm^2 is the most appropriate parameter). Other quantification parameters used are the number of vascular branches and vessel diameter. Both should be used in addition to but should not substitute for quantification of vessel density. The quantification of pericytes and other mural cells (smooth muscle cells, astrocytes, and podocytes) in association with vessels has also been included as important maturation criteria.

3.4.2.2. How to Count

In the past, quantification was done by recording the number of times that a vessel crossed a preorganized grid. Today, a number of computer-based programs are readily available (many of these such as the Angiotool, National Institutes of Health, can be downloaded for free). These programs have facilitated the process significantly and improved reproducibility (but not necessarily accuracy). Furthermore, standardization can be achieved, and larger areas can be evaluated. However, these methods rely heavily on the quality of the staining.

3.4.2.3. Where to Count

The selection of sampling and the location of the area(s) are critical to accurately assess vascular density. As Figure 5 shows, some tumors might show what appears to be "hotspots" of vessel growth, whereas others are clearly less dense. As a result of this inherent heterogeneity, selection of one of these areas versus another can yield directly opposite results. Furthermore, areas of contact between tumor and normal tissue are frequently more vascular than areas in the center of the tumor. Thus, sampling a small area is unlikely to provide representative vessel density, and because of these caveats, a broad assessment of the entire tumor mass is a must. This clearly affects the evaluation of human tumor biopsies. Thus, other modalities of vascular assessment (not invasive and relying on broader and repeated evaluation) have also been used. These include computed tomography, magnetic resonance imaging, positron emission tomography, single-photon emission computed tomography, and ultrasound.[91,92] These types of clinical imaging are most applicable to patients, and although they do not offer the degree of sensitivity of optical imaging, they are minimally invasive and safer than repeated biopsies. Therefore, they constitute a valid approach to determine responses to therapy.

3.4.3. Vessel Cooption

Whether a tumor actually recruits its own vasculature by inducing angiogenesis or coopts the existing vascular supply has been subject to controversy.[93] Probably both events coexist; however, from a therapeutic perspective, there are important differences. Angiogenesis involves EC proliferation and migration and 3D vascular morphogenesis, and angiogenic vessels are known to be leaky, poorly covered by pericytes, and more susceptible to antiangiogenic therapies. Coopted vessels, on the other hand, may be stable, have a well-formed basement membrane, and are

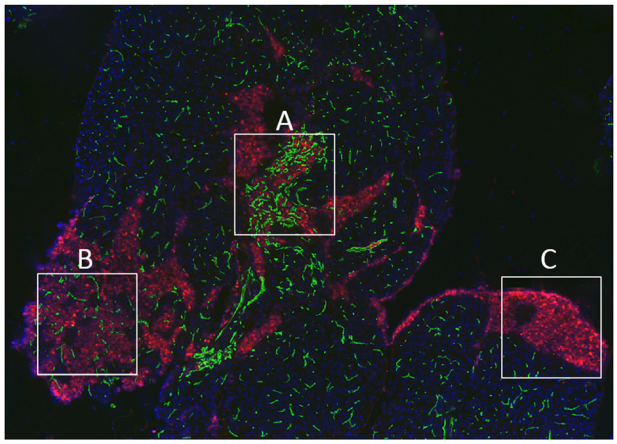

Figure 5. The heterogeneity of tumor vasculature. Confocal microscopy image showing a RIP-Tag insulinoma (endocrine pancreatic cancer) in the pancreas and the degree of vascular invasion. Pancreatic tumor from the Rip-Tag model demonstrating drastic heterogeneity in vascular density (boxes). Areas of very high vascular density (**A**) can be found in proximity to tumor regions with intermediate vascular density (**B**) and apparently avascular tumor zones (**C**). Tumor cells were identified with an antibody against large T-tumor antigen (Tag in red), and vascular profiles were identified with a MECA32 antibody (in green). Courtesy of Liz Allen and Doug Hanahan, EPFL, Lausanne, Switzerland.

well coated by mural cells, making them likely more difficult to target. How can we determine whether the vessels are in fact de novo branches of preexisting vascular beds? The best approach is to use cell cycle markers (Ki67 and phospho-histone H3 antibodies are good choices) and to determine proliferation kinetics (bromodeoxyuridine or similar labels).

3.4.4. Metabolic and Physiological Considerations

Ultimately, the role of blood vessels is to deliver oxygen and nutrients to either normal or pathological tissues. Thus, the level of oxygenation and the metabolic status of tissues have been considered important parameters in the evaluation of an adequate/sufficient or inadequate/insufficient vasculature. The use of "hypoxy-probes," either alone or in combination with hypoxia-inducible factor readouts (transcript or protein), has been a useful approach to indirectly determine the oxygenation status of tissues.[94] More recently, evaluation of glycolysis and glyconeogenesis has also revealed information on the efficacy of the vascular supply. In fact, this information in combination with vessel density is powerful in assessing general changes in metabolic patterns, in addition to vessel status.

3.5. Genetic Tools to Study Angiogenesis

Genetic tools provide important insights into the mechanisms of angiogenesis but can also be used to deliver therapeutic molecules. Because VEGF has been one of the most studied growth factors in this respect, this section illustrates the general methodologies that can be used to overexpress or inhibit gene expression in the context of angiogenesis with VEGF used as an example. The methodologies described below are equally applicable to other angiogenic and lymphangiogenic factors. Of note, various other tools for delivering or inhibiting angiogenic factors (eg, biomaterials, antibodies, VEGF traps) have been developed and are reviewed elsewhere.[95]

Genetic VEGF manipulations can be grossly divided into 2 categories. The first is based on delivery of VEGF-encoding DNA or a modified RNA to induce VEGF gain of function or to interfere with VEGF transcription or translation for VEGF loss-of-function studies. Delivery modes make use of a direct application of the respective nucleic acids, for example, by plasmids,[96] engraftment of ex vivo transduced cells, or, primarily, virus-mediated delivery.[97] The second category includes different transgenic models of VEGF gain of function and loss of function. Whereas the first category might be considered a more relevant approach to eventual implementation of VEGF-based therapies, models of the second category, by virtue of their much greater flexibility, are better suited to elucidate VEGF-related pathogenic mechanisms (Table 3).

3.5.1. Virus-Mediated Delivery of VEGF-Encoding DNA or RNA and VEGF Interfering RNA

Adenoviral vectors, adeno-associated virus–based vectors, and retrovirus, including lentivirus-based vectors, have been used to package VEGF cDNA, and different delivery modes are used to secure optimal transduction of the target organ. Several considerations apply to viral vector selection, including transduction efficacy, a preferential organ tropism, transduction of mitotic versus postmitotic cells, transient versus long-term expression, and adverse effects such as immunogenicity and oncogenic potential. For example, adenoviral vectors have a marked liver tropism, whereas adeno-associated virus vectors with different tropisms can be selected, including those displaying a specific tropism for skeletal muscle cells and cardiomyocytes, which render them particularly suitable for cardiovascular applications. Furthermore, adeno-associated virus vectors have the advantage (or disadvantage) of expressing the therapeutic gene in these cells for indefinite periods.[98] Lentivirus vectors can infect postmitotic cells, whereas vectors based on other retroviruses infect only dividing cells and thus allow a choice of vector suitable for intended VEGF transduction of particular cell subpopulations.[97]

Viral vectors used to transduce VEGF in larger animals, including pig models of myocardial infarction and rabbit models of peripheral vascular disease, can be delivered in a variety of ways. Direct intramyocardial or muscular injection is generally favored over systemic intravenous or intra-arterial injection. Percutaneous selective pressure-regulated retroinfusion revealed favorable results compared with surgical and percutaneous intramyocardial injection techniques.[99] Another methodology of VEGF gene transfer into muscle involves retrovirus-mediated transduction of myoblasts, selection of clones expressing desirable VEGF levels, and injection of those clones into the muscle tissue. This procedure circumvents the heterogeneity of VEGF production after viral transduction in vivo and prevents excessive VEGF production and resultant edema. For VEGF gene transfer to the brain, both adeno-associated virus vectors and lentivirus vectors are being used in conjunction with a stereotactic injection into defined cerebral regions. Replacing DNA vectors, the use of VEGF-encoding synthetic modified RNA was recently introduced.

Table 3. Delivery of DNA and RNA With VEGF as an Example

	Purpose	Transduced/Delivered NA	Route	Features	Examples of Use
Plasmid-mediated delivery	Intended CA and PA therapies	VEGF-encoding plasmids	IM, IMC, TREC	Advantage: Safety, ease Disadvantage: transiency	Clinical trials for CAD and PAD
Modified RNA delivery	Improve heart function	VEGF modified RNA	IMC	Advantage: Sustained effect	Mouse MI model
Adenovirus	Robust VEGF secretion	Different VEGF isoforms	IV, IM, IMC, TREC	Inflammation, hepatotropism	Clinical trials for CAD and PAD
AAV	Sustained VEGF secretion/VEGF inhibition	VEGF/shRNA	IM, IMC, IC, IO	Nonimmunogenic or inflammatory, sustained, postmitotic cell tropism, ease of combinatorial delivery; inducible vectors	VEGF production in preclinical models of myocardial, ocular, and brain angiogenesis, limb ischemia, neurogenesis
Lentivirus	Sustained VEGF secretion/VEGF inhibition	VEGF/shRNA	IM, IMC, IC, IO	Efficient, stable transduction; transduce both dividing and postmitotic cells, inducible constructs	VEGF production in preclinical models of myocardial, peripheral, ocular, and cerebral angiogenesis; VEGF silencing in tumors
VEGF ectopic/ overexpression, conditional	Ectopic/overexpression of VEGF in selected organs or cell types	Different VEGF isoforms	Transgenesis	Organ/cell-type specificity dictated by the choice of driving promoter; temporal controls by tamoxifen inducibility	Conditional VEGF induction in many different organs and by specific cell types therein
VEGF ectopic/ overexpression, conditional and reversible	Ectopic/overexpression of VEGF in selected organs or cell types in a reversible manner	Different VEGF isoforms	Transgenesis	VEGF on and off switching regulated by doxycycline	Distinguishing phenotypes requiring continuous VEGF from “hit-and-run” actions
Transgenic modifications of endogenous VEGF	Replacing endogenous VEGF gene (or its regulatory sequences) with a modified version	A construct targeting the VEGF locus	Gene replacement	Enables precise mutations in both coding and noncoding regions affecting any facet of VEGF biology	Transgenic reporter for endogenous VEGF expression; VEGF hypomorphic alleles; VEGF with altered splicing pattern; hypoxia nonresponsive VEGF (an ALS model)
Conditional VEGF LOF	Precluding endogenous VEGF production	VEGF deletion using the Cre/lox system	Option of delivering Cre via viral infection	Enables VEGF deletion in organ/cell type of choice using floxed VEGF and a tissue-specific Cre recombinase	VEGF deletion in almost every adult organ; uncovers the whole spectrum of nonvascular VEGF functions
Conditional and reversible VEGF LOF	Reversible inhibition of endogenous VEGF signaling	Conditional induction of a transgene encoding a VEGF trap	Inducer added in drinking water	On and off switching of a doxycycline-regulated VEGF decoy receptor	Produce hypoperfused myocardium for modeling ischemic heart disease; study reversibility of phenotypes caused by VEGF blockade or insufficient perfusion

AAV indicates adeno-associated virus: ALS, amyotrophic lateral sclerosis; CA, cardiac angiogenesis; CAD, coronary artery disease; IC, intracerebral; IM, intramuscular; IMC, intramyocardial; IO, intraocular; IV, intravascular; LOF, loss of function; MI, myocardial infarction; PA, peripheral angiogenesis; PAD, peripheral artery disease; shRNA, short hairpin RNA; TREC, transendocardial (catheter-aided); and VEGF, vascular endothelial growth factor.

Direct comparison of myocardially injected modified RNA with DNA vectors in an experimental MI model revealed increased efficacy of the former.[100]

For the purpose of VEGF loss of function, extensive use is being made of viral vectors expressing short hairpin RNA sequences complementary to VEGF mRNA and inhibiting endogenous VEGF production by either targeting its mRNA for destruction or interfering with its translation. The same criteria for selecting vectors and delivery modes discussed above also apply for short hairpin RNA application.

3.5.2. Transgenic Mouse Models of VEGF Manipulation

Because the VEGF dose is exquisitely controlled during embryonic development, with even a small deviation from its normal level of expression during critical developmental stages resulting in early embryonic lethality, transgenic manipulations designed for VEGF overexpression or underexpression ought to be conditional. The most commonly used approaches for conditional VEGF induction are the systems based on either doxycycline-regulated expression of VEGF or tamoxifen-activatable Cre expression.[101] The former is a bitransgenic system composed of a doxycycline-regulated VEGF responder transgene that is activated in trans by a doxycycline-regulated driver transgene in the form of a transactivator protein driven by a tissue-specific promoter. This allows one to induce and, in turn, to deinduce VEGF in the tissue of choice by adding or removing doxycycline to the drinking water ("tet-on" and "tet-off" versions of the system, respectively). A large panel of doxycycline-regulated driver mice is available and allows VEGF induction specifically in almost any organ of choice and on a predetermined time schedule. Using a doxycycline-releasing mini-pump implanted in a pregnant mouse also allows extending VEGF induction to defined developmental time windows with the intention of modeling VEGF-related congenital defects. A significant drawback of the system is the limited ability to control the level of induced VEGF, which may become excessive and result in the formation of an abnormal and leaky vasculature, underscoring the need to uncouple the angiogenic and permeability-promoting activities of VEGF.

Exercising a VEGF on/off manipulation provides an opportunity to distinguish nonvascular from vascular VEGF functions. In these experimental protocols, VEGF is switched off after it has acted to generate a durable vascular network. Phenotypes persisting after VEGF withdrawal can therefore be attributed to effects of the newly acquired vasculature rather than VEGF per se. For conditional VEGF knockouts, a floxed VEGF allele is usually used in conjunction with a tissue specific Cre recombinase to restrict VEGF deletion to the desired tissue or cell type. The use of a tamoxifen-regulated Cre provides temporal control over VEGF nullification. Another approach for VEGF loss of function is based on the doxycycline-regulated model described above in which the responder transgene encodes a soluble VEGF receptor chimeric protein acting as a VEGF trap. A clear advantage of this system is the option of conditional resumption of normal VEGF signaling (using the on/off mode), an impossible option with Cre-mediated VEGF deletion. Variable durations of the VEGF blockade in this system allow escalation in the severity of the ensuing phenotypes, notably the levels of vascular and perfusion deficits that can then be used to model different manifestations of ischemic heart disease.

3.6. Hind-Limb and Coronary Models

Arteriogenesis, the process of the formation of arterial conduits, is a promising therapeutic approach to the treatment of a number of ischemic vascular diseases. The term arteriogenesis refers to development of larger vessels, that is, arterial blood conduits such as arterioles and arteries. Collateral formation represents a specific case of arteriogenesis. By definition, collateral vessels provide artery-to-artery connections and are thought to play a protective role by providing alternative routes to blood flow.[102]

3.6.1. Brief Description of Arteriogenesis

Arteriogenesis takes place during embryonic development, but it can also occur in adult tissues. In the latter case, arteriogenesis typically occurs at sites of occlusion (atherosclerosis) or physical disruption (eg, ligation, trauma) of preexisting arterial conduits. It can also occur in growing organs (eg, myocardial hypertrophy) or tumors. Molecular signals and processes responsible for arteriogenesis are poorly understood and are subject to considerable controversy. The 2 most commonly considered mechanisms are the expansion of preexisting collaterals and de novo arteriogenesis.[103] Clearly, both scenarios can produce new arteries, but their contribution varies, depending on the experimental model tested.

It is widely thought that a larger number of preexisting collaterals serves as a predictor of better flow recovery after ligation of a major arterial trunk. Indeed, mouse strains with higher numbers of collaterals show better blood flow recovery after common femoral artery ligation than mouse species with fewer collaterals.[104] Similarly, among larger animals, a higher number of visible preexisting collaterals predicts better recovery. This is an important consideration because studies in humans have demonstrated a wide variability in the extent of preexisting, recruitable collaterals and suggested a protective clinical role of preexisting collaterals.[105] However, more recent studies demonstrated that not all preexisting collaterals are equal and that, under certain circumstances, a larger number of collaterals does not improve or might even worsen the outcome of an acute arterial occlusion (eg, see the work by Skuli et al[106]).

3.6.2. Hind-Limb Ischemia Models: General Considerations

Hind-limb ischemia models are typically performed in smaller species (mice, rats), although studies have also been conducted in larger animals (rabbits, pigs). There are 2 distinct versions of hind-limb ischemia models: a less severe collateral remodeling model that results in proximal arterial flow restriction but no rest ischemia in the distal limb and a more severe model that leads to severe rest ischemia that may result in a certain amount of tissue loss.[107,108] Blood flow recovery in both of these models is thought to be dependent primarily on arteriogenesis, with most new arteries forming above the site of ligation, although arteriogenesis also takes place below the knee. Some flow recovery is undoubtedly attributable to angiogenesis in the ischemic part of the limb. Unfortunately, the exact contributions of neovascularization in these 3 sites to the total flow recovery have never been accurately defined.

As alluded to above, the extent of arteriogenesis in this model is heavily dependent on the mouse or rat strain and the species being used.[104] Whereas C57Bl6 mice recover almost fully without any therapeutic interference, other mouse strains (eg, Balb/C) and rabbits do not.[104,109] However, genetic components responsible for these differences have not been identified. Other key parameters affecting blood flow recovery include the age of the animals (reduced in older animals)[110] and the presence of atherosclerosis or diabetes mellitus.[111] It is important to keep in mind when hind-limb ischemia models are being used that, although they are excellent for studying

the mechanisms of neovascularization, they have significant limitations as a readout for potential therapeutic agents because results obtained through experimental testing in young, healthy animals does not readily translate into efficacy in older patients with systemic vascular diseases.

3.6.2.1. Hind-Limb Ischemia Models: Readouts

The key readouts of the model include blood flow recovery in the ischemic foot, the extent of arteriogenesis above and below the knee, and the extent of angiogenesis in the calf. Additional readouts may include vasodilator reserve, the extent of mononuclear cell infiltration of ischemic and nonischemic tissues, and changes in gene expression of key molecules involved in arteriogenic and angiogenic responses.

The most critical functional readout of the assay is the extent and time course of blood flow recovery in the ischemic foot. This is usually accomplished with the use of a deeply penetrating laser Doppler positioned on the skin to determine a ratio of blood flow in the ischemic foot and normal foot.[107] Occasionally, a Doppler probe positioned directly over the blood vessel of interest is used. The method, although seemingly simple, is subject to many factors that can affect the readout, including the temperature of the animal and the extremities, depth of anesthesia, choice of anesthetic, and quantification of the Doppler images. It is important to assess blood flow not only at a given time point but also over a period of time. Typical time points include flow determination immediately after ischemia induction and then at 3, 7, and 14 days. In some cases, it may be necessary to extend the experiment for 3 or 4 weeks, in which case additional flow measurements should be made.

In addition to flow assessment, the extent of arteriogenesis should be directly quantified. Micro–computed tomographic (CT) imaging has emerged as a gold standard, given its high resolution and the quantifiable nature of the images (Figure 6). However, the technique is not straightforward and requires accurate filling of the distal arterial bed with a contrast agent without this agent entering capillaries and the venous circulation. Underfilling is also a common problem and may substantially affect quantification.[112] In general, all animals should be processed on the same day to minimize variability. Other imaging modalities, including magnetic resonance (MR) angiography and high-resolution x-ray angiography, can be used, but they lack the resolution of a micro-CT image.

Histological assessment of arteriogenesis also is sometimes used by staining with smooth muscle cell markers such as α-smooth muscle actin followed by quantification of vessel diameter (grouped by size, eg, <50, 50–100, >100 μm). The key challenge is a large variability in arteriolar density between different muscle groups or even different sections within the same muscle group. In all cases, a sufficient number of sections should be counted, and the assessment should be carried out by investigators blinded to the genetic or treatment group to which the animal under study belongs.

3.6.3. Ameroid Constrictor and Reduction Stent Models

Ameroid occluders are used to induce gradual occlusion of a coronary artery, creating a collateral-dependent myocardial territory. Although ameroid occluders have been used in both dogs and pigs, pigs are the preferred model, given the relatively small abundance of coronary collateral circulation. If done correctly, with the occlusion developing over 5 to 7 days, there is only a minimal area of left ventricular (LV) wall necrosis (myocardial infarction). Coronary angiography demonstrates peri-ameroid collaterals that are sufficient to maintain baseline myocardial perfusion under normal but not stress (exercise or pacing) conditions. Functional studies demonstrate normal global and regional LV function at rest and regional myocardial dysfunction under stress conditions.

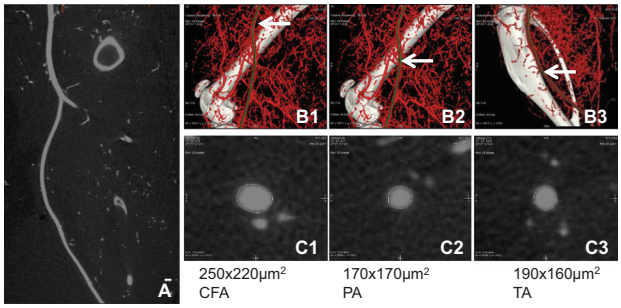

Figure 6. Multiplanar images for quantitative angiogram in the hind limb in mice. The curved image shows the whole course of the conduit artery in the normal leg (**A**). Three-dimensional micro–computed tomographic images indicate the locations of the representative vessels with a **white arrow** (**B1**–**B3**). Two-dimensional axial images show the sizes of the vessels in **B1** through **B3** images of the common femoral artery (CFA), popliteal artery (PA), and tibia artery (TA; **C1**–**C3**). Bar indicates 200 μm in **A**.

The principal mechanism of adaptation to the ameroid occlusion in pigs is de novo arteriogenesis. Although pigs demonstrate de novo arteriogenesis, there are a small number of preformed collaterals; the principal development here is the formation of peri-ameroid collaterals, although large epicardial collaterals from normal to ischemic territory have also been observed. Angiogenesis is also observed in the ameroid territory; its contribution to overall flow restoration in this model is considered minimal, but there are no extensive quantitative studies documenting this.

The ameroid model is typically carried out in young (≈6 weeks old) Yorkshire pigs, with animals nearly doubling in size during the experimental period (from ≈40 to 80 lb). This growth clearly complicates data interpretation because any collateral growth is superimposed on the normal coronary artery growth process that also occurs during this period. Alternatively, minipigs and microswine have been used for these studies. These animals are substantially smaller than Yorkshire pigs, but they still tend to be used when fairly young, at 2 to 3 months of age. Very little ameroid work has been done in atherosclerotic pigs. Consequently, as with rodent hind-limb ischemia models, the data are more suitable for mechanistic than therapeutic studies.

Alternatively, percutaneous implantation of a reduction stent graft has been used to decrease blood supply over the long term.[113] Therefore, stents are implanted into the left anterior descending artery (LAD) but are not fully expanded, resulting in an initial stenosis of 75% of the luminal diameter that progressively develops into a (sub)total occlusion of the LAD and hibernating myocardium at day 28.

3.6.3.1. Ameroid Constrictor and Reduction Stent Models: Readouts

A number of techniques are used to assess both the anatomical extent of blood flow recovery and its functional impact. Blood flow improvement in the ischemic zone is typically assessed with microspheres (radioactive or colored), although MR imaging has also been used. Functional improvement is assessed with 2-dimensional echocardiography to obtain indexes of regional and global LV function.

3.6.4. Acute Coronary Occlusion Models

There are several models in both small[114-117] and large animals[118-121] in which a major coronary artery or multiple branches are occluded for the specific purpose of inducing significant myocardial ischemia and infarction for the subsequent analysis of neovasculogenesis and arteriogenesis in response to experimental therapies (Table 4). These models can entail permanent occlusion or a prolonged occlusion followed by reperfusion.[122] The result is an area of myocardial necrosis and, in some models, an ischemic border zone around the infarct territory. Regional or even global myocardial contractile function is usually impaired. Adverse ventricular remodeling also occurs over a period of time, leading, in the case of extensive myocardial damage, to the development of heart failure.

The small animal coronary occlusion model typically uses either mice or rats. In both models, the LAD is ligated to create an extremely reproducible and survivable 35% LV infarct. The advantage of mice is the availability of a wide range of transgenic animals, along with the development of LV remodeling and heart failure within 2 to 4 weeks. Mice, however, pose a relative technical challenge compared with rats in terms of intubation and LAD ligation. Rats remodel and develop heart failure in 4 to 6 weeks. This model can be used in both an acute and chronic approach. An intervention, whether it directly involves the myocardium or systemic administration of an agent, can be initiated immediately after infarction[123] or several weeks postoperatively[124] to model a more chronic process. The major limitation of this model is that open access to the myocardium is needed for intervention, which does not directly translate to the majority of clinical scenarios.

The small animal reperfusion model is similar to the permanent ligation model except that the LAD is occluded temporarily, typically for 30 to 90 minutes, followed by a comparable reperfusion period.[125,126] When cats or rabbits are used rather than mice or rats, the ischemia and reperfusion periods tend to be somewhat longer. Additionally, the LAD is occluded just distal to the first diagonal.[127,128] The intervention can be performed at any time point but commonly occurs just before and after reperfusion.

The large animal acute coronary occlusion model can be accomplished via embolization,[129,130] microspheres,[131] balloon,[132] and ligation.[118-120] Canine, ovine, and porcine models are described extensively in the literature. With the embolization or microsphere approach, 4 to 14 injections are typically required until the reduced goal ejection fraction is achieved. Global LV ischemia occurs without a localized area of infarction. The mortality is high at 30% to 50%, but the advantage of this model is its utility in creating chronic LV dysfunction for up to 6 months. The coronary ligation approach possesses the ability to model both myocardial and valvular pathology. In sheep, it is possible to induce an acute LV infarct followed by LV thinning, aneurysm formation, and heart failure over an 8-week period by ligating the distal LAD and second diagonal. Chronic ischemic mitral regurgitation can be modeled over 8 weeks in the sheep by ligating the second and third circumflex oblique arteries. Acute severe mitral regurgitation can be induced in 1 hour by ligation of the second and third circumflex oblique arteries combined with the posterior descending artery. Overall, the ovine coronary occlusion approach can model a variety of cardiac pathologies. Potential interventions at various time points include systemic and localized cell-based therapy, cytokine-based therapy, and mechanical devices.

For large animal reperfusion, the common models are canine and porcine. In the canine model,[122] the LAD is occluded for 60 to 90 minutes just distal to the first diagonal, and reperfusion is allowed for ≥4 hours. Function and histology have been assessed up to 48 hours after the procedure. The model is frequently used to assess biochemical and antioxidant therapies.[133] An alternative to this approach is the repetitive ischemia canine model in which the left circumflex is briefly occluded for 2 minutes at 30- to 60-minute intervals.[134] This model has been used to evaluate collateral growth and recently been scaled down to a small animal model.[135] In the porcine model,[136] the LAD is balloon occluded just distal to the second diagonal. Ischemia and reperfusion times are similar to those in the canine model and evaluate similar therapeutic approaches.

Overall, these permanent occlusion and ischemia-reperfusion models are usually used to establish a framework in which molecular, cellular, genetic, and tissue engineering experimental therapies are evaluated for their efficacy in both restoring perfusion in the border zone and improving regional and global LV function. Myocardial regeneration is also often examined in this context.

3.6.4.1. Acute Coronary Occlusion Models: Readouts

There are a multitude of methodologies for data collection in these models, including but not limited to microsphere assessment of blood flow, determination of oxygen tension, echocardiography, MR imaging, angiography, and invasive pressure-volume hemodynamic assessment. Additionally, standard histology, immunohistochemistry, and genetic analyses are frequently performed to assess gross and biomolecular changes.

Microsphere assessment is accomplished by injection of radiolabeled microspheres, frequently directly into the left atrium, followed by assessment of the myocardium by the use of gamma counters to measure tracer decay, correlating to regional perfusion.[137] Extending from this, regional oxygen tension can be assessed by intramyocardial injection of a phosphorescent probe that is quenched by oxygen. Briefly, the phosphorescent decay is optically measured and correlated to oxygen tension.[138] Echocardiography is readily available in both small and large animal models for geometric analysis of LV dimensions, along with functional evaluation of ejection fraction and fractional shortening. Cardiac MR imaging can play a significant role in demonstrating 3D ventricular geometry, intraventricular flow, global function, regional strain, and even biochemical changes.[119,139] Angiography can be implemented in large animal models with Rentrop scoring used to evaluate vascular collateralization.[119] Invasive LV

Table 4. Mammalian Models for Testing Neovascularization

Model	Species	Technique	Outcome
Acute coronary ligation	Sheep	Distal LAD and second diagonal	LV infarct expansion by 4 h followed by LV thinning over 2 mo and development of CHF
Acute coronary ligation	Sheep	Second and third marginal of Cx	20% PW MI
			Chronic mitral regurgitation
Acute coronary ligation	Sheep	Second and third marginal of Cx and PDA	40% PW MI
			Severe mitral regurgitation <1 h
Acute coronary ligation	Rat	Proximal LAD	AW MI and CHF in 3–6 wk
Acute coronary ligation	Mouse	Proximal LAD	AW MI and CHF in 2 wk
Ischemia/reperfusion	Dog	Ligation of LAD distal to first diagonal for 90 min, 4 h of reperfusion	LV function at 48 h
			Histology at 48 h
Ischemia/reperfusion	Baboon	Ligation of LAD distal to first diagonal for 120 min, 60 min of reperfusion to 1 wk	LV function, ischemic-zone wall thickness, regional myocardial blood flow, arrhythmias, infarction
Ischemia/reperfusion	Rabbit	Ligation of LAD distal to first diagonal for 90 min, 120 min of reperfusion	Hypokinesis at 10 min after reperfusion
			LV dysfunction and infarct evaluation/histology at 4 wk
Ischemia/reperfusion	Mouse/rat	Snare proximal LAD occlusion for 30 min, 30 min of reperfusion	Immediate LV dysfunction and histological changes
Repetitive ischemia	Dog	Occlude LCx for 2 min at 30–60 min intervals	Stimulation of collateralization
Repetitive ischemia	Rat	Occlude proximal-mid LAD for 40 s at 20-min intervals; repeated for 10 d	Stimulation of collateralization
Ameroid	Dog	Proximal LAD	CHF within 60 d
Ameroid	Pig	Proximal Cx	Chronic ischemia in 3 wk
Embolization	Dog	Intracoronary sequential latex microsphere injection until EF 35%	Global ischemia, no localized MI; 30%–50% mortality
Embolization	Sheep	Sequential intracoronary 90-μm microsphere injection until EF of 35%	4 and 26 wk after CHF establishment: LV end-systolic elastance, preload recruitable stroke work
Reduction stent	Pig	Percutaneous implantation of a reduction stent in the LAD (75% stenosis)	(Sub)total occlusion of the LAD and hibernating myocardium at day 28, functional analysis at day 49

AW indicates anterior wall; CHF, congestive heart failure; Cx, circumflex artery; EF, ejection fraction; LAD, left anterior descending artery; LCx, left circumflex; LV, left ventricular; MI, myocardial infarction; PDA, posterior descending artery; and PW, posterior wall.

hemodynamic measurements are acquired with the use of a pressure-volume catheter. The catheter is preferably introduced into the LV in a closed chest, frequently via the right carotid artery. This approach is widely used in both small and large animal models.

3.7. Carotid Remodeling

Carotid artery remodeling is a complex physiological process governed by hemodynamic alterations and multicellular responses. The integral need for remodeling has been well defined by Mulvany and Glagov (whose principles are now commonly called the Glagov law). Their collective works state that a blood vessel undergoes compensatory morphological changes via either inward or outward remodeling to maintain a physiological state of blood flow. Vessel remodeling is typically associated with pathophysiological conditions such as atherosclerosis; however, it is also important for arteriogenesis and vessel maturation. The demand on the vessel wall to grow, thereby regulating a homeostatic environment, is controlled primarily by a balance between EC, vascular smooth muscle cell, inflammatory cell, and progenitor cell signaling. In response to stimuli such as changes in blood flow, EC damage, or inflammation, vessel wall thickness either increases (outward) or decreases (inward with narrow lumen) in size (Figure 7). Both situations involve dynamic extracellular matrix remodeling and vascular smooth muscle cell and progenitor cell migration, proliferation, and apoptosis.

The degree and type of remodeling that occurs are highly complex and largely governed by genetic factors and the extent of vascular perturbation. Several animal models have been designed to better study carotid remodeling processes. Each model presents advantages and disadvantages in terms of large vessel remodeling. Table 5 summarizes the advantages, limitations, and challenges of current animal models.

4. Special Issues

4.1. Lymphangiogenesis: Developmental and Therapeutic Models

4.1.1. Lymphangiogenesis During Development

For the analysis of lymphangiogenesis during mouse development, whole-mount immunofluorescent imaging is more informative than standard immunohistochemistry and allows better simultaneous interrogation of the tissue microenvironment and cellular interactions.[148] Lymphatic vessels can also be imaged in vivo by the use of one of several mouse lines in which lymph vessels express a fluorescent reporter or luciferase (Table 2). Ultramicroscopy has provided the most detailed

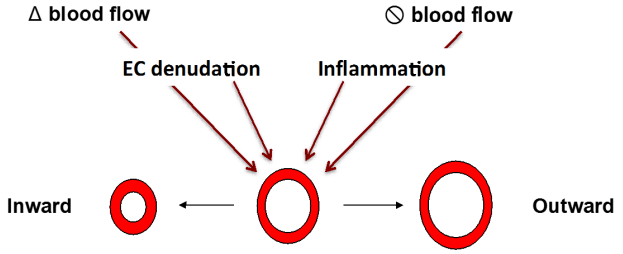

Figure 7. Carotid remodeling. Vascular perturbations in the form of changes (Δ) in blood flow (ie, turbulent or low shear stress), blood flow cessation, endothelium damage, or inflammation induce vascular wall remodeling. The vessel wall either increases (outward) or decreases (inward) in size. The extent and degree of remodeling are governed by the type of perturbation. EC indicates endothelial cell.

views of the earliest steps in the formation of lymphatic vessels in mouse embryos.[28] Identification of lymphatic ECs requires the use of several markers such as VEGFR3, Prox1, Lyve-1, and podoplanin[89] (Table 6). After midgestation, lymphatic vessels can be visualized best in the skin and in the mesenterium, where lymphangiogenic sprouting, EC proliferation, and collecting lymphatic vessel maturation, including recruitment of smooth muscle cells, deposition of basal lamina components, and valve formation, can be discerned.[149,150] Postnatally, lymphatic vessel development can be visualized in ventral and tail skin[151,152] and in the mesentery.[153] In late postnatal and adult mice, the ear skin represents the best tissue to simultaneously visualize lymphatic capillaries and collecting vessels.[148,150]

Key steps in lymphangiogenesis and lymphatic vascular diseases can be evaluated in a number of mouse mutants.[154] Genetic models are available for the most direct acting, and specific growth and transcription factors include deletion of VEGF-C, collagen- and calcium-binding EGF domain protein-1, neuropilin-2, Sox18, Prox1 or FoxC2 transcription factors, and missense point mutation of VEGFR3 and include transgenic mice expressing a soluble form of VEGFR3. Mutations in VEGFR3, VEGF-C, collagen- and calcium-binding EGF domain protein-1, Sox18, and FoxC2 have been found to be associated with human lymphedema.[155]

4.1.2. Therapeutic Lymphangiogenesis

Therapeutic manipulation of lymphangiogenesis aims at repair of damaged or malfunctioning lymphatic vessels to alleviate lymphedema or inhibition of pathological lymphangiogenesis and lymphatic metastasis. Experimental models of primary lymphedema include VEGF-C heterozygous[156] and VEGFR3 missense point mutant mice,[157] and models for secondary lymphedema include incision of mouse tail[158] or rabbit ear[159] and excision of lymph nodes and associated vessels in mice and pigs.[160,161] Preclinical studies so far have used gene therapy for the induction of lymphangiogenesis, vessel remodeling, and maturation. Adenoviral expression of VEGF-C is transient but results in the proliferation of lymphatic capillaries, which mature functionally and can undergo differentiation into collecting lymphatic vessels.[160] The efficacy of VEGF-C–induced lymphangiogenesis may be boosted by simultaneous administration of a vector encoding the collagen- and calcium-binding EGF domain protein-1.[162] The use of lymphangiogenic growth factor proteins is hampered by their fast redistribution and short half-life in tissues. Tissue transplantation, including lymph nodes from uninvolved areas, with the promotion of lymphatic vessel reconnection has been used to re-establish functional lymphatic vessels.[163] Lymphatic function can be imaged by fluorescent lymphangiography in which vessel size and the smooth muscle contractions that allow the lymphatic pump function can be quantified.[164] Molecular clearance analysis, for example, using labeled albumin and interstitial tissue pressure, provides a complementary analysis of fluid homeostasis in tissues with compromised lymphatic vessels.[165]

Lymphangiogenesis-blocking agents such as antibodies targeting VEGF-C, VEGFR3, or its coreceptor neuropilin-2, as well as soluble VEGFR3 and certain tyrosine kinase inhibitors, have been found to inhibit lymphatic metastasis in xenotransplanted tumors and in transgenic mice. Such experiments commonly use luciferase- or green fluorescent protein–expressing tumor cells that can be imaged in the target tissues.

The mouse trachea provides a convenient tissue model to analyze inflammatory lymphangiogenesis induced by mycoplasma infection in which various modulators can be tested.[166] Recent results suggest that inflammatory bowel disease models also involve lymphangiogenesis, which can be monitored in the gut wall.[167]

4.2. Assessment of Vascular Permeability

Depending on its host organ, the vascular endothelium has structurally distinct barrier functions that are adapted to local microenvironmental needs (continuous endothelium, discontinuous endothelium, fenestrated endothelium). When serving as a barrier between the bloodstream and the interstitium, the endothelium controls the transport of fluids and hydrophilic solutes and the transfer of cells across the vascular wall. Vascular and, in particular, microvascular permeability refers to the transport to and from the circulation of fluid and solutes by transcellular transport through the endothelial layer and by regulated opening of intercellular junctions. The basal permeability of normal microvessels can be distinguished from increased microvascular permeability because the latter occurs, for example, during the early stages of acute inflammation. Likewise, regulated permeability needs to be discriminated from uncontrolled vascular leakage resulting from microvascular damage.[168]

Vascular permeability can be studied in vitro and in vivo. Cellular assays use confluent layers of cultured ECs grown between the 2 compartments of a transwell system. Readouts of permeability and barrier function in these assays are the transfer of dye from one compartment to the other or the analysis of electric resistance as a measure of endothelial barrier function.[169] Both approaches can be considered suitable in vitro surrogates of permeability. However, generally speaking, the barrier function of isolated endothelial monolayers devoid of their microenvironment (extracellular matrix, pericytes, luminal fluid shear stress) tends to be substantially lower than in comparable conditions in vivo.

A plethora of assays have been developed to measure specific physiological permeability parameters such as fluid filtration,

Table 5. Models of Carotid Remodeling*

Model	Animal	Insight	Advantages	Disadvantages	Reference*
Aortic banding	Mouse	Carotid remodeling results from changes in pulsatile pressure and turbulent blood flow Hypertensive model	Provides a correlative and mathematical analysis of the effects of pulsatile pressure There is less neointimal formation	Data obtained in mice cannot be easily extrapolated to humans because of differences in cardiac output and function	140
Adventitial $FeCl_3$ and $CaCl_2$	Rat, mouse	External application to the vessel wall Induces remodeling with significant inflammation	Technically easy Remodeling is mediated by inflammation	Thrombus formation occurs and influences vessel remodeling Severe injury model	141
Arteriovenous fistula	Rat, mouse, rabbit	EC-mediated response to high shear stress	Large adaptive outward remodeling	Stenosis development and reduced long-term vessel patency	142
Balloon angioplasty	Rat, pig, rabbit	EC denudation induces significantly enhanced VSMC proliferation and dynamic ECM remodeling	VSMC signaling response and neointimal hyperplasia are consistent Rat models are well developed and characterized	Not technically reproducible Balloon injury in mouse carotids is difficult	143
Complete carotid ligation	Mouse	Primarily VSMC-mediated remodeling Extent of remodeling is determined by length of blood flow cessation	Highly reproducible Technically easy to perform Phenotype primarily governed by blood flow cessation and not surgical manipulation	Thrombus formation can occur and influence vessel remodeling beyond blood flow cessation	144
Partial carotid ligation	Rat, mouse rabbit	Primarily VSMC-mediated remodeling Extent of remodeling is determined by both percent reduction and length of blood flow cessation	Highly reproducible Preferable to complete ligation to study physiological remodeling in response to low blood flow Inward and outward remodeling is genetically determined Less likelihood of thrombus and vessel occlusion	Rats and rabbits form less neointimal hyperplasia and remodeling relative to mice Anatomic variation among mouse strains can affect blood flow reduction after ligation	144, 145
Photochemical exposure	Rat, mouse	Internal application causes endothelium injury Induces remodeling with significant inflammation	Remodeling is specifically mediated by inflammation More subtle injury compared with $FeCl_3$ and $CaCl_2$	Severe injury model	146
Wire injury	Rat, mouse, rabbit	Remodeling is a result of EC denudation Neointimal formation ceases after re-endovascularization	Re-endovascularization occurs symmetrically after EC denudation	Technically challenging Thrombus formation and subsequent lesion development are common	147

EC indicates endothelial cell; ECM, extracellular matrix; and VSMC, vascular smooth muscle cell.
*Only representative references are provided.

hydraulic conductivity, solute permeability coefficient, and osmotic reflection coefficient.[170] The most widely used in vivo assay to measure permeability is the Miles dye transfer assay.[171] In this assay, an inert dye is intravenously injected into mice and allowed to systemically circulate. This assay originally used Pontamine Sky Blue but nowadays mostly uses the 961-Da molecule Evans Blue, which strongly associates with albumin. Baseline permeability in different organs can be measured after a specific time period by dye extraction from isolated organs after washing out of the circulating dye.[172] This approach can, for example, be used to comparatively study baseline permeability in wild-type and genetically engineered mice. To analyze induced hyperpermeability, the Miles assay can be used by locally injecting a permeability-inducing compound into a dye-loaded mouse, followed by quantification of extracted dye from tissue at the application site.[173]

Table 6. Markers of Endothelial Cells

Markers	Comments
Pan endothelial markers	
CD31	Also expressed in inflammatory cells
	Some of the commercial antibodies will require epitope unmasking
Isolectin B4	Also binds to microglia/inflammatory cells
	Works only in mouse
	Can be used to visualize perfused vessels after systemic intravenous infusion
Lycopersicum esculentum	Mouse and human
	Works well when perfused in the circulatory system because it binds to the inner surface of the endothelium
VEGFR2	Is also expressed in hematopoietic cells and in some tumor cells
	Binds better to arterial ECs than vein ECs but is present in both and in capillaries
	Also labels retinal neurons
VE-cadherin	Specifically stains ECs
ZO-1	Labels EC junctions
Claudin5	Labels EC junctions
CD34	Also expressed in hematopoietic stem cells
	Works particularly well in human tissue and to detect transplanted human cells in mice (spheroid model)
Arterial EC markers	
Ephrin B2	Preferentially stains arterial ECs
Neuropilin-1	Preferentially stains arterial ECs but also is expressed on other cells (eg, neurons)
UNC5B	Similar to Nrp1 but no labeling of neurons
Cx40	Expressed only on arterial ECs
Sox18	Should be used only in combination with other EC markers
Venous EC markers	
EphB4	Preferentially labels venous ECs
Neuropilin-2	Preferentially labels venous ECs; also labels lymphatic ECs on tissue sections
LEC markers	
Prox1	Most genuine LEC marker, not expressed by brain ECs
	Highly expressed by lymphatic valves and capillaries, less by lymphangiomas
	Expressed also by some venous ECs in embryonic or postnatal intestines/mesenteries, but staining is weaker compared with LECs
	Expressed by all LECs in vitro
	Also expressed by certain cancer cells, lens epithelial cells, some neuronal cells, hepatocytes, pancreas, adrenal medulla, megakaryocytes, platelets, skeletal and cardiac muscle cells, venous valves, cardiac valves
Lyve1	Expressed by lymphatic capillaries but not collecting vessels
	Also expressed by certain embryonic blood vessels and activated macrophages
Vegfr3	Expressed mostly by LECs, in lymphatic capillaries and collecting vessels
	Also expressed in certain blood vessels during embryogenesis and angiogenesis, fenestrated endothelium and high endothelial venules, certain neuronal cells, monocytes/macrophages, and megakaryocytic progenitors
Podoplanin	Expressed by lymphatic vessels
	Also expressed by kidney podocytes, some tumor stromal cells, fibroblastic reticular cells in LNs, among other cell types
Itga9	Marks lymphatic valves
FoxC2	Marks lymphatic valves
Podoplanin	Expressed by lymphatic vessels
	Also expressed by kidney podocytes, some tumor stromal cells, fibroblastic reticular cells in LNs, among other cell types

EC indicates endothelial cell; LEC, lymphatic endothelial cell; and LN, lymph node.

The Miles assay with its various modifications is a useful readout for extravasation. However, there are limitations that need to be considered. Most notably, the distribution of intravenous tracers is affected by hemodynamics; that is, a permeability-inducing compound such as VEGF may also cause vasodilation, which results in an increase in vessel surface area and blood flow volume, both of which will affect the amount of extravasated dye. Moreover, to reduce baseline permeability in local induction experiments, baseline permeability is quenched in many studies by antihistamine pretreatment of the experimental animals, which must be taken into consideration in the interpretation of the results.

An alternative method to measure permeability is the tracheal microsphere assay.[173] In this assay, mice are systemically loaded with microspheres of a defined size. After injection of a permeability-inducing agent, tracheas are harvested, and the associated vasculature is analyzed by whole-mount techniques, allowing direct morphological analysis of extravasated microspheres, which are trapped by the periendothelial extracellular matrix.

High-resolution morphological techniques are also useful to study in detail the mechanisms of vascular permeability and leakage. Dye transfer techniques measure only the net outcome of extravasation, whereas morphological techniques (including electron microscopic tracing techniques) enable the detailed analysis of transcellular versus pericellular mechanisms. For dynamic analysis, intravital microscopy techniques, including high-resolution 2-photon techniques, and noninvasive near-infrared imaging have proven useful.[174,175]

4.3. Evaluation of Microvascular Function, Perfusion, and Angiogenesis Imaging

Although it is possible to directly measure certain aspects of vascular growth, for example, collateral development with the use of angiography, these techniques are invasive. Angiography has also been used to estimate microvascular function and microvascular growth.[176,177] A limitation of this approach is that only measurements of vasodilator reserve are obtained, not measurements of volume flow. Vasodilator reserve can be affected by downstream angiogenesis and influenced by the basal tone of the vasculature. Indirect measures of tissue perfusion, hypoxia, or metabolism can be used (under certain conditions) to provide estimates of vascular growth. Measurements of perfusion during maximal dilation can provide an assessment of minimal vascular resistance, the quotient of perfusion pressure and flow, which can reflect vascular growth at the capillary and arteriolar levels.[178-180] For optimization of this approach, the circulation of the organ must be maximally dilated, and perfusion must be quantified in units of flow per mass of tissue. However, to provide estimates of minimal resistance (or maximal conductance, the reciprocal of minimal resistance), the investigator must implement an intervention to provide maximal dilation, along with simultaneous measurements of arterial pressure, with invasive or noninvasive methods. Impaired vascular growth or rarefaction of vessels can be identified as increased minimal resistance or decreased maximal conductance.[181]

Noninvasive imaging strategies are critical to define the in vivo spatial distribution and temporal characteristics of angiogenesis and arteriogenesis and to assess the efficacy of angiogenic therapies in preclinical animal models. Standard noninvasive imaging strategies have focused on the evaluation of the physiological changes in tissue hypoxia, perfusion, or vascular permeability associated with angiogenesis; however, these strategies may not be sensitive enough to evaluate early changes in vascularization in animal models used to evaluate angiogenesis. There has been a push to develop more sensitive and specific imaging strategies that can directly evaluate angiogenesis and track this process noninvasively. Molecular targeted imaging of angiogenesis has focused on EC targets (eg, VEGF, growth factor receptors, integrins, CD13, cell adhesion molecules), extracellular matrix proteins, and matrix proteases, or even associated non-EC targets (eg, monocytes, macrophages, and stem cells), and has been reviewed recently.[182-184]

Several imaging modalities have been applied to evaluate angiogenesis and arteriogenesis in preclinical experimental animal models and are summarized in Table 7. Optical imaging approaches, in particular laser Doppler, have traditionally been used to evaluate changes in superficial perfusion associated with angiogenesis in models of hind-limb ischemia. This approach is technically challenging, is affected by environmental conditions, and generally is less effective for evaluating the angiogenic process in deeper structures like the heart. Ultrasound imaging has also been applied to assess angiogenesis for the evaluation of tissue perfusion both with and without molecular targeted imaging. Contrast echocardiography has been used extensively to measure blood flow in many organ systems.[212-214] Molecular imaging with ultrasound relies on the application of targeted contrast agents. Contrast-enhanced ultrasound is performed by the acoustic detection of microbubble or gas-containing nanoscale contrast agents that remain within the intravascular compartment but can be targeted to EC markers.[184] Peripheral angiogenesis can be tracked in a rodent model of hind-limb ischemia with the use of a microbubble contrast agent with conjugated arginylglycylaspartic acid (RGD)-bearing echistatin that targets integrin activation.[198] Other investigators have used microbubbles to

Table 7. Methods for the Evaluation of Perfusion and Molecular Imaging of Angiogenesis

	Perfusion/Blood Flow	Angiogenesis
SPECT imaging	^{201}Tl[185]	^{111}In-RP748[186]
	^{99m}Tc-sestamibi[186]	^{99m}Tc-NC100692[187]
	^{99m}Tc-tetrofosmin[147]	^{111}In-VEGF$_{121}$[188]
		^{125}I-c[RGD(l)yV][189]
PET imaging	^{15}O-water[190]	^{76}Br-nanoprobe[191]
		^{68}Ga-NOTA-RGD[192]
	^{13}N-ammonia[193]	^{64}Cu-DOTA-CANF-comb[194]
		^{64}Cu-NOTA-TRC$_{105}$[195]
		^{64}Cu-DOTA-VEGF$_{121}$[196]
Ultrasound imaging	Microbubble contrast[197]	Echistatin microbubble[198]
		P-selectin microbubble[197]
		VCAM-1 microbubble[199]
		ICAM-1 microbubble[200]
MR imaging	Gd-DTPA[201]	Integrin/nalectin-1[202]
		RGD nanoparticle[203]
Optical imaging	IVM[204]	cNGR/CD13[205]
	Laser Doppler[206]	VCAM-1[207]
		$\alpha v\beta 3$[208]
		VEGF[209]
Photoacoustic imaging	Oxygen saturation[210]	$\alpha v\beta 3$-GNBs[211]

ICAM-1 indicates intracellular cell adhesion molecule-1; IVM, in vivo microscopy; MR, magnetic resonance; PET, positron emission tomography; RGD, arginylglycylaspartic acid; SPECT, single-photon emission tomography; VCAM-1, vascular cell adhesion molecule-1; and VEGF, vascular endothelial growth factor.

target activated neutrophils, VEGF, and vascular cell adhesion molecule-1.[199]

MR imaging has also been applied to evaluate changes in tissue perfusion and permeability in association with angiogenesis. Regional tissue perfusion can be assessed with MR imaging after administration of gadolinium-based contrast agents[215] or with noncontrast imaging approaches that apply arterial spin labeling.[216] Some attempts at molecular imaging of angiogenesis have been made, including αvβ3-targeted nanoparticles for MR imaging,[203] although the MR approach in general lacks sensitivity for targeted molecular imaging. MR targeted imaging approaches that use nanoparticles have also incorporated targeted therapy of angiogenesis with fumagillin.[217]

The radiotracer-based imaging approaches provide the highest sensitivity and, when applied with biologically targeted radiotracers, offer a novel approach to investigate neovascularization or vascular remodeling. This nuclear approach can provide an assessment of tissue perfusion, oxygenation, and metabolism, along with the direct targeted evaluation of signaling events modulating the angiogenic and arteriogenic processes. The high-sensitivity images obtained with single-photon emission tomography and positron emission tomography can now be colocalized with high-resolution x-ray CT anatomical images to better identify and quantify radiotracer uptake within the cardiovascular system with the availability of hybrid imaging systems. Radiotracer imaging, including hybrid single-photon emission tomography/CT approaches, has been applied to evaluate angiogenesis and arteriogenesis in rodent models of hind-limb ischemia[218] and myocardial ischemia,[187] as well as in larger canine and porcine models of ischemia-induced angiogenesis.[185,186] Figure 8 illustrates the integration of physiological perfusion imaging and targeted molecular imaging of angiogenesis using hybrid single-photon emission tomography/CT imaging in a murine model of hind-limb ischemia and the application of serial perfusion imaging for the evaluation of angiogenesis in a porcine model of hind-limb ischemia.

X-ray angiography in vivo after the administration of an iodinated contrast agent can provide information about both perfusion and arteriogenesis, characterizing vessels as small as 25 to 50 μm in diameter. Micro-CT imaging after the intra-arterial administration of a contrast medium can provide high-resolution ex vivo images of vessels as small as 8 μm in diameter. This high-resolution micro-CT approach has become a standard approach to evaluate arteriogenesis in animal models of myocardial and hind-limb ischemia.[219,220] High-resolution ex vivo micro-CT images of the microvasculature can be characterized and quantified with the use of vascular image analysis approaches that incorporate physiological principles to establish connectivity.[221] Figure 9 illustrates the value of micro-CT imaging for the evaluation of arteriogenesis and the associated changes in perfusion and permeability in models of hind-limb ischemia.

Photoacoustic tomography is a newer approach that combines optical and acoustic imaging to generate high-resolution images of microvasculature. Pan et al[211] have developed, characterized, and demonstrated a vascular-constrained, αvβ3-targeted gold nanobeacon for the sensitive and specific discrimination of immature angiogenic endothelial vessels from mature microvasculature.

The imaging of the microcirculation can be extended to the capillary level with intravital microscopic imaging, including fluorescent microscopy and multiphoton laser scanning microscopy. These approaches allow evaluation of structure and intravascular flow velocities, circulating cells, and EC interactions.[204,222] The integration of fluorescence molecular imaging agents with high-resolution in vivo microscopy has facilitated the in vivo serial assessment of angiogenesis and arteriogenesis.[223] Confocal in vivo microscopy can sense events up to 200 μm below the surface. Spinning disk confocal microscopy systems provide faster imaging frame rates (hundreds per second) but cannot provide the same depth of penetration. This spinning disk confocal microscopy approach is best suited for dynamic in vivo microscopy studies of fluorescently labeled cells. Multiphoton microscopy has enabled imaging of cellular interactions at depths approaching 500 μm. A wide array of imaging probes are available for molecular imaging of the vasculature. Injectable fluorescence molecular imaging agents have emerged for detecting key biological processes underlying vascular diseases, including

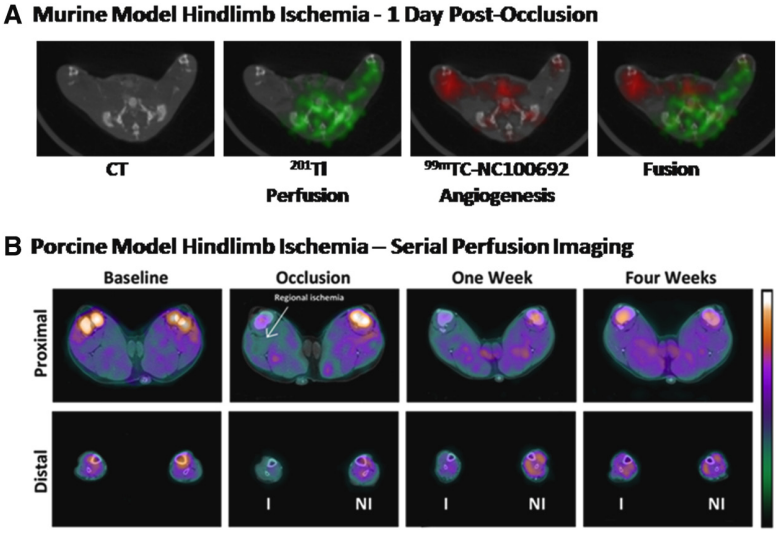

Figure 8. Integration of ^{201}Tl perfusion and targeted imaging of angiogenesis with hybrid single-photon emission computed tomography (SPECT)/computed tomography (CT) imaging in a mouse 1 day after femoral artery occlusion (**A**). Color-coded SPECT ^{201}Tl images (green) and ^{99m}Tc-NC100692 images (red) of integrin activation are superimposed on CT images (black and white) of the hind limb. Serial images of ^{201}Tl perfusion before and after femoral artery occlusion in a pig (**B**). Decreased perfusion is seen in the ischemic limb, which slowly improves over the 4 weeks after occlusion. I indicates ischemic; and NI, nonischemic. Modified with permission from Stacy et al.[185] Copyright © 2014, American Heart Association, Inc.

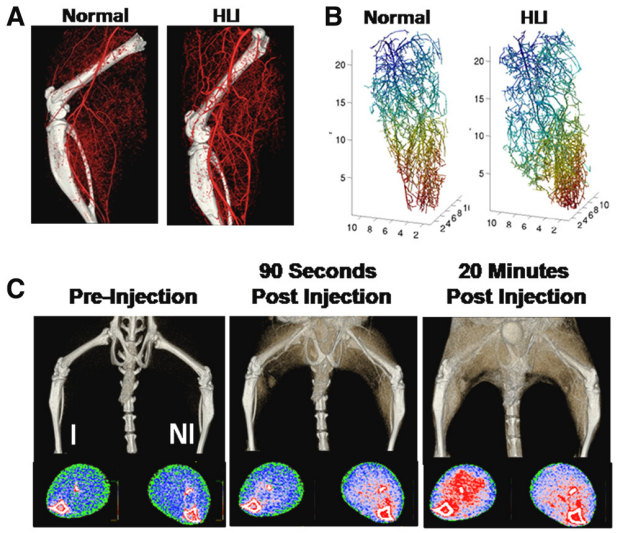

Figure 9. Ex vivo micro–computed tomography (micro-CT) images (**A**) after vascular casting of control mouse hind limb and mouse after creation of hind-limb ischemia (HLI). These images were analyzed by use of a 3-dimensional computational reconstruction of the arterial tree. Branching levels are indicated by color (**B**). Serial in vivo micro-CT images of mouse with HLI after contrast injection (**C**) with volume rendering and cross sections through the calf color coded for image contrast intensity. The ischemic (I) limb demonstrates an initial decrease in perfusion (90 seconds after injection) and increased vascular permeability (20 minutes after injection). NI indicates nonischemic.

inflammation, angiogenesis, apoptosis, oxidative stress, and calcification.[223] Novel protease-activatable near-infrared fluorescence reporters have provided insights into thrombin, cathepsin, and matrix metalloproteinase activities in vivo within the vascular tree.

Other imaging approaches allow the evaluation of intravascular blood volume and vascular permeability with the use of intravascular nanoparticulate contrast agents having a range of sizes. This imaging approach can assess vascular leakiness. Macromolecular intravascular MR contrast agents containing iron oxides, gadolinium, albumin, or dendrimers[224] or CT contrast agents containing iodine or other heavy metals can provide an index of the barrier function of angiogenic vessels. This imaging requires dynamic or serial imaging for the evaluation of temporal changes in contrast delivery, clearance, and retention.

4.4. Histological Assessment of the Vasculature

A wide variety of markers are available for the identification of ECs, as summarized in Table 6. In their selection, it is important to note that antibodies may vary, depending on the sources, and details in protocols strongly affect the results; therefore, the recommendations provided in this section should be seen as general guide. In addition, even across endothelium there is heterogeneity, for example, between venous and arterial endothelium or ECs from different vascular beds. A classic arterial phenotype marker is EphrinB2, but a variety of other preferentially arterially expressed proteins also are useful (Table 6). Venous markers are EphB4 and neuropilin-2. Pan-endothelial markers include CD31 and VE-cadherin, with additional markers such as von Willebrand factor and Tie2, but von Willebrand factor stainings have to be viewed with caution because the protein is secreted. For visualization of the embryonic vasculature, staining against endomycin is very suitable. Besides antibodies, lectins (specifically *Griffonia simplicifolia* I isolectin B4 for mouse tissue) can be used to mark ECs. Of note, lectins can also be infused to identify the perfused vessels. However, especially in injury states, care should be taken to avoid cross-reactivity with platelets or hematopoietic antigens, which can occur with lectins or CD31.

For markers of surrounding smooth muscle cells, α-smooth muscle actin provides an index of arterioles and venules and can be used to distinguish these structures from capillaries. The following are markers of pericytes: platelet-derived growth factor receptor-α and -β, desmin, nestin aminopeptidase A, aminopeptidase N (CD13), and NG2.

4.5. Models of Microcirculation/Macrocirculation Pathology in Diabetes Mellitus

Here, we review the dominant clinical features of human diabetic vascular disease to discuss the relevant animal models. We classify diabetic vascular disease into early versus late stages, disease affecting the large (conduit) and small (resistance) vessels or the microvascular capillary network, and disease occurring with profound hyperglycemia and low insulin production (ie, human type 1) or only moderate hyperglycemia with normal or elevated circulating insulin levels (type 2).

Early in diabetes mellitus, the predominant injury is to the vascular endothelium, with abnormal flow-mediated vasodilation of the brachial artery (a conduit vessel) and forearm blood flow in response to acetylcholine (regulated by microvascular tone) called endothelial dysfunction. Endothelial dysfunction occurs across levels of hyperglycemia, and the defect is not correctable with insulin. The abnormal vasodilation is a manifestation of abnormal cell-cell (mainly endothelial–vascular smooth muscle) interactions that occur without evidence of arterial structural disease.[225] In selected vascular beds, one observes evidence of alterations in capillary (microvascular) function such as microalbuminuria, likely caused by an abnormality in the permeability of the glomerular endothelium. However, in many capillary beds, capillary number, structure, and function may be normal at this early stage.

Aspects of abnormal vascular reactivity in humans occurs when diabetes mellitus is induced in rodents with streptozotocin or alloxan to induce hyperglycemia and to mimic type 1 diabetes mellitus or after high-fat or high-fructose feeding to mimic the metabolic disturbance observed in type II diabetes mellitus in humans, that is, hyperinsulinemia, hyperglycemia, and dyslipidemia. In human and preclinical studies, the early endothelial vasodilator dysfunction observed is due predominantly to an elevation in reactive oxygen species from mitochondrial dysfunction, increased activity of vascular NADPH oxidase, and the infiltration of immune cells. The increase in reactive oxygen species has global effects on cell signaling, for example, degradation of endothelium-derived nitric oxide.[226] Also contributing to the vascular dysfunction are vasoconstrictor prostanoids and endogenous nitric oxide synthase

antagonists.[227] These alterations may be mediated in part by the receptor for advanced glycosylation end products.[228]

Alterations in vascular compliance occur before obstructive arterial disease. The reduction in vascular compliance in human diabetics is believed to be attributable to increased fibrosis and perhaps alterations in connective tissue caused by aberrant protein glycosylation. The obstructive arterial atherosclerosis seen in diabetic patients includes at least 4 intriguing differences from that seen in nondiabetic individuals. First, the disease is typically more diffuse than atherosclerosis in nondiabetics and extends more distally in the arterial tree.[229] Second, atherosclerosis in diabetes mellitus is more often associated with extensive vascular calcification of the coronary and peripheral vessels, often extending into the digital arteries, which has implications for imaging and the accuracy of diagnostic testing.[230] Third, whereas atherosclerosis and hypertension increase the risk of aneurysm formation in the aorta and peripheral vessels in nondiabetic individuals, subjects with diabetes mellitus seem to be protected against aortic aneurysms. Finally, diabetes mellitus is a particularly potent risk factor for occlusive atherosclerosis in vessels of the lower extremity.[231]

Mouse and rodent models of diabetic atherosclerosis have shown some similarities to human disease. Of all the models, the hyperlipidemic, diabetic swine appear to best mimic the composition and complexity of atherosclerotic lesions in diabetic humans.[232] Rodent models are far less faithful with respect to plaque composition and complexity but mimic the endothelial vasodilator dysfunction of human diabetic vascular disease and thus allow detailed testing of mechanisms of disease.

One critical feature the rodent model mimics is the impairment of angiogenesis in diabetes mellitus that occurs in response to arterial occlusion.[233] Clinically, this is one of the mechanisms that places diabetics at risk for nonhealing ulcers, particularly in the foot. Murine models of impaired angiogenesis have been studied extensively in the hind-limb ischemia model in which a number of proposed mechanisms include the accumulation of advanced glycation end products, generation of reactive oxygen species, decreased bone marrow mononuclear cells, impaired endothelial progenitor cell mobilization, increased inflammation, impaired hypoxia-inducible factor-1α expression, increased thioredoxin-interacting protein expression, and alterations in the activation of the VEGF receptor ligand family. Incidentally, retinal neovascularization is paradoxically enhanced in diabetics, even though angiogenesis is generally impaired in other organs. The paradox of proliferative retinal angiogenesis may be explained in part by high intraocular levels of VEGF.

Several problems need to be highlighted in the study of animal models of diabetes mellitus. In murine models of diabetes mellitus, the largest problem is the manner in which diabetes mellitus is induced. Streptozotocin administration is the most common and tested method, but in addition to injuring islet cells of the pancreas, it can damage other cells, including vascular cells. Furthermore, this is a model for type 1 but not type 2 diabetes mellitus. Even as a model for type 1 diabetes mellitus, blood glucose values remain chronically elevated and are far in excess of those seen in patients.[234] Unlike human type 1 diabetes mellitus, there are almost never periods of normoglycemia or fluctuations in blood sugar that are associated with the effects of insulin replacement therapy. Other type 1 models such as Akita knockout mice may offer an alternative because some level of circulating insulin is present.[235] In patients with type 2 diabetes mellitus, insulin resistance underlies the elevated blood sugars, and often hypertension and obesity are superimposed. Mouse models that include a high-fat diet mimic the metabolic abnormalities, but this model is time consuming and costly and, like the type 1 model, is not associated with systemic atherosclerosis.[236]

A novel and potentially useful approach to modeling the genetic and epigenetic abnormalities underlying diabetic vascular disease is provided by human induced pluripotent stem cells. The induced pluripotent stem cells may be generated from human somatic cells by the forced expression of transcription factors that activate the core genes involved in pluripotency.[237] Subsequently, the induced pluripotent stem cells may be differentiated into vascular cells.[238] For example, one could potentially study induced pluripotent stem cell–derived vascular cells derived from diabetics to understand the genetic or epigenetic mechanisms responsible for the individual variations in the severity of vascular disease with similar levels of metabolic abnormality.

4.6. Summary of Models for Preclinical Testing of Therapeutic Applications

One of the major challenges in translational medicine relates to the identification of relevant preclinical models to test novel therapeutic strategies. We have made considerable progress with respect to understanding how angiogenesis works at the basic levels, but we have so far failed to predict which therapeutic approaches will be effective in patients. Despite multiple "cures" in mouse, rat, rabbit, and pig models of hind-limb and coronary ischemia, no approach to date has worked in patients.[239] Given the absence of even a single positive clinical outcome, it is obviously difficult to claim that any particular model is predictive of a clinical outcome. In fact, as stated above, no model to date is predictive at all. There are numerous reasons for this state of affairs. One reason is that animal studies are typically carried out in young, healthy animals. This is just the opposite of what happens in clinical practice in which old, ill, and frequently "no option" patients are enrolled in trials. We know that numerous disease states, including diabetes mellitus and atherosclerosis, interfere with proangiogenic growth factor signaling. In those rare cases in which old or diseased animals are used, the data are much less promising and still do not translate to clinical practice. Another consideration is that we may have the biology wrong. Although VEGF and related proangiogenic molecules are absolutely necessary during development and are very efficient in stimulating vessel growth in the setting of VEGF (or another specific growth factor) deficiency, it is not clear that most patients enrolled in therapeutic angiogenesis studies suffer from a VEGF-deficient state. In fact, most likely they do not. What they do suffer from is abnormal/impaired VEGF (or another growth factor) signaling.[240,241] The assumption that flooding the system with an excess of a growth factor will take care of an intracellular signaling defect may simply be wrong. For example, large doses

Table 8. Comparison of Animal Models for Therapeutic Neovascularization

Target Tissue	Model	Species	Advantages	Disadvantages
Heart	Ischemia/reperfusion	Mice, rats	Established reliable model	Only usable for testing acute endothelium-protective and particularly cardioprotective effects
Heart	Chronic ligation	Mice, rats	Established reliable model	Longer-term remodeling can be determined in mice with large infarcts
			Limited clinical relevance	
Heart	Ischemia/reperfusion model	Pig	Established model	Comorbidities and current state of the art therapy are not reflected in current studies
			Clinically relevant	
			Possibility to test delivery strategies	Use of diabetic and hypercholesterolemic pigs may solve some of these issues
Heart	Chronic ischemia/hibernation model	Pig	Established model	Difficult to mimic the clinically relevant conditions
			Useful for studying effects on vascularization	Patients show variable degrees of reversible ischemia vs scar tissue and development of collaterals
Hind limb	Chronic femoral artery ligation	Mice, rats, rabbits	Established model	Predominantly dependent on arteriogenesis

of insulin are frequently not the answer in managing blood glucose in patients with type 2 diabetes mellitus. Finally, it is not obvious that a single growth factor therapy may be sufficient to induce blood vessel growth in a complex disease state. For all these reasons, we do not have an animal model or approach that is predictive of clinical outcome. This section summarizes the pros and cons of currently available models and discusses the their limitations (Table 8).

In vitro models are ideally suited to discover mechanisms of angiogenesis and vessel formation and can be robustly used as platforms for screening and target identification. However, it is very challenging to rebuild in vitro the complex vascular structure, which not only is dependent on ECs but also includes pericytes, extracellular matrix, and particularly mechanical activation. Therefore, model organisms such as the zebrafish or the reliable and robust postnatal mouse retina assays can be used to further elucidate the relevance of a target in vivo. Particularly, the oxygen-induced retinopathy model may be useful to study treatment strategies for retinopathies. Of note, the impact of ischemic injury, which affects not only ECs but the entire tissue and significantly modifies the milieu in which capillaries or vessels are growing, is not yet well mimicked in the currently available in vitro culture assays or model organisms. Moreover, the disturbed vessel growth and functions that occur, for example, in diabetes mellitus are difficult to copy in model organisms or during vascular development. Recent efforts to introduce pathophysiological conditions such as diabetes mellitus or hypercholesterolemia into model organisms such as the zebrafish may help to provide appropriate context to study more pathophysiologically relevant conditions.

Models in adult mice are the next best choice to test putative therapeutic strategies. The hind-limb and coronary ligation models are well established for addressing the benefit of therapeutic strategies for peripheral artery disease or ischemic coronary artery disease. However, as discussed, there are also several disadvantages. Chronic ligation, as is done in most cases, does not mimic the clinical situation, in which the majority of patients are revascularized. Moreover, patients with peripheral artery disease and coronary artery disease have comorbidities that are not present in healthy young mice. Therefore, the use of diabetic or aged mice may provide a more relevant context. A second limitation of the mouse model is that the recovery after ischemia is driven largely by collateralization, which occurs to a small extent in some but not all patients for reasons that are not well understood.

The pig model is considered most appropriate for preclinical testing. The vascular architecture and response are similar, and pigs can be easily instrumented for local cardiac or vascular delivery of therapeutic substances. In addition, the ischemia/reperfusion setting very closely resembles the clinical condition. However, other conditions that may warrant proangiogenic therapy such as chronic ischemia (which occurs in patients with ischemic heart failure) or microcirculatory dysfunction (which is observed in patients with dilated cardiomyopathy) are difficult to model. Chronic heart failure may be studied after longer observation of pigs with ischemia/reperfusion. Moreover, as outlined above, some first attempts have been made to induce chronic ischemia by ameroid occluders or reduction stents. However, in this model, only limited cardiac injury is induced, which may mimic angina but not heart failure. Finally, pig models with comorbidities are currently being developed but are not yet well established and will be quite expensive.

Acknowledgments

We thank Elisabeth Allen and Doug Hanahan for providing Figure 1; M. Dewerchin, Leuven, Belgium, and Elaine Smolock, Rochester, MN, for their contributions to sections 2.3. and 3.7, respectively; Zhen W Zhuang, Yale, New Haven, CT, for providing Figure 6 and components of Figure 9; and Wei Zheng and Georgia Zarkada, Helsinki, Finland, for assistance with Table 2.

Disclosures

Writing Group Disclosures

Writing Group Member	Employment	Research Grant	Other Research Support	Speakers' Bureau/ Honoraria	Expert Witness	Ownership Interest	Consultant/ Advisory Board	Other
Stefanie Dimmeler	University of Frankfurt	DFG†	None	None	None	T2cure GmbH*	Miragen*	None
Michael Simons	Yale University School of Medicine	None	None	None	None	None	None	None
Kari Alitalo	University of Helsinki	None	None	None	None	Herantis Pharma*	Herantis Pharma*	None
Brian H. Annex	University of Virginia	None	None	None	None	None	None	None
Hellmut G. Augustin	German Cancer Research Center	None	None	None	None	None	None	None
Craig Beam	CBRE Health Care	None	None	None	None	None	None	None
Bradford C. Berk	University of Rochester	None	None	None	None	None	Merck*	None
Tatiana Byzova	Cleveland Clinic	None	None	None	None	None	None	None
Peter Carmeliet	Vesalius Research Center KU Leuven	None	None	None	None	None	None	None
William Chilian	Northeast Ohio Medical University	None	None	None	None	None	None	None
John P. Cooke	Houston Methodist Research Institute	None	NHLBI†	None	None	Fibralign*; Armetheon*	Pfizer*; Novartis*	None
George E. Davis	University of Missouri	NIH†	None	None	None	None	None	None
Anne Eichmann	Inserm College de France	None	None	None	None	None	None	None
M. Luisa Iruela-Arispe	UCLA	None	None	None	None	None	None	None
Eli Keshet	Hebrew University of Jerusalem	None	None	None	None	None	None	None
Christiana Ruhrberg	University College London	Wellcome Trust*; British Heart Foundation*	None	None	None	None	None	None
Albert J. Sinusas	Yale University	GE Healthcare*; Siemens*	None	None	None	None	None	None
Y. Joseph Woo	Stanford University School of Medicine	None	None	None	None	None	None	None

This table represents the relationships of writing group members that may be perceived as actual or reasonably perceived conflicts of interest as reported on the Disclosure Questionnaire, which all members of the writing group are required to complete and submit. A relationship is considered to be "significant" if (a) the person receives $10 000 or more during any 12-month period, or 5% or more of the person's gross income; or (b) the person owns 5% or more of the voting stock or share of the entity, or owns $10 000 or more of the fair market value of the entity. A relationship is considered to be "modest" if it is less than "significant" under the preceding definition.

*Modest.

†Significant.

Reviewer Disclosures

Reviewer	Employment	Research Grant	Other Research Support	Speakers' Bureau/ Honoraria	Expert Witness	Ownership Interest	Consultant/ Advisory Board	Other
Elisabetta Dejana	IFOM, FIRC Institute of Molecular Oncology (Italy)	None	None	None	None	None	None	None
Christian Kupatt	Ludwig-Maximilians-University Munich (Germany)	None	None	None	None	None	None	None
Douglas Losordo	Northwestern University	None	None	None	None	None	None	None

This table represents the relationships of reviewers that may be perceived as actual or reasonably perceived conflicts of interest as reported on the Disclosure Questionnaire, which all reviewers are required to complete and submit. A relationship is considered to be "significant" if (a) the person receives $10 000 or more during any 12-month period, or 5% or more of the person's gross income; or (b) the person owns 5% or more of the voting stock or share of the entity, or owns $10 000 or more of the fair market value of the entity. A relationship is considered to be "modest" if it is less than "significant" under the preceding definition.

References

1. Iruela-Arispe ML, Davis GE. Cellular and molecular mechanisms of vascular lumen formation. *Dev Cell*. 2009;16:222–231. doi: 10.1016/j.devcel.2009.01.013.
2. Xu K, Cleaver O. Tubulogenesis during blood vessel formation. *Semin Cell Dev Biol*. 2011;22:993–1004. doi: 10.1016/j.semcdb.2011.05.001.
3. Nakatsu MN, Hughes CC. An optimized three-dimensional in vitro model for the analysis of angiogenesis. *Methods Enzymol*. 2008;443:65–82. doi: 10.1016/S0076-6879(08)02004-1.
4. Koh W, Stratman AN, Sacharidou A, Davis GE. In vitro three dimensional collagen matrix models of endothelial lumen formation during vasculogenesis and angiogenesis. *Methods Enzymol*. 2008;443:83–101. doi: 10.1016/S0076-6879(08)02005-3.
5. Korff T, Augustin HG. Tensional forces in fibrillar extracellular matrices control directional capillary sprouting. *J Cell Sci*. 1999;112(pt 19):3249–3258.
6. Aplin AC, Fogel E, Zorzi P, Nicosia RF. The aortic ring model of angiogenesis. *Methods Enzymol*. 2008;443:119–136. doi: 10.1016/S0076-6879(08)02007-7.
7. Stratman AN, Malotte KM, Mahan RD, Davis MJ, Davis GE. Pericyte recruitment during vasculogenic tube assembly stimulates endothelial basement membrane matrix formation. *Blood*. 2009;114:5091–5101. doi: 10.1182/blood-2009-05-222364.
8. Hughes CS, Postovit LM, Lajoie GA. Matrigel: a complex protein mixture required for optimal growth of cell culture. *Proteomics*. 2010;10:1886–1890. doi: 10.1002/pmic.200900758.
9. Vernon RB, Angello JC, Iruela-Arispe ML, Lane TF, Sage EH. Reorganization of basement membrane matrices by cellular traction promotes the formation of cellular networks in vitro. *Lab Invest*. 1992;66:536–547.
10. Senger DR, Davis GE. Angiogenesis. *Cold Spring Harb Perspect Biol*. 2011;3:a005090. doi: 10.1101/cshperspect.a005090.
11. Davis GE, Stratman AN, Sacharidou A, Koh W. Molecular basis for endothelial lumen formation and tubulogenesis during vasculogenesis and angiogenic sprouting. *Int Rev Cell Mol Biol*. 2011;288:101–165. doi: 10.1016/B978-0-12-386041-5.00003-0.
12. Saunders WB, Bohnsack BL, Faske JB, Anthis NJ, Bayless KJ, Hirschi KK, Davis GE. Coregulation of vascular tube stabilization by endothelial cell TIMP-2 and pericyte TIMP-3. *J Cell Biol*. 2006;175:179–191. doi: 10.1083/jcb.200603176.
13. Stratman AN, Davis GE. Endothelial cell-pericyte interactions stimulate basement membrane matrix assembly: influence on vascular tube remodeling, maturation, and stabilization. *Microsc Microanal*. 2012;18:68–80. doi: 10.1017/S1431927611012402.
14. Nehls V, Drenckhahn D. A microcarrier-based cocultivation system for the investigation of factors and cells involved in angiogenesis in three-dimensional fibrin matrices in vitro. *Histochem Cell Biol*. 1995;104:459–466.
15. Alajati A, Laib AM, Weber H, Boos AM, Bartol A, Ikenberg K, Korff T, Zentgraf H, Obodozie C, Graeser R, Christian S, Finkenzeller G, Stark GB, Héroult M, Augustin HG. Spheroid-based engineering of a human vasculature in mice. *Nat Methods*. 2008;5:439–445. doi: 10.1038/nmeth.1198.
16. Laib AM, Bartol A, Alajati A, Korff T, Weber H, Augustin HG. Spheroid-based human endothelial cell microvessel formation in vivo. *Nat Protoc*. 2009;4:1202–1215. doi: 10.1038/nprot.2009.96.
17. Bayless KJ, Kwak HI, Su SC. Investigating endothelial invasion and sprouting behavior in three-dimensional collagen matrices. *Nat Protoc*. 2009;4:1888–1898. doi: 10.1038/nprot.2009.221.
18. Montesano R, Pepper MS, Vassalli JD, Orci L. Phorbol ester induces cultured endothelial cells to invade a fibrin matrix in the presence of fibrinolytic inhibitors. *J Cell Physiol*. 1987;132:509–516. doi: 10.1002/jcp.1041320313.
19. Bruyère F, Melen-Lamalle L, Blacher S, Roland G, Thiry M, Moons L, Frankenne F, Carmeliet P, Alitalo K, Libert C, Sleeman JP, Foidart JM, Noël A. Modeling lymphangiogenesis in a three-dimensional culture system. *Nat Methods*. 2008;5:431–437. doi: 10.1038/nmeth.1205.
20. Drake CJ, Fleming PA. Vasculogenesis in the day 6.5 to 9.5 mouse embryo. *Blood*. 2000;95:1671–1679.
21. Hsu YH, Moya ML, Hughes CC, George SC, Lee AP. A microfluidic platform for generating large-scale nearly identical human microphysiological vascularized tissue arrays. *Lab Chip*. 2013;13:2990–2998. doi: 10.1039/c3lc50424g.
22. Miller JS, Stevens KR, Yang MT, Baker BM, Nguyen DH, Cohen DM, Toro E, Chen AA, Galie PA, Yu X, Chaturvedi R, Bhatia SN, Chen CS. Rapid casting of patterned vascular networks for perfusable engineered three-dimensional tissues. *Nat Mater*. 2012;11:768–774. doi: 10.1038/nmat3357.
23. Morgan JP, Delnero PF, Zheng Y, Verbridge SS, Chen J, Craven M, Choi NW, Diaz-Santana A, Kermani P, Hempstead B, López JA, Corso TN, Fischbach C, Stroock AD. Formation of microvascular networks in vitro. *Nat Protoc*. 2013;8:1820–1836. doi: 10.1038/nprot.2013.110.
24. Liu H, Kennard S, Lilly B. NOTCH3 expression is induced in mural cells through an autoregulatory loop that requires endothelial-expressed JAGGED1. *Circ Res*. 2009;104:466–475. doi: 10.1161/CIRCRESAHA.108.184846.
25. Risau W. Mechanisms of angiogenesis. *Nature*. 1997;386:671–674. doi: 10.1038/386671a0.
26. Jones EA, le Noble F, Eichmann A. What determines blood vessel structure? Genetic prespecification vs. hemodynamics. *Physiology (Bethesda)*. 2006;21:388–395. doi: 10.1152/physiol.00020.2006.
27. Potente M, Gerhardt H, Carmeliet P. Basic and therapeutic aspects of angiogenesis. *Cell*. 2011;146:873–887. doi: 10.1016/j.cell.2011.08.039.
28. Hägerling R, Pollmann C, Andreas M, Schmidt C, Nurmi H, Adams RH, Alitalo K, Andresen V, Schulte-Merker S, Kiefer F. A novel multistep mechanism for initial lymphangiogenesis in mouse embryos based on ultramicroscopy. *EMBO J*. 2013;32:629–644. doi: 10.1038/emboj.2012.340.
29. Walls JR, Coultas L, Rossant J, Henkelman RM. Three-dimensional analysis of vascular development in the mouse embryo. *PLoS One*. 2008;3:e2853. doi: 10.1371/journal.pone.0002853.
30. Arora R, Papaioannou VE. The murine allantois: a model system for the study of blood vessel formation. *Blood*. 2012;120:2562–2572. doi: 10.1182/blood-2012-03-390070.
31. Benedito R, Rocha SF, Woeste M, Zamykal M, Radtke F, Casanovas O, Duarte A, Pytowski B, Adams RH. Notch-dependent VEGFR3 upregulation allows angiogenesis without VEGF-VEGFR2 signalling. *Nature*. 2012;484:110–114. doi: 10.1038/nature10908.
32. Gustafsson E, Brakebusch C, Hietanen K, Fässler R. Tie-1-directed expression of Cre recombinase in endothelial cells of embryoid bodies and transgenic mice. *J Cell Sci*. 2001;114(pt 4):671–676.
33. Kisanuki YY, Hammer RE, Miyazaki J, Williams SC, Richardson JA, Yanagisawa M. Tie2-Cre transgenic mice: a new model for endothelial cell-lineage analysis in vivo. *Dev Biol*. 2001;230:230–242. doi: 10.1006/dbio.2000.0106.
34. Licht AH, Raab S, Hofmann U, Breier G. Endothelium-specific Cre recombinase activity in flk-1-Cre transgenic mice. *Dev Dyn*. 2004;229:312–318. doi: 10.1002/dvdy.10416.
35. Alva JA, Zovein AC, Monvoisin A, Murphy T, Salazar A, Harvey NL, Carmeliet P, Iruela-Arispe ML. VE-Cadherin-Cre-recombinase transgenic mouse: a tool for lineage analysis and gene deletion in endothelial cells. *Dev Dyn*. 2006;235:759–767. doi: 10.1002/dvdy.20643.
36. Pham TH, Baluk P, Xu Y, Grigorova I, Bankovich AJ, Pappu R, Coughlin SR, McDonald DM, Schwab SR, Cyster JG. Lymphatic endothelial cell sphingosine kinase activity is required for lymphocyte egress and lymphatic patterning. *J Exp Med*. 2010;207:17–27. doi: 10.1084/jem.20091619.
37. Pitulescu ME, Schmidt I, Benedito R, Adams RH. Inducible gene targeting in the neonatal vasculature and analysis of retinal angiogenesis in mice. *Nat Protoc*. 2010;5:1518–1534. doi: 10.1038/nprot.2010.113.
38. Claxton S, Kostourou V, Jadeja S, Chambon P, Hodivala-Dilke K, Fruttiger M. Efficient, inducible Cre-recombinase activation in vascular endothelium. *Genesis*. 2008;46:74–80. doi: 10.1002/dvg.20367.
39. Bazigou E, Lyons OT, Smith A, Venn GE, Cope C, Brown NA, Makinen T. Genes regulating lymphangiogenesis control venous valve formation and maintenance in mice. *J Clin Invest*. 2011;121:2984–2992. doi: 10.1172/JCI58050.
40. Srinivasan RS, Dillard ME, Lagutin OV, Lin FJ, Tsai S, Tsai MJ, Samokhvalov IM, Oliver G. Lineage tracing demonstrates the venous origin of the mammalian lymphatic vasculature. *Genes Dev*. 2007;21:2422–2432. doi: 10.1101/gad.1588407.
41. Martínez-Corral I, Olmeda D, Diéguez-Hurtado R, Tammela T, Alitalo K, Ortega S. In vivo imaging of lymphatic vessels in development, wound healing, inflammation, and tumor metastasis. *Proc Natl Acad Sci USA*. 2012;109:6223–6228. doi: 10.1073/pnas.1115542109.
42. Choi I, Chung HK, Ramu S, Lee HN, Kim KE, Lee S, Yoo J, Choi D, Lee YS, Aguilar B, Hong YK. Visualization of lymphatic vessels by Prox1-promoter directed GFP reporter in a bacterial artificial chromosome-based transgenic mouse. *Blood*. 2011;117:362–365. doi: 10.1182/blood-2010-07-298562.

43. Hägerling R, Pollmann C, Kremer L, Andresen V, Kiefer F. Intravital two-photon microscopy of lymphatic vessel development and function using a transgenic Prox1 promoter-directed mOrange2 reporter mouse. *Biochem Soc Trans*. 2011;39:1674–1681. doi: 10.1042/BST20110722.
44. Truman LA, Bentley KL, Smith EC, Massaro SA, Gonzalez DG, Haberman AM, Hill M, Jones D, Min W, Krause DS, Ruddle NH. ProxTom lymphatic vessel reporter mice reveal Prox1 expression in the adrenal medulla, megakaryocytes, and platelets. *Am J Pathol*. 2012;180:1715–1725. doi: 10.1016/j.ajpath.2011.12.026.
45. Motoike T, Loughna S, Perens E, Roman BL, Liao W, Chau TC, Richardson CD, Kawate T, Kuno J, Weinstein BM, Stainier DY, Sato TN. Universal GFP reporter for the study of vascular development. *Genesis*. 2000;28:75–81.
46. Iljin K, Petrova TV, Veikkola T, Kumar V, Poutanen M, Alitalo K. A fluorescent Tie1 reporter allows monitoring of vascular development and endothelial cell isolation from transgenic mouse embryos. *FASEB J*. 2002;16:1764–1774. doi: 10.1096/fj.01-1043com.
47. Wang Y, Nakayama M, Pitulescu ME, Schmidt TS, Bochenek ML, Sakakibara A, Adams S, Davy A, Deutsch U, Lüthi U, Barberis A, Benjamin LE, Mäkinen T, Nobes CD, Adams RH. Ephrin-B2 controls VEGF-induced angiogenesis and lymphangiogenesis. *Nature*. 2010;465:483–486. doi: 10.1038/nature09002.
48. Ruhrberg C, Bautch VL. Neurovascular development and links to disease. *Cell Mol Life Sci*. 2013;70:1675–1684. doi: 10.1007/s00018-013-1277-5.
49. Connor KM, Krah NM, Dennison RJ, Aderman CM, Chen J, Guerin KI, Sapieha P, Stahl A, Willett KL, Smith LE. Quantification of oxygen-induced retinopathy in the mouse: a model of vessel loss, vessel regrowth and pathological angiogenesis. *Nat Protoc*. 2009;4:1565–1573. doi: 10.1038/nprot.2009.187.
50. Fantin A, Vieira JM, Plein A, Maden CH, Ruhrberg C. The embryonic mouse hindbrain as a qualitative and quantitative model for studying the molecular and cellular mechanisms of angiogenesis. *Nat Protoc*. 2013;8:418–429.
51. Fruttiger M. Development of the retinal vasculature. *Angiogenesis*. 2007;10:77–88. doi: 10.1007/s10456-007-9065-1.
52. Sawamiphak S, Ritter M, Acker-Palmer A. Preparation of retinal explant cultures to study ex vivo tip endothelial cell responses. *Nat Protoc*. 2010;5:1659–1665. doi: 10.1038/nprot.2010.130.
53. Teillet MA, Ziller C, Le Douarin NM. Quail-chick chimeras. *Methods Mol Biol*. 2008;461:337–350. doi: 10.1007/978-1-60327-483-8_24.
54. Pardanaud L, Altmann C, Kitos P, Dieterlen-Lievre F, Buck CA. Vasculogenesis in the early quail blastodisc as studied with a monoclonal antibody recognizing endothelial cells. *Development*. 1987;100: 339–349.
55. Wilting J, Birkenhäger R, Eichmann A, Kurz H, Martiny-Baron G, Marmé D, McCarthy JE, Christ B, Weich HA. VEGF121 induces proliferation of vascular endothelial cells and expression of flk-1 without affecting lymphatic vessels of chorioallantoic membrane. *Dev Biol*. 1996;176:76–85.
56. Sato Y, Lansford R. Transgenesis and imaging in birds, and available transgenic reporter lines. *Dev Growth Differ*. 2013;55:406–421. doi: 10.1111/dgd.12058.
57. Hogan BM, Bos FL, Bussmann J, Witte M, Chi NC, Duckers HJ, Schulte-Merker S. Ccbe1 is required for embryonic lymphangiogenesis and venous sprouting. *Nat Genet*. 2009;41:396–398. doi: 10.1038/ng.321.
58. Karlsson J, von Hofsten J, Olsson PE. Generating transparent zebrafish: a refined method to improve detection of gene expression during embryonic development. *Mar Biotechnol (NY)*. 2001;3:522–527. doi: 10.1007/s1012601-0053-4.
59. Lawson ND, Weinstein BM. In vivo imaging of embryonic vascular development using transgenic zebrafish. *Dev Biol*. 2002;248:307–318.
60. Pelster B, Burggren WW. Disruption of hemoglobin oxygen transport does not impact oxygen-dependent physiological processes in developing embryos of zebra fish (*Danio rerio*). *Circ Res*. 1996;79:358–362.
61. Lawson ND, Wolfe SA. Forward and reverse genetic approaches for the analysis of vertebrate development in the zebrafish. *Dev Cell*. 2011;21:48–64. doi: 10.1016/j.devcel.2011.06.007.
62. Hwang WY, Fu Y, Reyon D, Maeder ML, Tsai SQ, Sander JD, Peterson RT, Yeh JR, Joung JK. Efficient genome editing in zebrafish using a CRISPR-Cas system. *Nat Biotechnol*. 2013;31:227–229. doi: 10.1038/nbt.2501.
63. Kettleborough RN, Busch-Nentwich EM, Harvey SA, Dooley CM, de Bruijn E, van Eeden F, Sealy I, White RJ, Herd C, Nijman IJ, Fényes F, Mehroke S, Scahill C, Gibbons R, Wali N, Carruthers S, Hall A, Yen J, Cuppen E, Stemple DL. A systematic genome-wide analysis of zebrafish protein-coding gene function. *Nature*. 2013;496:494–497. doi: 10.1038/nature11992.
64. Isogai S, Horiguchi M, Weinstein BM. The vascular anatomy of the developing zebrafish: an atlas of embryonic and early larval development. *Dev Biol*. 2001;230:278–301. doi: 10.1006/dbio.2000.9995.
65. Jensen LD, Rouhi P, Cao Z, Länne T, Wahlberg E, Cao Y. Zebrafish models to study hypoxia-induced pathological angiogenesis in malignant and nonmalignant diseases. *Birth Defects Res C Embryo Today*. 2011;93:182–193. doi: 10.1002/bdrc.20203.
66. Herwig L, Blum Y, Krudewig A, Ellertsdottir E, Lenard A, Belting HG, Affolter M. Distinct cellular mechanisms of blood vessel fusion in the zebrafish embryo. *Curr Biol*. 2011;21:1942–1948. doi: 10.1016/j.cub.2011.10.016.
67. Proulx K, Lu A, Sumanas S. Cranial vasculature in zebrafish forms by angioblast cluster-derived angiogenesis. *Dev Biol*. 2010;348:34–46. doi: 10.1016/j.ydbio.2010.08.036.
68. van Impel A, Zhao Z, Hermkens DM, Roukens MG, Fischer JC, Peterson-Maduro J, Duckers H, Ober EA, Ingham PW, Schulte-Merker S. Divergence of zebrafish and mouse lymphatic cell fate specification pathways. *Development*. 2014;141:1228–1238. doi: 10.1242/dev.105031.
69. Ellertsdóttir E, Lenard A, Blum Y, Krudewig A, Herwig L, Affolter M, Belting HG. Vascular morphogenesis in the zebrafish embryo. *Dev Biol*. 2010;341:56–65. doi: 10.1016/j.ydbio.2009.10.035.
70. Carmeliet P, Tessier-Lavigne M. Common mechanisms of nerve and blood vessel wiring. *Nature*. 2005;436:193–200. doi: 10.1038/nature03875.
71. Zhong TP, Childs S, Leu JP, Fishman MC. Gridlock signalling pathway fashions the first embryonic artery. *Nature*. 2001;414:216–220. doi: 10.1038/35102599.
72. De Bock K, Georgiadou M, Schoors S, Kuchnio A, Wong BW, Cantelmo AR, Quaegebeur A, Ghesquière B, Cauwenberghs S, Eelen G, Phng LK, Betz I, Tembuyser B, Brepoels K, Welti J, Geudens I, Segura I, Cruys B, Bifari F, Decimo I, Blanco R, Wyns S, Vangindertael J, Rocha S, Collins RT, Munck S, Daelemans D, Imamura H, Devlieger R, Rider M, Van Veldhoven PP, Schuit F, Bartrons R, Hofkens J, Fraisl P, Telang S, Deberardinis RJ, Schoonjans L, Vinckier S, Chesney J, Gerhardt H, Dewerchin M, Carmeliet P. Role of PFKFB3-driven glycolysis in vessel sprouting. *Cell*. 2013;154:651–663. doi: 10.1016/j.cell.2013.06.037.
73. Bussmann J, Wolfe SA, Siekmann AF. Arterial-venous network formation during brain vascularization involves hemodynamic regulation of chemokine signaling. *Development*. 2011;138:1717–1726. doi: 10.1242/dev.059881.
74. Traver D, Paw BH, Poss KD, Penberthy WT, Lin S, Zon LI. Transplantation and in vivo imaging of multilineage engraftment in zebrafish bloodless mutants. *Nat Immunol*. 2003;4:1238–1246. doi: 10.1038/ni1007.
75. Amaya E, Offield MF, Grainger RM. Frog genetics: *Xenopus tropicalis* jumps into the future. *Trends Genet*. 1998;14:253–255.
76. Ny A, Koch M, Vandevelde W, Schneider M, Fischer C, Diez-Juan A, Neven E, Geudens I, Maity S, Moons L, Plaisance S, Lambrechts D, Carmeliet P, Dewerchin M. Role of VEGF-D and VEGFR-3 in developmental lymphangiogenesis, a chemicogenetic study in *Xenopus* tadpoles. *Blood*. 2008;112:1740–1749. doi: 10.1182/blood-2007-08-106302.
77. Levine AJ, Munoz-Sanjuan I, Bell E, North AJ, Brivanlou AH. Fluorescent labeling of endothelial cells allows in vivo, continuous characterization of the vascular development of *Xenopus laevis*. *Dev Biol*. 2003;254:50–67.
78. Ny A, Vandevelde W, Hohensinner P, Beerens M, Geudens I, Diez-Juan A, Brepoels K, Plaisance S, Krieg PA, Langenberg T, Vinckier S, Luttun A, Carmeliet P, Dewerchin M. A transgenic *Xenopus laevis* reporter model to study lymphangiogenesis. *Biol Open*. 2013;2:882–890. doi: 10.1242/bio.20134739.
79. Cleaver O, Krieg PA. VEGF mediates angioblast migration during development of the dorsal aorta in *Xenopus*. *Development*. 1998;125: 3905–3914.
80. Shimizu T, Hoshino Y, Miyazaki H, Sato E. Angiogenesis and microvasculature in the female reproductive organs: physiological and pathological implications. *Curr Pharm Des*. 2012;18:303–309.
81. Burton GJ, Charnock-Jones DS, Jauniaux E. Regulation of vascular growth and function in the human placenta. *Reproduction*. 2009;138:895–902. doi: 10.1530/REP-09-0092.
82. Reynolds LP, Borowicz PP, Vonnahme KA, Johnson ML, Grazul-Bilska AT, Wallace JM, Caton JS, Redmer DA. Animal models of placental angiogenesis. *Placenta*. 2005;26:689–708. doi: 10.1016/j.placenta.2004.11.010.

83. Muthig V, Gilsbach R, Haubold M, Philipp M, Ivacevic T, Gessler M, Hein L. Upregulation of soluble vascular endothelial growth factor receptor 1 contributes to angiogenesis defects in the placenta of alpha 2B-adrenoceptor deficient mice. *Circ Res*. 2007;101:682–691. doi: 10.1161/CIRCRESAHA.107.151563.
84. Lu J, Zhang S, Nakano H, Simmons DG, Wang S, Kong S, Wang Q, Shen L, Tu Z, Wang W, Wang B, Wang H, Wang Y, van Es JH, Clevers H, Leone G, Cross JC, Wang H. A positive feedback loop involving Gcm1 and Fzd5 directs chorionic branching morphogenesis in the placenta. *PLoS Biol*. 2013;11:e1001536. doi: 10.1371/journal.pbio.1001536.
85. Malinda KM. In vivo Matrigel migration and angiogenesis assay. *Methods Mol Biol*. 2009;467:287–294. doi: 10.1007/978-1-59745-241-0_17.
86. Volkmann I, Kumarswamy R, Pfaff N, Fiedler J, Dangwal S, Holzmann A, Batkai S, Geffers R, Lother A, Hein L, Thum T. MicroRNA-mediated epigenetic silencing of sirtuin1 contributes to impaired angiogenic responses. *Circ Res*. 2013;113:997–1003. doi: 10.1161/CIRCRESAHA.113.301702.
87. Heeschen C, Weis M, Aicher A, Dimmeler S, Cooke JP. A novel angiogenic pathway mediated by non-neuronal nicotinic acetylcholine receptors. *J Clin Invest*. 2002;110:527–536. doi: 10.1172/JCI14676.
88. Regan ER, Aird WC. Dynamical systems approach to endothelial heterogeneity. *Circ Res*. 2012;111:110–130. doi: 10.1161/CIRCRESAHA.111.261701.
89. Baluk P, McDonald DM. Markers for microscopic imaging of lymphangiogenesis and angiogenesis. *Ann NY Acad Sci*. 2008;1131:1–12. doi: 10.1196/annals.1413.001.
90. Mazzetti S, Frigerio S, Gelati M, Salmaggi A, Vitellaro-Zuccarello L. Lycopersicon esculentum lectin: an effective and versatile endothelial marker of normal and tumoral blood vessels in the central nervous system. *Eur J Histochem*. 2004;48:423–428.
91. Choyke PL, Dwyer AJ, Knopp MV. Functional tumor imaging with dynamic contrast-enhanced magnetic resonance imaging. *J Magn Reson Imaging*. 2003;17:509–520. doi: 10.1002/jmri.10304.
92. Furman-Haran E, Margalit R, Grobgeld D, Degani H. Dynamic contrast-enhanced magnetic resonance imaging reveals stress-induced angiogenesis in MCF7 human breast tumors. *Proc Natl Acad Sci USA*. 1996;93:6247–6251.
93. Ziyad S, Iruela-Arispe ML. Molecular mechanisms of tumor angiogenesis. *Genes Cancer*. 2011;2:1085–1096. doi: 10.1177/1947601911432334.
94. Lin WY, Mannikarottu A, Li S, Juan YS, Schuler C, Javed Z, Blaivas J, Levin RM. Correlation of in vivo bladder blood flow measurements with tissue hypoxia. *World J Urol*. 2011;29:165–170. doi: 10.1007/s00345-008-0369-6.
95. Hsu JY, Wakelee HA. Monoclonal antibodies targeting vascular endothelial growth factor: current status and future challenges in cancer therapy. *BioDrugs*. 2009;23:289–304. doi: 10.2165/11317600-000000000-00000.
96. Williams PD, Kingston PA. Plasmid-mediated gene therapy for cardiovascular disease. *Cardiovasc Res*. 2011;91:565–576. doi: 10.1093/cvr/cvr197.
97. Giacca M, Zacchigna S. VEGF gene therapy: therapeutic angiogenesis in the clinic and beyond. *Gene Ther*. 2012;19:622–629. doi: 10.1038/gt.2012.17.
98. Tafuro S, Ayuso E, Zacchigna S, Zentilin L, Moimas S, Dore F, Giacca M. Inducible adeno-associated virus vectors promote functional angiogenesis in adult organisms via regulated vascular endothelial growth factor expression. *Cardiovasc Res*. 2009;83:663–671. doi: 10.1093/cvr/cvp152.
99. Raake P, von Degenfeld G, Hinkel R, Vachenauer R, Sandner T, Beller S, Andrees M, Kupatt C, Schuler G, Boekstegers P. Myocardial gene transfer by selective pressure-regulated retroinfusion of coronary veins: comparison with surgical and percutaneous intramyocardial gene delivery. *J Am Coll Cardiol*. 2004;44:1124–1129. doi: 10.1016/j.jacc.2004.05.074.
100. Zangi L, Lui KO, von Gise A, Ma Q, Ebina W, Ptaszek LM, Später D, Xu H, Tabebordbar M, Gorbatov R, Sena B, Nahrendorf M, Briscoe DM, Li RA, Wagers AJ, Rossi DJ, Pu WT, Chien KR. Modified mRNA directs the fate of heart progenitor cells and induces vascular regeneration after myocardial infarction. *Nat Biotechnol*. 2013;31:898–907. doi: 10.1038/nbt.2682.
101. May D, Gilon D, Djonov V, Itin A, Lazarus A, Gordon O, Rosenberger C, Keshet E. Transgenic system for conditional induction and rescue of chronic myocardial hibernation provides insights into genomic programs of hibernation. *Proc Natl Acad Sci USA*. 2008;105:282–287. doi: 10.1073/pnas.0707778105.
102. Chilian WM, Penn MS, Pung YF, Dong F, Mayorga M, Ohanyan V, Logan S, Yin L. Coronary collateral growth: back to the future. *J Mol Cell Cardiol*. 2012;52:905–911. doi: 10.1016/j.yjmcc.2011.12.006.
103. Mac Gabhann F, Peirce SM. Collateral capillary arterialization following arteriolar ligation in murine skeletal muscle. *Microcirculation*. 2010;17:333–347. doi: 10.1111/j.1549-8719.2010.00034.x.
104. Chalothorn D, Faber JE. Strain-dependent variation in collateral circulatory function in mouse hindlimb. *Physiol Genomics*. 2010;42:469–479. doi: 10.1152/physiolgenomics.00070.2010.
105. Meier P, Gloekler S, Zbinden R, Beckh S, de Marchi SF, Zbinden S, Wustmann K, Billinger M, Vogel R, Cook S, Wenaweser P, Togni M, Windecker S, Meier B, Seiler C. Beneficial effect of recruitable collaterals: a 10-year follow-up study in patients with stable coronary artery disease undergoing quantitative collateral measurements. *Circulation*. 2007;116:975–983. doi: 10.1161/CIRCULATIONAHA.107.703959.
106. Skuli N, Majmundar AJ, Krock BL, Mesquita RC, Mathew LK, Quinn ZL, Runge A, Liu L, Kim MN, Liang J, Schenkel S, Yodh AG, Keith B, Simon MC. Endothelial HIF-2α regulates murine pathological angiogenesis and revascularization processes. *J Clin Invest*. 2012;122:1427–1443. doi: 10.1172/JCI57322.
107. Limbourg A, Korff T, Napp LC, Schaper W, Drexler H, Limbourg FP. Evaluation of postnatal arteriogenesis and angiogenesis in a mouse model of hind-limb ischemia. *Nat Protoc*. 2009;4:1737–1746. doi: 10.1038/nprot.2009.185.
108. Niiyama H, Huang NF, Rollins MD, Cooke JP. Murine model of hindlimb ischemia. *J Vis Exp*. 2009;21. doi: 10.3791/1035.
109. Zhou YF, Stabile E, Walker J, Shou M, Baffour R, Yu Z, Rott D, Yancopoulos GD, Rudge JS, Epstein SE. Effects of gene delivery on collateral development in chronic hypoperfusion: diverse effects of angiopoietin-1 versus vascular endothelial growth factor. *J Am Coll Cardiol*. 2004;44:897–903. doi: 10.1016/j.jacc.2004.05.046.
110. Rivard A, Fabre JE, Silver M, Chen D, Murohara T, Kearney M, Magner M, Asahara T, Isner JM. Age-dependent impairment of angiogenesis. *Circulation*. 1999;99:111–120.
111. Tirziu D, Moodie KL, Zhuang ZW, Singer K, Helisch A, Dunn JF, Li W, Singh J, Simons M. Delayed arteriogenesis in hypercholesterolemic mice. *Circulation*. 2005;112:2501–2509. doi: 10.1161/CIRCULATIONAHA.105.542829.
112. Simons M. Chapter 14: assessment of arteriogenesis. *Methods Enzymol*. 2008;445:331–342. doi: 10.1016/S0076-6879(08)03014-0.
113. Kupatt C, Hinkel R, von Brühl ML, Pohl T, Horstkotte J, Raake P, El Aouni C, Thein E, Dimmeler S, Feron O, Boekstegers P. Endothelial nitric oxide synthase overexpression provides a functionally relevant angiogenic switch in hibernating pig myocardium. *J Am Coll Cardiol*. 2007;49:1575–1584. doi: 10.1016/j.jacc.2006.11.047.
114. Brunner S, Winogradow J, Huber BC, Zaruba MM, Fischer R, David R, Assmann G, Herbach N, Wanke R, Mueller-Hoecker J, Franz WM. Erythropoietin administration after myocardial infarction in mice attenuates ischemic cardiomyopathy associated with enhanced homing of bone marrow-derived progenitor cells via the CXCR-4/SDF-1 axis. *FASEB J*. 2009;23:351–361. doi: 10.1096/fj.08-109462.
115. Hiesinger W, Perez-Aguilar JM, Atluri P, Marotta NA, Frederick JR, Fitzpatrick JR 3rd, McCormick RC, Muenzer JR, Yang EC, Levit RD, Yuan LJ, Macarthur JW, Saven JG, Woo YJ. Computational protein design to reengineer stromal cell-derived factor-1alpha generates an effective and translatable angiogenic polypeptide analog. *Circulation*. 2011;124(suppl):S18–S26.
116. Nishina T, Nishimura K, Yuasa S, Miwa S, Sakakibara Y, Ikeda T, Komeda M. A rat model of ischemic cardiomyopathy for investigating left ventricular volume reduction surgery. *J Card Surg*. 2002;17:155–162.
117. Woo YJ, Grand TJ, Berry MF, Atluri P, Moise MA, Hsu VM, Cohen J, Fisher O, Burdick J, Taylor M, Zentko S, Liao G, Smith M, Kolakowski S, Jayasankar V, Gardner TJ, Sweeney HL. Stromal cell-derived factor and granulocyte-monocyte colony-stimulating factor form a combined neovasculogenic therapy for ischemic cardiomyopathy. *J Thorac Cardiovasc Surg*. 2005;130:321–329. doi: 10.1016/j.jtcvs.2004.11.041.
118. Llaneras MR, Nance ML, Streicher JT, Lima JA, Savino JS, Bogen DK, Deac RF, Ratcliffe MB, Edmunds LH Jr. Large animal model of ischemic mitral regurgitation. *Ann Thorac Surg*. 1994;57:432–439.
119. Macarthur JW Jr, Cohen JE, McGarvey J, Shudo Y, Patel JB, Trubelja A, Fairman A, Edwards BB, Hung G, Goldstone AB, Hiesinger W, Atluri P, Wilensky RL, Pilla J, Gorman JH 3rd, Gorman RC, Woo YJ. Preclinical evaluation of the engineered stem cell chemokine stromal cell-derived

factor 1α analog in a translational ovine myocardial infarction model. *Cir Res*. 2014;114:650–659. doi: 10.1161/CIRCRESAHA.114.302884.
120. Markovitz LJ, Savage EB, Ratcliffe MB, Bavaria JE, Kreiner G, Iozzo RV, Hargrove WC 3rd, Bogen DK, Edmunds LH Jr. Large animal model of left ventricular aneurysm. *Ann Thorac Surg*. 1989;48:838–845.
121. Moainie SL, Guy TS, Gorman JH 3rd, Plappert T, Jackson BM, St John-Sutton MG, Edmunds LH Jr, Gorman RC. Infarct restraint attenuates remodeling and reduces chronic ischemic mitral regurgitation after postero-lateral infarction. *Ann Thorac Surg*. 2002;74:444–449.
122. Horwitz LD, Fennessey PV, Shikes RH, Kong Y. Marked reduction in myocardial infarct size due to prolonged infusion of an antioxidant during reperfusion. *Circulation*. 1994;89:1792–1801.
123. Shudo Y, Cohen JE, Macarthur JW, Atluri P, Hsiao PF, Yang EC, Fairman AS, Trubelja A, Patel J, Miyagawa S, Sawa Y, Woo YJ. Spatially oriented, temporally sequential smooth muscle cell-endothelial progenitor cell bi-level cell sheet neovascularizes ischemic myocardium. *Circulation*. 2013;128(suppl 1):S59–S68. doi: 10.1161/CIRCULATIONAHA.112.000293.
124. Jayasankar V, Bish LT, Pirolli TJ, Berry MF, Burdick J, Woo YJ. Local myocardial overexpression of growth hormone attenuates postinfarction remodeling and preserves cardiac function. *Ann Thorac Surg*. 2004;77:2122–2129. doi: 10.1016/j.athoracsur.2003.12.043.
125. Aicher A, Heeschen C, Mildner-Rihm C, Urbich C, Ihling C, Technau-Ihling K, Zeiher AM, Dimmeler S. Essential role of endothelial nitric oxide synthase for mobilization of stem and progenitor cells. *Nat Med*. 2003;9:1370–1376. doi: 10.1038/nm948.
126. Cohen JE, Atluri P, Taylor MD, Grand TJ, Liao GP, Panlilio CM, Suarez EE, Zentko SE, Hsu VM, Berry MF, Smith MJ, Gardner TJ, Sweeney HL, Woo YJ. Fructose 1,6-diphosphate administration attenuates post-ischemic ventricular dysfunction. *Heart Lung Circ*. 2006;15:119–123. doi: 10.1016/j.hlc.2005.12.004.
127. Masuzawa A, Black KM, Pacak CA, Ericsson M, Barnett RJ, Drumm C, Seth P, Bloch DB, Levitsky S, Cowan DB, McCully JD. Transplantation of autologously derived mitochondria protects the heart from ischemia-reperfusion injury. *Am J Physiol Heart Circ Physiol*. 2013;304:H966–H982. doi: 10.1152/ajpheart.00883.2012.
128. Yang DH, Kim TH, Choi JW, Kim ST, Yoon JH, Shin JH, Seo JB, Lim TH. Manganese dipyridoxyl diphosphate (MnDPDP)-enhanced magnetic resonance imaging of acute reperfused myocardial injury in a cat model, part II: comparison with cine magnetic resonance imaging. *Invest Radiol*. 2005;40:56–61.
129. Blaustein AS, Hoit BD, Wexler LF, Ashraf M, Ramrakhyani K, Matoba R, Gabel M, Millard RW. Characteristics of chronic left ventricular dysfunction induced by coronary embolization in a canine model. *Am J Cardiovasc Pathol*. 1995;5:32–48.
130. Saavedra WF, Tunin RS, Paolocci N, Mishima T, Suzuki G, Emala CW, Chaudhry PA, Anagnostopoulos P, Gupta RC, Sabbah HN, Kass DA. Reverse remodeling and enhanced adrenergic reserve from passive external support in experimental dilated heart failure. *J Am Coll Cardiol*. 2002;39:2069–2076.
131. Huang Y, Kawaguchi O, Zeng B, Carrington RA, Horam CJ, Yuasa T, Abdul-Hussein N, Hunyor SN. A stable ovine congestive heart failure model: a suitable substrate for left ventricular assist device assessment. *ASAIO J*. 1997;43:M408–M413.
132. Chen Y, Shao DB, Zhang FX, Zhang J, Yuan W, Man YL, Du W, Liu BX, Wang DW, Li XR, Cao KJ. Establishment and evaluation of a swine model of acute myocardial infarction and reperfusion-ventricular fibrillation-cardiac arrest using the interventional technique. *J Chin Med Assoc*. 2013;76:491–496. doi: 10.1016/j.jcma.2013.05.013.
133. Feuerstein GZ, Yue TL, Cheng HY, Ruffolo RR Jr. Myocardial protection by the novel vasodilating beta-blocker, carvedilol: potential relevance of anti-oxidant activity. *J Hypertens Suppl*. 1993;11:S41–S48.
134. Fujita M, McKown DP, McKown MD, Hartley JW, Franklin D. Evaluation of coronary collateral development by regional myocardial function and reactive hyperaemia. *Cardiovasc Res*. 1987;21:377–384. Doi: http://dx.doi.org/10.1093/cvr/21.5.377 377-384.
135. Toyota E, Warltier DC, Brock T, Ritman E, Kolz C, O'Malley P, Rocic P, Focardi M, Chilian WM. Vascular endothelial growth factor is required for coronary collateral growth in the rat. *Circulation.* 2005;112:2108–2113. doi: 10.1161/CIRCULATIONAHA.104.526954.
136. Bune LT, Larsen JR, Thaning P, Bune NE, Rasmussen P, Rosenmeier JB. Adenosine diphosphate reduces infarct size and improves porcine heart function after myocardial infarct. *Physiol Rep*. 2013;1:e00003. doi: 10.1002/PHY2.3.
137. Reinhardt CP, Dalhberg S, Tries MA, Marcel R, Leppo JA. Stable labeled microspheres to measure perfusion: validation of a neutron activation assay technique. *Am J Physiol Heart Circ Physiol*. 2001;280:H108–H116.
138. Hiesinger W, Vinogradov SA, Atluri P, Fitzpatrick JR 3rd, Frederick JR, Levit RD, McCormick RC, Muenzer JR, Yang EC, Marotta NA, MacArthur JW, Wilson DF, Woo YJ. Oxygen-dependent quenching of phosphorescence used to characterize improved myocardial oxygenation resulting from vasculogenic cytokine therapy. *J Appl Physiol (1985)*. 2011;110:1460–1465. doi: 10.1152/japplphysiol.01138.2010.
139. Haris M, Singh A, Cai K, Kogan F, McGarvey J, Debrosse C, Zsido GA, Witschey WR, Koomalsingh K, Pilla JJ, Chirinos JA, Ferrari VA, Gorman JH, Hariharan H, Gorman RC, Reddy R. A technique for in vivo mapping of myocardial creatine kinase metabolism. *Nat Med*. 2014;20:209–214. doi: 10.1038/nm.3436.
140. Eberth JF, Gresham VC, Reddy AK, Popovic N, Wilson E, Humphrey JD. Importance of pulsatility in hypertensive carotid artery growth and remodeling. *J Hypertens*. 2009;27:2010–2021. doi: 10.1097/HJH.0b013e32832e8dc8.
141. Zhang J, Nie L, Razavian M, Ahmed M, Dobrucki LW, Asadi A, Edwards DS, Azure M, Sinusas AJ, Sadeghi MM. Molecular imaging of activated matrix metalloproteinases in vascular remodeling. *Circulation*. 2008;118:1953–1960. doi: 10.1161/CIRCULATIONAHA.108.789743.
142. Castier Y, Brandes RP, Leseche G, Tedgui A, Lehoux S. p47phox-dependent NADPH oxidase regulates flow-induced vascular remodeling. *Circ Res*. 2005;97:533–540. doi: 10.1161/01.RES.0000181759.63239.21.
143. Pollman MJ, Hall JL, Gibbons GH. Determinants of vascular smooth muscle cell apoptosis after balloon angioplasty injury: influence of redox state and cell phenotype. *Circ Res*. 1999;84:113–121.
144. Rudic RD, Bucci M, Fulton D, Segal SS, Sessa WC. Temporal events underlying arterial remodeling after chronic flow reduction in mice: correlation of structural changes with a deficit in basal nitric oxide synthesis. *Circ Res*. 2000;86:1160–1166.
145. Miyashiro JK, Poppa V, Berk BC. Flow-induced vascular remodeling in the rat carotid artery diminishes with age. *Circ Res*. 1997;81:311–319.
146. Saniabadi AR, Umemura K, Matsumoto N, Sakuma S, Nakashima M. Vessel wall injury and arterial thrombosis induced by a photochemical reaction. *Thromb Haemost*. 1995;73:868–872.
147. Miyamoto M, Yasutake M, Takano H, Takagi H, Takagi G, Mizuno H, Kumita S, Takano T. Therapeutic angiogenesis by autologous bone marrow cell implantation for refractory chronic peripheral arterial disease using assessment of neovascularization by 99mTc-tetrofosmin (TF) perfusion scintigraphy. *Cell Transplant*. 2004;13:429–437.
148. Tammela T, Saaristo A, Lohela M, Morisada T, Tornberg J, Norrmén C, Oike Y, Pajusola K, Thurston G, Suda T, Yla-Herttuala S, Alitalo K. Angiopoietin-1 promotes lymphatic sprouting and hyperplasia. *Blood*. 2005;105:4642–4648. doi: 10.1182/blood-2004-08-3327.
149. Norrmén C, Ivanov KI, Cheng J, Zangger N, Delorenzi M, Jaquet M, Miura N, Puolakkainen P, Horsley V, Hu J, Augustin HG, Ylä-Herttuala S, Alitalo K, Petrova TV. FOXC2 controls formation and maturation of lymphatic collecting vessels through cooperation with NFATc1. *J Cell Biol*. 2009;185:439–457. doi: 10.1083/jcb.200901104.
150. Lutter S, Xie S, Tatin F, Makinen T. Smooth muscle-endothelial cell communication activates Reelin signaling and regulates lymphatic vessel formation. *J Cell Biol*. 2012;197:837–849. doi: 10.1083/jcb.201110132.
151. Dellinger M, Hunter R, Bernas M, Gale N, Yancopoulos G, Erickson R, Witte M. Defective remodeling and maturation of the lymphatic vasculature in Angiopoietin-2 deficient mice. *Dev Biol*. 2008;319:309–320. doi: 10.1016/j.ydbio.2008.04.024.
152. Xu Y, Yuan L, Mak J, Pardanaud L, Caunt M, Kasman I, Larrivée B, Del Toro R, Suchting S, Medvinsky A, Silva J, Yang J, Thomas JL, Koch AW, Alitalo K, Eichmann A, Bagri A. Neuropilin-2 mediates VEGF-C-induced lymphatic sprouting together with VEGFR3. *J Cell Biol*. 2010;188:115–130. doi: 10.1083/jcb.200903137.
153. Mäkinen T, Adams RH, Bailey J, Lu Q, Ziemiecki A, Alitalo K, Klein R, Wilkinson GA. PDZ interaction site in ephrinB2 is required for the remodeling of lymphatic vasculature. *Genes Dev*. 2005;19:397–410. doi: 10.1101/gad.330105.
154. Koltowska K, Betterman KL, Harvey NL, Hogan BM. Getting out and about: the emergence and morphogenesis of the vertebrate lymphatic vasculature. *Development*. 2013;140:1857–1870. doi: 10.1242/dev.089565.

155. Schulte-Merker S, Sabine A, Petrova TV. Lymphatic vascular morphogenesis in development, physiology, and disease. *J Cell Biol*. 2011;193:607–618. doi: 10.1083/jcb.201012094.
156. Karkkainen MJ, Haiko P, Sainio K, Partanen J, Taipale J, Petrova TV, Jeltsch M, Jackson DG, Talikka M, Rauvala H, Betsholtz C, Alitalo K. Vascular endothelial growth factor C is required for sprouting of the first lymphatic vessels from embryonic veins. *Nat Immunol*. 2004;5:74–80. doi: 10.1038/ni1013.
157. Karkkainen MJ, Saaristo A, Jussila L, Karila KA, Lawrence EC, Pajusola K, Bueler H, Eichmann A, Kauppinen R, Kettunen MI, Yla-Herttuala S, Finegold DN, Ferrell RE, Alitalo K. A model for gene therapy of human hereditary lymphedema. *Proc Natl Acad Sci USA*. 2001;98:12677–12682. doi: 10.1073/pnas.221449198.
158. Rutkowski JM, Moya M, Johannes J, Goldman J, Swartz MA. Secondary lymphedema in the mouse tail: lymphatic hyperplasia, VEGF-C upregulation, and the protective role of MMP-9. *Microvasc Res*. 2006;72:161–171. doi: 10.1016/j.mvr.2006.05.009.
159. Szuba A, Skobe M, Karkkainen MJ, Shin WS, Beynet DP, Rockson NB, Dakhil N, Spilman S, Goris ML, Strauss HW, Quertermous T, Alitalo K, Rockson SG. Therapeutic lymphangiogenesis with human recombinant VEGF-C. *FASEB J*. 2002;16:1985–1987. doi: 10.1096/fj.02-0401fje.
160. Tammela T, Saaristo A, Holopainen T, Lyytikkä J, Kotronen A, Pitkonen M, Abo-Ramadan U, Ylä-Herttuala S, Petrova TV, Alitalo K. Therapeutic differentiation and maturation of lymphatic vessels after lymph node dissection and transplantation. *Nat Med*. 2007;13:1458–1466. doi: 10.1038/nm1689.
161. Lähteenvuo M, Honkonen K, Tervala T, Tammela T, Suominen E, Lähteenvuo J, Kholová I, Alitalo K, Ylä-Herttuala S, Saaristo A. Growth factor therapy and autologous lymph node transfer in lymphedema. *Circulation*. 2011;123:613–620. doi: 10.1161/CIRCULATIONAHA.110.965384.
162. Jeltsch M, Jha SK, Tvorogov D, Anisimov A, Leppanen VM, Holopainen T, Kivela R, Ortega S, Karpanen T, Alitalo K. CCBE1 enhances lymphangiogenesis via A disintegrin and metalloprotease with thrombospondin motifs-3-mediated vascular endothelial growth factor-C activation. *Circulation*. 2014;129:1962–1971. doi: 10.1161/CIRCULATIONAHA.113.002779.
163. Hartiala P, Saaristo AM. Growth factor therapy and autologous lymph node transfer in lymphedema. *Trends Cardiovasc Med*. 2010;20:249–253. doi: 10.1016/j.tcm.2011.11.008.
164. Proulx ST, Luciani P, Christiansen A, Karaman S, Blum KS, Rinderknecht M, Leroux JC, Detmar M. Use of a PEG-conjugated bright near-infrared dye for functional imaging of rerouting of tumor lymphatic drainage after sentinel lymph node metastasis. *Biomaterials*. 2013;34:5128–5137. doi: 10.1016/j.biomaterials.2013.03.034.
165. Karlsen TV, McCormack E, Mujic M, Tenstad O, Wiig H. Minimally invasive quantification of lymph flow in mice and rats by imaging depot clearance of near-infrared albumin. *Am J Physiol Heart Circ Physiol*. 2012;302:H391–H401. doi: 10.1152/ajpheart.00842.2011.
166. Baluk P, Tammela T, Ator E, Lyubynska N, Achen MG, Hicklin DJ, Jeltsch M, Petrova TV, Pytowski B, Stacker SA, Ylä-Herttuala S, Jackson DG, Alitalo K, McDonald DM. Pathogenesis of persistent lymphatic vessel hyperplasia in chronic airway inflammation. *J Clin Invest*. 2005;115:247–257. doi: 10.1172/JCI22037.
167. Jurisic G, Sundberg JP, Detmar M. Blockade of VEGF receptor-3 aggravates inflammatory bowel disease and lymphatic vessel enlargement. *Inflamm Bowel Dis*. 2013;19:1983–1989. doi: 10.1097/MIB.0b013e31829292f7.
168. Michel CC, Curry FE. Microvascular permeability. *Physiol Rev*. 1999;79:703–761.
169. Albelda SM, Sampson PM, Haselton FR, McNiff JM, Mueller SN, Williams SK, Fishman AP, Levine EM. Permeability characteristics of cultured endothelial cell monolayers. *J Appl Physiol (1985)*. 1988;64:308–322.
170. Yuan SY, Rigor RR. *Regulation of Endothelial Barrier Function*. San Rafael CA: Morgan & Claypool Life Sciences; 2010.
171. Miles AA, Miles EM. Vascular reactions to histamine, histamine-liberator and leukotaxine in the skin of guinea-pigs. *J Physiol*. 1952;118:228–257.
172. Radu M, Chernoff J. An in vivo assay to test blood vessel permeability. *J Vis Exp*. 2013:e50062. doi: 10.3791/50062.
173. Benest AV, Kruse K, Savant S, Thomas M, Laib AM, Loos EK, Fiedler U, Augustin HG. Angiopoietin-2 is critical for cytokine-induced vascular leakage. *PLoS One*. 2013;8:e70459. doi: 10.1371/journal.pone.0070459.
174. Egawa G, Nakamizo S, Natsuaki Y, Doi H, Miyachi Y, Kabashima K. Intravital analysis of vascular permeability in mice using two-photon microscopy. *Sci Rep*. 2013;3:1932. doi: 10.1038/srep01932.
175. Proulx ST, Luciani P, Alitalo A, Mumprecht V, Christiansen AJ, Huggenberger R, Leroux JC, Detmar M. Non-invasive dynamic near-infrared imaging and quantification of vascular leakage in vivo. *Angiogenesis*. 2013;16:525–540. doi: 10.1007/s10456-013-9332-2.
176. Eigler NL, Schühlen H, Whiting JS, Pfaff JM, Zeiher A, Gu S. Digital angiographic impulse response analysis of regional myocardial perfusion: estimation of coronary flow, flow reserve, and distribution volume by compartmental transit time measurement in a canine model. *Circ Res*. 1991;68:870–880. doi: 10.1161/01.RES.68.3.870.
177. Erbs S, Linke A, Schachinger V, Assmus B, Thiele H, Diederich KW, Hoffmann C, Dimmeler S, Tonn T, Hambrecht R, Zeiher AM, Schuler G. Restoration of microvascular function in the infarct-related artery by intracoronary transplantation of bone marrow progenitor cells in patients with acute myocardial infarction: the Doppler Substudy of the Reinfusion of Enriched Progenitor Cells and Infarct Remodeling in Acute Myocardial Infarction (REPAIR-AMI) trial. *Circulation*. 2007;116:366–374. doi: 10.1161/CIRCULATIONAHA.106.671545.
178. Chilian WM, Wangler RD, Peters KG, Tomanek RJ, Marcus ML. Thyroxine-induced left ventricular hypertrophy in the rat: anatomical and physiological evidence for angiogenesis. *Circ Res*. 1985;57:591–598. doi: 10.1161/01.RES.57.4.591.
179. Marcus ML, Harrison DG, Chilian WM, Koyanagi S, Inou T, Tomanek RJ, Martins JB, Eastham CL, Hiratzka LF. Alterations in the coronary circulation in hypertrophied ventricles. *Circulation*. 1987;75(pt 2):I19–I25.
180. Tomanek RJ, Searls JC, Lachenbruch PA. Quantitative changes in the capillary bed during developing, peak, and stabilized cardiac hypertrophy in the spontaneously hypertensive rat. *Circ Res*. 1982;51:295–304. doi: 10.1161/01.RES.51.3.295.
181. Chilian WM, Marcus ML. Coronary vascular adaptations to myocardial hypertrophy. *Annu Rev Physiol*. 1987;49:477–487. doi: 10.1146/annurev.ph.49.030187.002401.
182. Lindner JR, Sinusas A. Molecular imaging in cardiovascular disease: which methods, which diseases? *J Nucl Cardiol*. 2013;20:990–1001. doi: 10.1007/s12350-013-9785-0.
183. Orbay H, Hong H, Zhang Y, Cai W. PET/SPECT imaging of hindlimb ischemia: focusing on angiogenesis and blood flow. *Angiogenesis*. 2013;16:279–287. doi: 10.1007/s10456-012-9319-4.
184. Dobrucki LW, de Muinck ED, Lindner JR, Sinusas AJ. Approaches to multimodality imaging of angiogenesis. *J Nucl Med*. 2010;51(suppl 1):66S–79S. doi: 10.2967/jnumed.109.074963.
185. Stacy MR, Yu da Y, Maxfield MW, Jaba IM, Jozwik BP, Zhuang ZW, Lin BA, Hawley CL, Caracciolo CM, Pal P, Tirziu D, Sampath S, Sinusas AJ. Multimodality imaging approach for serial assessment of regional changes in lower extremity arteriogenesis and tissue perfusion in a porcine model of peripheral arterial disease. *Circ Cardiovasc Imaging*. 2014;7:92–99. doi: 10.1161/CIRCIMAGING.113.000884.
186. Meoli DF, Sadeghi MM, Krassilnikova S, Bourke BN, Giordano FJ, Dione DP, Su H, Edwards DS, Liu S, Harris TD, Madri JA, Zaret BL, Sinusas AJ. Noninvasive imaging of myocardial angiogenesis following experimental myocardial infarction. *J Clin Invest*. 2004;113:1684–1691. doi: 10.1172/JCI20352.
187. Dobrucki LW, Tsutsumi Y, Kalinowski L, Dean J, Gavin M, Sen S, Mendizabal M, Sinusas AJ, Aikawa R. Analysis of angiogenesis induced by local IGF-1 expression after myocardial infarction using microSPECT-CT imaging. *J Mol Cell Cardiol*. 2010;48:1071–1079. doi: 10.1016/j.yjmcc.2009.10.008.
188. Lu E, Wagner WR, Schellenberger U, Abraham JA, Klibanov AL, Woulfe SR, Csikari MM, Fischer D, Schreiner GF, Brandenburger GH, Villanueva FS. Targeted in vivo labeling of receptors for vascular endothelial growth factor: approach to identification of ischemic tissue. *Circulation*. 2003;108:97–103. doi: 10.1161/01.CIR.0000079100.38176.83.
189. Lee KH, Jung KH, Song SH, Kim DH, Lee BC, Sung HJ, Han YM, Choe YS, Chi DY, Kim BT. Radiolabeled RGD uptake and alphav integrin expression is enhanced in ischemic murine hindlimbs. *J Nucl Med*. 2005;46:472–478.
190. Fischman AJ, Hsu H, Carter EA, Yu YM, Tompkins RG, Guerrero JL, Young VR, Alpert NM. Regional measurement of canine skeletal muscle blood flow by positron emission tomography with H2(15)O. *J Appl Physiol (1985)*. 2002;92:1709–1716. doi: 10.1152/japplphysiol.00445.2001.
191. Almutairi A, Rossin R, Shokeen M, Hagooly A, Ananth A, Capoccia B, Guillaudeu S, Abendschein D, Anderson CJ, Welch MJ, Fréchet JM.

Biodegradable dendritic positron-emitting nanoprobes for the noninvasive imaging of angiogenesis. *Proc Natl Acad Sci USA*. 2009;106:685–690. doi: 10.1073/pnas.0811757106.
192. Jeong JM, Hong MK, Chang YS, Lee YS, Kim YJ, Cheon GJ, Lee DS, Chung JK, Lee MC. Preparation of a promising angiogenesis PET imaging agent: 68Ga-labeled c(RGDyK)-isothiocyanatobenzyl-1,4,7-triazacyclononane-1,4,7-triacetic acid and feasibility studies in mice. *J Nucl Med*. 2008;49:830–836. doi: 10.2967/jnumed.107.047423.
193. Peñuelas I, Aranguren XL, Abizanda G, Martí-Climent JM, Uriz M, Ecay M, Collantes M, Quincoces G, Richter JA, Prósper F. (13)N-ammonia PET as a measurement of hindlimb perfusion in a mouse model of peripheral artery occlusive disease. *J Nucl Med*. 2007;48:1216–1223. doi: 10.2967/jnumed.106.039180.
194. Liu Y, Pressly ED, Abendschein DR, Hawker CJ, Woodard GE, Woodard PK, Welch MJ. Targeting angiogenesis using a C-type atrial natriuretic factor-conjugated nanoprobe and PET. *J Nucl Med*. 2011;52:1956–1963. doi: 10.2967/jnumed.111.089581.
195. Orbay H, Hong H, Koch JM, Valdovinos HF, Hacker TA, Theuer CP, Barnhart TE, Cai W. Pravastatin stimulates angiogenesis in a murine hindlimb ischemia model: a positron emission tomography imaging study with (64)Cu-NOTA-TRC105. *Am J Transl Res*. 2013;6:54–63.
196. Willmann JK, Chen K, Wang H, Paulmurugan R, Rollins M, Cai W, Wang DS, Chen IY, Gheysens O, Rodriguez-Porcel M, Chen X, Gambhir SS. Monitoring of the biological response to murine hindlimb ischemia with 64Cu-labeled vascular endothelial growth factor-121 positron emission tomography. *Circulation*. 2008;117:915–922. doi: 10.1161/CIRCULATIONAHA.107.733220.
197. Carr CL, Qi Y, Davidson B, Chadderdon S, Jayaweera AR, Belcik JT, Benner C, Xie A, Lindner JR. Dysregulated selectin expression and monocyte recruitment during ischemia-related vascular remodeling in diabetes mellitus. *Arterioscler Thromb Vasc Biol*. 2011;31:2526–2533. doi: 10.1161/ATVBAHA.111.230177.
198. Leong-Poi H, Christiansen J, Klibanov AL, Kaul S, Lindner JR. Noninvasive assessment of angiogenesis by ultrasound and microbubbles targeted to alpha(v)-integrins. *Circulation*. 2003;107:455–460. doi: 10.1161/01.CIR.0000044916.05919.8B.
199. Behm CZ, Kaufmann BA, Carr C, Lankford M, Sanders JM, Rose CE, Kaul S, Lindner JR. Molecular imaging of endothelial vascular cell adhesion molecule-1 expression and inflammatory cell recruitment during vasculogenesis and ischemia-mediated arteriogenesis. *Circulation*. 2008;117:2902–2911. doi: 10.1161/CIRCULATIONAHA.107.744037.
200. Weller GE, Villanueva FS, Tom EM, Wagner WR. Targeted ultrasound contrast agents: in vitro assessment of endothelial dysfunction and multi-targeting to ICAM-1 and sialyl Lewisx. *Biotechnol Bioeng*. 2005;92:780–788. doi: 10.1002/bit.20625.
201. Luo Y, Mohning KM, Hradil VP, Wessale JL, Segreti JA, Nuss ME, Wegner CD, Burke SE, Cox BF. Evaluation of tissue perfusion in a rat model of hind-limb muscle ischemia using dynamic contrast-enhanced magnetic resonance imaging. *J Magn Reson Imaging*. 2002;16:277–283. doi: 10.1002/jmri.10169.
202. Kluza E, van der Schaft DW, Hautvast PA, Mulder WJ, Mayo KH, Griffioen AW, Strijkers GJ, Nicolay K. Synergistic targeting of alphavbeta3 integrin and galectin-1 with heteromultivalent paramagnetic liposomes for combined MR imaging and treatment of angiogenesis. *Nano Lett*. 2010;10:52–58. doi: 10.1021/nl902659g.
203. Winter PM, Caruthers SD, Allen JS, Cai K, Williams TA, Lanza GM, Wickline SA. Molecular imaging of angiogenic therapy in peripheral vascular disease with alphanubeta3-integrin-targeted nanoparticles. *Magn Reson Med*. 2010;64:369–376. doi: 10.1002/mrm.22447.
204. Fukumura D, Jain RK. Imaging angiogenesis and the microenvironment. *APMIS*. 2008;116:695–715. doi: 10.1111/j.1600-0463.2008.01148.x.
205. Mulder WJ, Strijkers GJ, Nicolay K, Griffioen AW. Quantum dots for multimodal molecular imaging of angiogenesis. *Angiogenesis*. 2010;13:131–134. doi: 10.1007/s10456-010-9177-x.
206. Briers JD. Laser Doppler, speckle and related techniques for blood perfusion mapping and imaging. *Physiol Meas*. 2001;22:R35–R66.
207. Kelly KA, Allport JR, Tsourkas A, Shinde-Patil VR, Josephson L, Weissleder R. Detection of vascular adhesion molecule-1 expression using a novel multimodal nanoparticle. *Circ Res*. 2005;96:327–336. doi: 10.1161/01.RES.0000155722.17881.dd.
208. Mulder WJ, Castermans K, van Beijnum JR, Oude Egbrink MG, Chin PT, Fayad ZA, Löwik CW, Kaijzel EL, Que I, Storm G, Strijkers GJ, Griffioen AW, Nicolay K. Molecular imaging of tumor angiogenesis using alphavbeta3-integrin targeted multimodal quantum dots. *Angiogenesis*. 2009;12:17–24. doi: 10.1007/s10456-008-9124-2.
209. Backer MV, Levashova Z, Patel V, Jehning BT, Claffey K, Blankenberg FG, Backer JM. Molecular imaging of VEGF receptors in angiogenic vasculature with single-chain VEGF-based probes. *Nat Med*. 2007;13:504–509. doi: 10.1038/nm1522.
210. Zhang HF, Maslov K, Stoica G, Wang LV. Functional photoacoustic microscopy for high-resolution and noninvasive in vivo imaging. *Nat Biotechnol*. 2006;24:848–851. doi: 10.1038/nbt1220.
211. Pan H, Myerson JW, Ivashyna O, Soman NR, Marsh JN, Hood JL, Lanza GM, Schlesinger PH, Wickline SA. Lipid membrane editing with peptide cargo linkers in cells and synthetic nanostructures. *FASEB J*. 2010;24:2928–2937. doi: 10.1096/fj.09-153130.
212. Vandenberg BF, Kieso R, Fox-Eastham K, Chilian W, Kerber RE. Quantitation of myocardial perfusion by contrast echocardiography: analysis of contrast gray level appearance variables and intracyclic variability. *J Am Coll Cardiol*. 1989;13:200–206.
213. Kaufmann BA, Wei K, Lindner JR. Contrast echocardiography. *Curr Probl Cardiol*. 2007;32:51–96. doi: 10.1016/j.cpcardiol.2006.10.004.
214. Le DE, Jayaweera AR, Wei K, Coggins MP, Lindner JR, Kaul S. Changes in myocardial blood volume over a wide range of coronary driving pressures: role of capillaries beyond the autoregulatory range. *Heart*. 2004;90:1199–1205. doi: 10.1136/hrt.2003.020875.
215. Coolen BF, Moonen RP, Paulis LE, Geelen T, Nicolay K, Strijkers GJ. Mouse myocardial first-pass perfusion MR imaging. *Magn Reson Med*. 2010;64:1658–1663. doi: 10.1002/mrm.22588.
216. Campbell-Washburn AE, Price AN, Wells JA, Thomas DL, Ordidge RJ, Lythgoe MF. Cardiac arterial spin labeling using segmented ECG-gated Look-Locker FAIR: variability and repeatability in preclinical studies. *Magn Reson Med*. 2013;69:238–247. doi: 10.1002/mrm.24243.
217. Winter PM, Neubauer AM, Caruthers SD, Harris TD, Robertson JD, Williams TA, Schmieder AH, Hu G, Allen JS, Lacy EK, Zhang H, Wickline SA, Lanza GM. Endothelial alpha(v)beta3 integrin-targeted fumagillin nanoparticles inhibit angiogenesis in atherosclerosis. *Arterioscler Thromb Vasc Biol*. 2006;26:2103–2109. doi: 10.1161/01.ATV.0000235724.11299.76.
218. Dobrucki LW, Dione DP, Kalinowski L, Dione D, Mendizabal M, Yu J, Papademetris X, Sessa WC, Sinusas AJ. Serial noninvasive targeted imaging of peripheral angiogenesis: validation and application of a semiautomated quantitative approach. *J Nucl Med*. 2009;50:1356–1363. doi: 10.2967/jnumed.108.060822.
219. Jaba IM, Zhuang ZW, Li N, Jiang Y, Martin KA, Sinusas AJ, Papademetris X, Simons M, Sessa WC, Young LH, Tirziu D. NO triggers RGS4 degradation to coordinate angiogenesis and cardiomyocyte growth. *J Clin Invest*. 2013;123:1718–1731. doi: 10.1172/JCI65112.
220. Moraes F, Paye J, Mac Gabhann F, Zhuang ZW, Zhang J, Lanahan AA, Simons M. Endothelial cell-dependent regulation of arteriogenesis. *Circ Res*. 2013;113:1076–1086. doi: 10.1161/CIRCRESAHA.113.301340.
221. Jiang Y, Zhuang ZW, Sinusas AJ, Staib LH, Papademetris X. Vessel connectivity using Murray's hypothesis. *Med Image Comput Comput Assist Interv*. 2011;14(pt 3):528–536.
222. McDonald DM, Choyke PL. Imaging of angiogenesis: from microscope to clinic. *Nat Med*. 2003;9:713–725. doi: 10.1038/nm0603-713.
223. Taqueti VR, Jaffer FA. High-resolution molecular imaging via intravital microscopy: illuminating vascular biology in vivo. *Integr Biol (Camb)*. 2013;5:278–290. doi: 10.1039/c2ib20194a.
224. Raatschen HJ, Simon GH, Fu Y, Sennino B, Shames DM, Wendland MF, McDonald DM, Brasch RC. Vascular permeability during antiangiogenesis treatment: MR imaging assay results as biomarker for subsequent tumor growth in rats. *Radiology*. 2008;247:391–399. doi: 10.1148/radiol.2472070363.
225. Rajwani A, Cubbon RM, Wheatcroft SB. Cell-specific insulin resistance: implications for atherosclerosis. *Diabetes Metab Res Rev*. 2012;28:627–634. doi: 10.1002/dmrr.2336.
226. Lassègue B, San Martín A, Griendling KK. Biochemistry, physiology, and pathophysiology of NADPH oxidases in the cardiovascular system. *Circ Res*. 2012;110:1364–1390. doi: 10.1161/CIRCRESAHA.111.243972.
227. Lin KY, Ito A, Asagami T, Tsao PS, Adimoolam S, Kimoto M, Tsuji H, Reaven GM, Cooke JP. Impaired nitric oxide synthase pathway in diabetes mellitus: role of asymmetric dimethylarginine and dimethylarginine dimethylaminohydrolase. *Circulation*. 2002;106:987–992. doi: 10.1161/01.CIR.0000027109.14149.67.
228. Goldin A, Beckman JA, Schmidt AM, Creager MA. Advanced glycation end products: sparking the development of diabetic vascular injury. *Circulation*. 2006;114:597–605. doi: 10.1161/CIRCULATIONAHA.106.621854.
229. Rosenfield K, Losordo DW, Ramaswamy K, Pastore JO, Langevin RE, Razvi S, Kosowsky BD, Isner JM. Three-dimensional reconstruction of human coronary and peripheral arteries from images recorded

during two-dimensional intravascular ultrasound examination. *Circulation*. 1991;84:1938–1956. doi:10.1161/01.CIR.84.5.1938.

230. Abedin M, Tintut Y, Demer LL. Vascular calcification: mechanisms and clinical ramifications. *Arterioscler Thromb Vasc Biol*. 2004;24:1161–1170. doi: 10.1161/01.ATV.0000133194.94939.42.
231. Beckman JA, Creager MA, Libby P. Diabetes and atherosclerosis: epidemiology, pathophysiology, and management. *JAMA*. 2002;287:2570–2581.
232. Cullen P, Baetta R, Bellosta S, Bernini F, Chinetti G, Cignarella A, von Eckardstein A, Exley A, Goddard M, Hofker M, Hurt-Camejo E, Kanters E, Kovanen P, Lorkowski S, McPheat W, Pentikäinen M, Rauterberg J, Ritchie A, Staels B, Weitkamp B, de Winther M; MAFAPS Consortium. Rupture of the atherosclerotic plaque: does a good animal model exist? *Arterioscler Thromb Vasc Biol*. 2003;23:535–542. doi: 10.1161/01.ATV.0000060200.73623.F8.
233. Annex BH. Therapeutic angiogenesis for critical limb ischaemia. *Nat Rev Cardiol*. 2013;10:387–396. doi: 10.1038/nrcardio.2013.70.
234. Handelsman Y, Mechanick JI, Blonde L, Grunberger G, Bloomgarden ZT, Bray GA, Dagogo-Jack S, Davidson JA, Einhorn D, Ganda O, Garber AJ, Hirsch IB, Horton ES, Ismail-Beigi F, Jellinger PS, Jones KL, Jovanovič L, Lebovitz H, Levy P, Moghissi ES, Orzeck EA, Vinik AI, Wyne KL; AACE Task Force for Developing a Diabetes Comprehensive Care Plan. American Association of Clinical Endocrinologists medical guidelines for clinical practice for developing a diabetes mellitus comprehensive care plan: executive summary. *Endocr Pract*. 2011;17:287–302.
235. Clee SM, Attie AD. The genetic landscape of type 2 diabetes in mice. *Endocr Rev*. 2007;28:48–83. doi: 10.1210/er.2006-0035.
236. Hazarika S, Dokun AO, Li Y, Popel AS, Kontos CD, Annex BH. Impaired angiogenesis after hindlimb ischemia in type 2 diabetes mellitus: differential regulation of vascular endothelial growth factor receptor 1 and soluble vascular endothelial growth factor receptor 1. *Circ Res*. 2007;101:948–956. doi: 10.1161/CIRCRESAHA.107.160630.
237. Inoue H, Nagata N, Kurokawa H, Yamanaka S. iPS cells: a game changer for future medicine. *EMBO J*. 2014;33:409–417. doi: 10.1002/embj.201387098.
238. Rufaihah AJ, Huang NF, Jamé S, Lee JC, Nguyen HN, Byers B, De A, Okogbaa J, Rollins M, Reijo-Pera R, Gambhir SS, Cooke JP. Endothelial cells derived from human iPSCS increase capillary density and improve perfusion in a mouse model of peripheral arterial disease. *Arterioscler Thromb Vasc Biol*. 2011;31:e72–e79. doi: 10.1161/ATVBAHA.111.230938.
239. Dragneva G, Korpisalo P, Ylä-Herttuala S. Promoting blood vessel growth in ischemic diseases: challenges in translating preclinical potential into clinical success. *Dis Model Mech*. 2013;6:312–322. doi: 10.1242/dmm.010413.
240. Simons M. Angiogenesis, arteriogenesis, and diabetes: paradigm reassessed? *J Am Coll Cardiol*. 2005;46:835–837. doi: 10.1016/j.jacc.2005.06.008.
241. Sasso FC, Torella D, Carbonara O, Ellison GM, Torella M, Scardone M, Marra C, Nasti R, Marfella R, Cozzolino D, Indolfi C, Cotrufo M, Torella R, Salvatore T. Increased vascular endothelial growth factor expression but impaired vascular endothelial growth factor receptor signaling in the myocardium of type 2 diabetic patients with chronic coronary heart disease. *J Am Coll Cardiol*. 2005;46:827–834. doi: 10.1016/j.jacc.2005.06.007.

KEY WORDS: AHA Scientific Statements ■ angiogenesis ■ assays ■ arteriogenesis ■ endothelial ■ imaging ■ models